Isotope Effects in the Chemistry of Atmospheric Trace Compounds†

C. A. M. Brenninkmeijer,*,§ C. Janssen,⊥ J. Kaiser,‡ T. Röckmann,⊥ T. S. Rhee,§ and S. S. Assonov§

Max Planck Institute for Chemistry, D-55128 Mainz, Germany, Max Planck Institute for Nuclear Physics, D-69117 Heidelberg, Germany, and Department of Geosciences, Princeton University, Princeton, New Jersey 08544

Received February 20, 2003

Contents

† Dedicated to Prof. Dr. Konrad Mauersberger.
* To whom correspondence should be addressed.
§ Max Planck Institute for Chemistry.
⊥ Max Planck Institute for Nuclear Physics.
‡ Princeton University.

1. Introduction

Three factors are currently driving the study of isotope variations in atmospheric trace gases and aerosols. First of all, isotope effects in nature provide information on a host of processes that are often difficult to quantify. Although isotope effects generally are subtle, they can mostly be measured precisely. Thus, just as much of the quantitative information we have on past climate changes is derived from isotope measurements on carbonates in sediments, or H_2O from ice cores, unique information is also contained in the isotopic composition of atmospheric trace gases. Therefore, in the normal course of better understanding the chemistry of the atmosphere, one increasingly studies isotopic composition, next to concentrations and fluxes.

The second factor is a development that perhaps has less to do with what isotopes can do for atmospheric chemistry than the opposite, namely, what atmospheric chemistry can do for better understanding isotope fractionation processes. In fact, through the investigation of isotopic processes in atmospheric trace gases, hitherto unknown effects have been discovered. Several of these effects were deemed as "anomalous" or "mass-independent", witnessing a truly exciting development at a time when it was generally conceived that most isotope effects were well understood at the molecular level. Besides this, the application of isotope analysis to atmospheric processes has forced a rethinking about precision, accuracy, traceability, and reference materials. Atmospheric chemistry has also helped some "traditional isotope scientists" to start to work on a set of scientific problems that are innately more quantitative than other applications in the earth sciences.

10.1021/cr020644k CCC: $44.00
Published on Web 11/08/2003

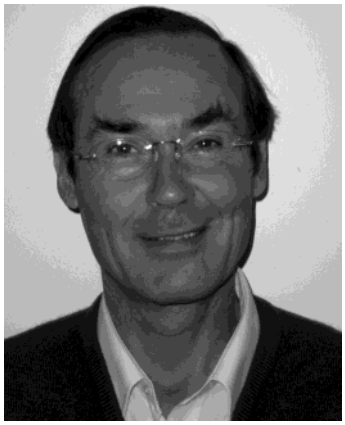

Dr. Carl Brenninkmeijer obtained his M.Sc. in experimental physics in The Netherlands (Prof. W. G. Mook) and subsequently worked at IGNS in Lower Hutt, New Zealand, on radiocarbon dating applications. After obtaining his Ph.D. in The Netherlands on isotope palaeoclimatology, he returned to IGNS (later NIWA), New Zealand, to work for 10 years on mass spectrometry and the development of atmospheric applications. He also was director of research of Scientific Solutions Ltd. In 1994, he moved with his family to Mainz to work in the Atmospheric Chemistry Division of the Max Planck Institute for Chemistry (Prof. Paul J. Crutzen). He is coordinator of CARIBIC (www.caribic-atmospheric.com).

Dr. Jan Kaiser completed his M.Sc. in chemistry at the Max Planck Institute for Marine Microbiology and the University of Bremen, Germany, in 1998, under the supervision of Prof. Bo Barker Jørgensen and Dr. Timothy G. Ferdelman. He received a Ph.D. from the Johannes Gutenberg University of Mainz in 2002 (subject: "Stable isotope investigations of atmospheric nitrous oxide") and performed research at the Max Planck Institute for Chemistry under the supervision of Prof. Paul J. Crutzen and Dr. Carl A. M. Brenninkmeijer. At present, he is working as a Hess Postdoctoral Fellow in the group of Prof. Michael L. Bender in the Department of Geosciences at Princeton University.

Dr. Christof Janssen received his M.Sc. in physics from the Ruprechts-Karls-Universität in Heidelberg in 1994. In 1999, he obtained his Ph.D. degree in physics from the same university. Currently he is a postdoctoral fellow at the Max-Planck-Institute for Nuclear Physics in Heidelberg with Prof. Konrad Mauersberger. His main research interests are atmospheric chemistry and isotope kinetic processes.

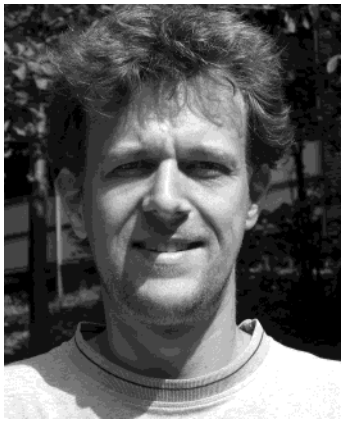

Dr. Thomas Röckmann is an atmospheric physicist, specializing in the development and application of isotope techniques to study a wide range of physical and chemical processes in the atmosphere. His "stable isotope life" began to tick during his M.Sc. research at the Stable Isotope Laboratory of the Institute of Arctic and Alpine Research (INSTAAR), University of Colorado at Boulder. He worked as a Ph.D. student and later as a postdoc in the laboratory of Carl A. M. Brenninkmeijer at the Max Planck Institute for Chemistry, Atmospheric Chemistry Division (Prof. Paul J. Crutzen), in Mainz, and obtained his Ph.D. degree from the University of Heidelberg. Since 2000, he is head of an independent "junior research group" funded by the German federal government (BmBF) and located at the Max Planck Institute for Nuclear Physics in Heidelberg.

Isotopic information about trace gases, be it in the troposphere or stratosphere, is increasingly incorporated into 2D and 3D modeling experiments.

The third factor is purely analytical development, namely the successful marriage between gas chromatography (a major tool in atmospheric chemistry) and isotope ratio mass spectrometry. This innovation, pioneered on two continents, has had a tremendous impact. For a long time it had been tacitly assumed that precise isotope ratio determinations could only be performed on at least micromole quantities of trace gases using magnetic sector mass spectrometers with a sample inlet system under high-vacuum conditions. This has changed radically, and over 90% of the instruments that are sold today are based on the introduction of the analyte into the mass spectrometer entrained in a flow of helium. In this way, nanomole quantities can be isotopically assayed by feeding the effluent of a gas chromatograph into a modified isotope ratio mass spectrometer. Even hydrogen gas can be analyzed this way, despite the massive background of He^+ ions. This background is generally fully suppressed by using an electrostatic filter. The GC−IRMS technique is fast and requires only the smallest of quantities. A good illustration of the new capability is that the measurement of, for instance, the carbon isotopic composition of methane presently requires only marginally more effort than measuring its concentration. With isotope measurements becoming so convenient, their benefits will increasingly outweigh the additional analytical efforts.

All in all, the combination of the generally growing use of isotopic information in earth sciences, the discovery of interesting new isotope effects—which

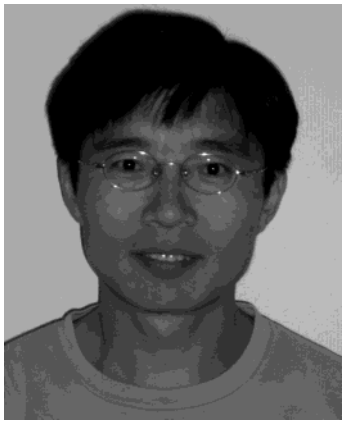

Dr. Tae Siek Rhee received his B.Sc. in plant pathology and M.Sc. in chemical oceanography from the Seoul National University. He studied air–sea gas exchange at the Max Plank Institute for Chemistry in Mainz and completed his doctoral thesis at the Texas A&M university in 2000, under the supervision of Professors D. Schink, R. A. Duce, and M. O. Andrea. After that, he joined the group of Dr. Carl A. M. Brenninkmeijer for postdoctoral research with several research topics (NMHC's, isotopes, etc.) in atmospheric chemistry.

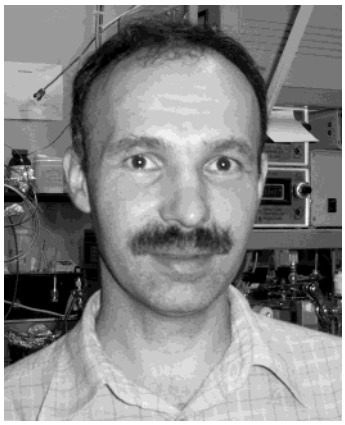

Dr. Sergey Assonov received his M.Sc. degree in geochemistry from the Moscow State University and his Ph.D. in geochemistry from the Vernadsky Institute of Analytical Chemistry (Russian Academy of Sciences, Moscow) in 1995 (topics: isotope dating and noble gas investigation of meteorites and lunar samples). In 1997, he was visiting fellow at the Open University (Planetary & Space Sciences Research Institute, Prof. C. Pillinger), and in 1999, he was visiting fellow at CRPG–CNRS, Nancy, France (research subject: isotope analyses of N in lunar samples in search of a solar nitrogen component). He is presently at the Max Planck Institute for Chemistry with Carl Brenninkmeijer, developing isotope tools for atmospheric applications and calibration and standardization issues of isotopic analyses.

already has sparked off theoretical work—and this elegant analytical breakthrough of GC−IRMS contributes to the coming-of-age of isotope studies in atmospheric chemistry. We quickly add to this that the application of spectroscopic (optical) detection techniques is likewise important, particularly for stratospheric research. The list of the atmospheric gases measured isotopically is considerable. It comprises most of the important trace gases: O_3, CH_4, CO_2, N_2O, CO, H_2, H_2O_2, HCHO, OCS, and interestingly also sulfate and nitrate. However, we do note that even atmospheric oxygen itself possesses a small but highly interesting isotopic anomaly. For a review concerning hydrocarbons and even halocarbons, we refer the reader to the paper by Goldstein in this issue.

This review discusses the isotope effects for each of several constituents or groups of constituents in turn: it cannot be exhaustive, and in some cases only the most recent work is touched upon. Ozone takes a dominant place. The amount of research is large and varied; ozone's isotope effects are very complex, are very substantial, and are being studied most intensively by experiment and by theory. Moreover, the special isotope effects of ozone are "inherited" by some trace gases. This all has made us give ozone the prominent role in this review. Nitrous oxide also will be highlighted, because the nitrogen isotopic distribution within this molecule has been analyzed for the first time very recently, and great progress was rapidly achieved by various groups. Overlap with existing reviews has been avoided as much as possible. For instance, relatively little of the extensive work on trace gas budgets and modeling is covered here. The emphasis is therefore somewhat more in the direction of atmospheric chemistry instead of global biogeochemical cycles. Before kicking off, we draw the reader's kind attention to the existence of other reviews, namely the classical extensive review from 1987 by Kaye,[1] a review by Johnson et al.,[2] reviews of mass-independent isotope effects by Thiemens[3] and by Weston,[4] and a review by Mauersberger et al.[5]

2. Definitions and Concepts

2.1. The Delta Notation and Standards

An isotope ratio R for a certain compound is generally defined as the atomic abundance ratio of a less abundant isotope to the most abundant isotope. Because (with the exception of deuterium) stable isotope variations in nature are small, these ratios are usually expressed in per mil (‰) relative deviation to the respective reference (often also called standard) material. We note that for making some formulas clearer, at times the factor of 1000 will be omitted. For the large isotope variations in ozone, % instead of ‰ is used. When we take ^{13}C as an example, and use SA for the sample and REF for the reference material, the conventional definition is $\delta^{13}C(SA) = (R_{SA}/R_{REF} - 1) \times 1000$. Thus, the expression for methane, $\delta^{13}CH_4$, is not officially defined, and δDCH_3 or δCDH_3 could be somewhat confusing. It would be clearer to use $\delta^{13}C(CH_4)$ for instance, or $\delta^{13}C\text{-}CH_4$. Note further that the molecular ratio of CDH_3 to CH_4 is 4 times the atomic ratio of D to H. The International Atomic Energy Agency supplies reference materials for a range of compounds. The following reference materials are in use for reporting δ values: Air N_2 for $^{15}N/^{14}N$,[6] VSMOW (Vienna Standard Mean Ocean Water) for D/H,[7] V-SMOW or Vienna Pee Dee Belemnite (VPDB) for $^{18}O/^{16}O$ and $^{17}O/^{16}O$[7] [at times also atmospheric oxygen is used as a reference material; this however complicates matters because it has a small deviation in its ^{17}O-to-^{18}O ratio (MIF)], VPDB for $^{13}C/^{12}C$,[7] and Vienna Cañon Diablo Troilite for sulfur isotope ratios.[8]

IUPAC defines an isotopologue as a molecular entity that differs only in isotopic composition (number of isotopic substitutions); e.g., CH_4, CH_3D, and

CH_2D_2 are isotopologues. Isotopomers (from "isotopic isomer") have the same number of each isotope but differ with respect to their position (e.g., the "heavy" isotopomers $CH_2DCH{=}O$ and $CH_3CD{=}O$, but also $^{14}N^{15}NO$ and $^{15}N^{14}NO$). For mixing of two reservoirs a and b, with delta values δ_a and δ_b, the resulting isotopic composition (r) is given by $\delta_r = f\delta_a + (1 - f)\delta_b$. Except for the case of small differences, δ values are not additive quantities. For a recent extensive overview of the range of natural variations of selected elements in naturally occurring materials, we refer to the USGS report by Coplen.[9]

2.2. Source Effects

Variations in the isotopic composition of atmospheric trace gases have two causes. One is that the various surface sources often exhibit characteristic isotopic compositions ("fingerprints"). For instance, the $^{13}C/^{12}C$ ratio of CH_4 produced in biomass burning tends to reflect that of the organic material (mainly cellulose) burned; $\delta^{13}C$ values of -25 to -30‰ are most common (note that the value for plants depends on the metabolic pathway of photosynthesis). However, when cellulose is processed by bacteria present in soils, in termites, or in cattle, CH_4 is released with $\delta^{13}C$ values of -40 to -100‰. Here, the substrate isotopic composition and the oxidation processes that preferentially remove the lighter isotopomer determine the delta value of the final product reaching the atmosphere. For the D/H ratio the situation is even more complicated, because the deuterium content of plant organic matter depends not only on biological processes but also on evapotranspiration and the isotopic composition of meteoric water. Unlike CH_4, CO does have in situ atmospheric sources, which of course all have to be considered. We finally remark that, although isotopes constitute excellent tracers, their variations do not affect the chemistry of the atmosphere. Cl, which consists of about 75% ^{35}Cl and 25% ^{37}Cl, in principle can possibly constitute an exception.

2.3. Sink Effects

The second origin of isotope variations in atmospheric trace gases—and this is of special interest to atmospheric chemists—is that isotope effects accompany the removal of trace gases from the atmosphere via reaction with mainly OH, or photolysis. These effects fractionate the trace gas remaining in the atmosphere and fall within the class of kinetic isotope effects. This is in contrast to equilibrium isotope effects in which the process is reversible, like the ^{18}O exchange between H_2O and CO_2 (via HCO_3^-). When certain atmospheric trace gases dissolve into ocean water or disappear in soils, isotopic fractionation occurs as well. In the first instance, the different rates of dissolution/diffusion of the isotopically substituted molecule have to be considered. Such sink effects are of a purely physical nature. Furthermore, microbial consumption in most cases will lead to fractionation as well. Thus, most sink processes cause isotopic changes, and the remaining, unreacted trace gas gradually acquires a different isotopic composition. For instance, a certain reservoir of CH_4 becomes enriched in ^{13}C and D through the reaction with OH (while CO depleted in ^{13}C is formed) and through consumption by aerobic processes in soils.

Whereas the delta notation is used to express the isotope ratio relative to a reference material, the isotopic difference between two reservoirs, phases, or molecule types in terms of a process-based relationship between them is given as a fractionation constant ϵ, likewise expressed in ‰, its value being related to the fractionation factor α (which invariably is close to 1 except for deuterium) by $\epsilon = \alpha - 1$. When a trace gas is removed from a closed reservoir by chemical reaction, the isotopic composition of the remaining fraction is mathematically expressed as a Raleigh process. We caution the reader that, due to the historical development of studying isotope fractionation, some inconsistencies have invaded the literature, which we point out next.

In atmospheric applications, α has increasingly been replaced by "KIE", that is, the kinetic isotope effect. Using the reaction $CH_4 + OH$ as an example, the KIE is taken to be the ratio of the respective reaction rate constants, $^{12}k/^{13}k$. This is convenient because the resulting ϵ is, in most cases, positive. Thus, atmospheric CH_4 becomes enriched in ^{13}C, because $^{13}CH_4$ reacts slower, and $\alpha \equiv \mathrm{KIE} > 1$. This practice follows IUPAC recommendations.[10] However, conforming to the convention of defining the ratio R as the rare over the abundant isotope, it is more logical to use the inverse, namely, $\alpha = {}^{13}k/{}^{12}k$. For most isotope fractionation processes, this implies negative values for ϵ. However, the expression describing the isotopic change of a reservoir, be it a photochemical reactor or an atmospheric pool, becomes straightforward, namely:

$$R = R_0(c/c_0)^{(\alpha-1)}$$

which gives the final ratio R as a function of the initial ratio R_0 and the ratio between the initial and final concentrations of the most abundant isotope of the gas. Thus, $\ln(R/R_0) = \ln(1 + \delta) = (\alpha - 1)\ln(c/c_0) = \epsilon \ln(c/c_0)$.

To avoid negative ϵ values, occasionally $\epsilon = 1 - \alpha$ is used. When steady-state conditions apply, the isotopic composition of a trace gas entering the atmosphere (which equals that of the combined sources) is identical to that of the gas which is removed in the sink processes. This means, in the case of CH_4, for instance, that the atmospheric inventory of the gas is enriched in ^{13}C relative to its combined sources. In reviewing existing work, both definitions of α (and both definitions of ϵ) are encountered, and the reader is referred to the original work for definitions of α and ϵ in each case. In this review, we follow the IUPAC-recommended convention of defining α as the reaction rate of the isotopically light species divided by the reaction rates of the heavy species, except for N_2O and OCS, where the inverse definition α is often used (with $\epsilon = \alpha - 1$). Where necessary, we have converted the values reported in the original publications to those consistent the IUPAC recommendation.

In most laboratory studies of kinetic isotope effects, the change in the source molecule has been followed rather than that of the product(s). Thus, the isotopic changes of H_2, CH_4, CO, and N_2O during reaction with radicals or under photolysis have been established. To our knowledge, isotope budgets for reactor experiments have been rarely measured. Kinetic isotope effects can be calculated using transition-state theories. For a review of the theoretical aspects, we refer the reader to the work of Weston.[4]

2.4. Intramolecular Isotope Distribution

Mass spectrometry has been a main analytical tool in earth sciences and has dominated isotope research in the atmosphere, which was focused mainly on CO_2, H_2, N_2, O_2, and SO_2. In the magnetic sector instruments commonly applied, mostly fixed Faraday cup collectors for the singly charged molecular ions of these gases are used. Even N_2O used to be converted to N_2 and CO_2. The direct analysis of N_2O (NNO) appears to be possible, but extreme care to avoid isobaric interference from traces of CO_2 has to be taken. By also considering the NO^+ ion beam, position-dependent isotope analysis could be realized (see N_2O section). Concerning atmospheric trace gases, O_3 and N_2O are the main molecules in which intramolecular isotopic distributions play an important role. In the analysis of propane, for instance, there are two distinct positions for H atoms to be considered, but this has received little attention. For the time being, a gas like propane will be burned to get CO_2 for ^{13}C analysis, while pyrolysis gives access to the overall D/H ratio. Furthermore, not only is position-dependent information inaccessible at times, or only in the investigative stage, but even establishing the $^{13}C/^{12}C$ and $^{18}O/^{16}O$ ratios of CO_2 is not without difficulty, because, as we will see, information on the $^{17}O/^{16}O$ ratio has to be assumed.

2.5. Mass-Independent Isotope Fractionation, MIF

The expression "mass-independent fractionation", abbreviated "MIF", is frequently used, but as will become clear later on, the concept is an oxymoron. Oxygen is the most abundant planetary element and possesses three stable isotopes. Because ^{17}O is less abundant than ^{18}O, and because most mass spectrometric measurements were based on the analysis of CO_2 (instead of O_2), in which mass 45 represents both ^{13}C- and ^{17}O-substituted CO_2 ($^{13}C^{16}O^{16}O$ and $^{12}C^{17}O$-^{16}O), and also because the theories of mass-dependent isotope effects, be it equilibrium or kinetic isotope effects, predict the variations in ^{17}O to be half as large as those in ^{18}O, ^{17}O was usually not analyzed at all. As early as 1973, however, Clayton et al.[11] found deviations for the Allende meteorite, which were attributed to nucleosynthetic processes. Notwithstanding, Thiemens and Heidenreich[12] discovered, in a simple experiment of producing ozone using an electrical discharge, that the degree of fractionation for ^{17}O was not half of that of ^{18}O. They found that $\delta^{17}O \approx \delta^{18}O$, contrary to the well-established theoretical framework, and contrary to experience with geological materials.

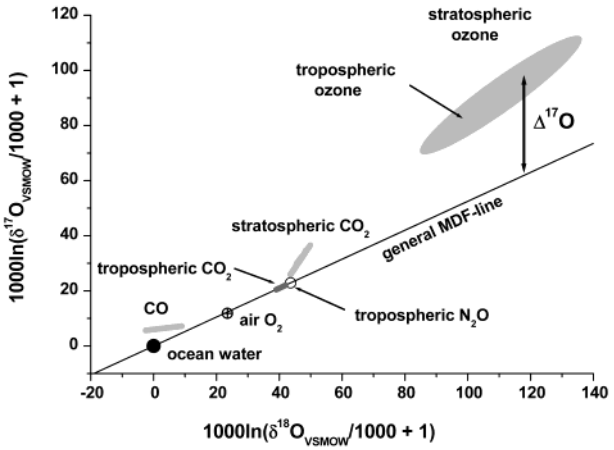

Figure 1. Schematic picture of the general mass-dependent relationship with $\ln(1 + \delta^{17}O)$ plotted against $\ln(1 + \delta^{18}O)$ using V-SMOW as reference. For small δ values, or as a general approximation, at times $\delta^{17}O$ is plotted directly against $\delta^{18}O$. The typical compositions for V-SMOW representing ocean water, atmospheric oxygen, CO, N_2O (arrow tip), stratospheric CO_2, and tropospheric and stratospheric O_3 are shown as a general guide.

The theoretical explanation of this effect in O_3 (the nonadherence to the common mass-dependent fractionation pattern), and likewise the laboratory experiments required to unravel the ozone system, would prove to be a major challenge indeed, and the nearly identical behaviors of ^{17}O and ^{18}O in ozone led to concepts and identifiers related to "symmetry", or "non-mass-dependent fractionation" (NOMAD), or more simply "mass-independent fractionation" (MIF), or just "anomalous".

For brevity, we will use the rather common expression MIF (MIF signature, MIF process, MIF effects) to indicate all deviations from the strict mass dependence (MDF) of which the theoretical foundations are well documented in the literature (we give a brief example below). The use of the unfortunate abbreviation MIF is not meant to imply that the isotopic fractionation is independent of the mass, which would leave only symmetry effects or nuclear spin, shape, or size effects as the possible causes for isotope fractionation in these cases.

A deviating composition for a certain compound may be due to a fundamental process hitherto not acknowledged, or due to a combination of several factors. Laboratory experiments should shed light on the reactions and mechanisms, but from many experiments it has been difficult even to find the exact origin, or reaction step, where the effect occurs.[4] Many different "slopes" and intersects have been recorded and discussed, often without being able to make fundamental progress. Thus, much work on MIF is currently at an exploratory stage, except perhaps for the systematic work conducted for the ozone reaction schemes.

As stated, the standard theories of isotope fractionation in equilibrium and kinetic conditions predict that the fractionation for ^{18}O is twice that for ^{17}O, and Figure 1 shows the concordant "mass-dependent" fractionation line. Analyses of the $^{17}O/^{16}O$ and $^{18}O/^{16}O$ ratios of nearly all oxygen-bearing terrestrial materials follow this relationship, with

small systematic differences depending on the actual fractionation processes involved. Striking is the phenomenon that several oxygen-bearing atmospheric trace gases show significant and even large deviations from it. Is this solely due to O_3 chemistry? There actually may be relatively few cases of MIF in atmospheric trace gases that are not due to its presence in O_3, as we will see later on.

The theories for mass-dependent behavior in fractionation which all yield a slope of about 0.5 are documented in the literature. Here we give the reader a little example, namely the isotope fractionation differences caused by the different diffusion coefficients (^{16}D, ^{17}D, and ^{18}D) for $H_2{}^{16}O$, $H_2{}^{17}O$, and $H_2{}^{18}O$ in air. The diffusion constants are proportional to the inverse of the square root of the reduced masses (basically with all molecules having the same kinetic energy, such that the translational speed—and with that the speed of diffusion—is proportional to the square root of the inverse of the reduced mass). Thus, looking at the three fluxes of isotopic molecules diffusing through air from a large well-mixed reservoir, the fractionation constants $^{17}\alpha$ and $^{18}\alpha$ are given by $^{16}D/^{17}D$ and $^{16}D/^{18}D$, respectively. For example, using mass 29 for air, we find

$$^{17}\alpha = (19/18)^{0.5}(47/48)^{0.5} = 1.01664 \quad \text{and}$$

$$^{18}\alpha = 1.03235$$

The relationship between the delta values (relative to the original vapor) of the emerging vapor is given by the ratio of the fractionation constants $^{17}\epsilon/^{18}\epsilon$, with $\epsilon = \alpha - 1$. Thus, the mass-dependent fractionation has a "slope" of 0.5144. By using different bath gases, one can see the changes in the mass-dependent behavior. For other isotope effects, the same proportionality to the inverse masses appears, thus invariably giving slopes close to 0.5 when the isotopic masses differ by one unit each. The derivation of the slope 0.5144 given here serves as an example only. Later we will show a more rigorous approach.

The deviations from the MIF line were initially expressed as $\Delta^{17}O \equiv \delta^{17}O - 0.5\delta^{18}O$. This gives a quick measure of MIF, i.e., basically the excess or deficiency in ^{17}O. The first problem is that the slope is not exactly 0.5. For certain compounds the mass-dependent slope has been established by analyzing samples from a wide range of origins. The simplest example is H_2O, for which $\delta^{18}O$ varies widely in meteoric waters, and indeed the $^{17}O-^{18}O$ relationship for meteoric waters forms a compact mass-dependent relationship.[13]

It is essential to note that, for the simple physical processes that fractionate H_2O, the theoretical values can, in principle, be accurately calculated. This is not so for most other processes. The ab initio calculation of isotope effects and the calculations using spectroscopic information are extremely difficult and do not always provide accurate results. The corollary to this is two-fold. Foremost, we rely on experimental data, i.e., measurements of isotopic composition for ^{17}O and ^{18}O to establish the exact mass-dependent relationship. Second, the occurrence of MIF can only be established for elements with three or more isotopes, and oxygen is the prominent case.

In light of this, we can revisit Figure 1 with different eyes and wonder what the basis for the mass-dependent line is. Without actually knowing the various underlying oxygen isotope fractionation processes, the mass-dependent relationship can only be an approximation; it may be compound- and process-specific. Therefore, the question posed in the Introduction, "what atmospheric chemistry can do for isotope research", can be answered. By first discovering MIF for ozone, and subsequently developing an increasingly quantitative approach, atmospheric chemistry provides an excellent framework for discovering new effects and testing new theories concerning isotope fractionation.

Next, we follow a more rigorous approach to deriving the relationship between $\delta^{17}O$ and $\delta^{18}O$ and apply it for equilibrium isotope effects, which leads to the following expression for the mass dependence:[13]

$$^{17}R/^{17}R_{st} = (^{18}R/^{18}R_{st})^{\beta} \quad \text{or}$$

$$\delta^{17}O + 1 = (\delta^{18}O + 1)^{\beta} \quad \text{or}$$

$$\ln(\delta^{17}O + 1) = \beta \ln(\delta^{18}O + 1)$$

This results in the approximation $\delta^{17}O \approx \beta\delta^{18}O$, in which the δ values are expressed in per mil.

It is on this basis that the degree of MIF is defined as $\Delta^{17}O \equiv \delta^{17}O - \beta\delta^{18}O$. The exact value of β depends on the process involved, and detailed analyses are given by Young et al.,[14] Matsuhisa et al.,[15] and Miller.[16] For meteoric waters, a value of 0.5281 was found.[13] This value is very precise but higher than other reported values. More sophisticated definitions or expressions for $\Delta^{17}O$ are currently in use.[16−18] We also refer to the section about N_2O, but a detailed discussion of the properties and the different definitions is beyond the scope of this work.

At this stage, it is clear that understanding the cause or causes of MIF at the molecular level is important and requires new theoretical work. For atmospheric applications, MIF provides in several instances a useful tracer or marker of certain processes. We emphasize that MIF is a special isotopic signature that cannot be erased or corrupted easily by mass-dependent (normal) fractionation. Thus, once a given pool of a trace substance has become "labeled" by MIF, normal isotope fractionation cannot, in most cases, erase this anymore. Referring to Figure 1, once the isotopic composition deviated from the mass-dependent fractionation line, normal fractionation caused only movements almost parallel to the line. For instance, if one extracts O_3 from air—which is a difficult process—and fractionation would occur due to nonquantitative trapping, the MIF signature would hardly be affected. Dilution and isotopic exchange do, however, directly reduce the degree of MIF and bring the respective substance gradually back to the mass-dependent fractionation line. We once more stress that there are small differences in the slope for mass-dependent fractionation. Thus, when substances are fractionated to a high degree following a slightly different slope, the

end product may be conceived as having a mass-independent composition, although the underlying process is mass-dependent.[14] The subtle differences between various processes related to the biosphere have been confirmed by Angert et al.[19]

Finally, we note that MIF as such alludes to one or more processes, several of which are not known yet. Basically, when the $^{17}O/^{16}O$ ratio of a given compound does not reflect its $^{18}O/^{16}O$ ratio as expected from the mass-dependent fractionation relationship, which has a slope of about 0.5, we can only infer that this compound has a mass-independent composition, which for convenience will be referred to as MIF.

Measurement of both ^{17}O and ^{18}O is necessary to determine MIF. For oxygen, isotope ratio mass spectrometry can be applied directly, using masses 32, 33, and 34. For water samples, the water can be electrolyzed to give O_2, which turns out to be rather difficult for routine measurement (H. Meijer, personal communication, 2002). Standard is the treatment of H_2O with BrF_5, and on-line techniques exist as well. For CO_2 gas, the widespread method of direct mass spectrometry using masses 44, 45, and 46 does not provide ^{17}O information because of the effect of the more abundant ^{13}C on the common mass 45. Therefore, treatment with BrF_5 to release O_2 is applied. This technique has been brought to perfection by Thiemens and co-workers. Brenninkmeijer and Röckmann[20] used a sapphire reactor to first convert CO_2 into CH_4 and H_2O using a nickel catalyst. Subsequently, the H_2O is reacted to O_2 using a mixture gas of 5% or 10% F_2 in He, which is usually applied for laser systems. This method avoids the use of the dangerous BrF_5. Assonov and Brenninkmeijer[21] developed an alternative $\Delta^{17}O$ method based on very precise measurement of CO_2 (masses 44, 45, and 46), followed by exchanging the oxygen atoms in the CO_2 using purified CeO_2 powder at 700 °C. After this exchange, the CO_2 is analyzed once more, and the change in mass 45 reflects the change in the ^{17}O content. This method is robust and safe, but the precision is intrinsically limited to 0.3‰ at its best. In the case of N_2O, simple thermal decomposition to N_2 and O_2 can be used without subsequent cryogenic[22] or gas chromatographic[23] separation of N_2 and O_2 followed by isotope ratio mass spectrometry of the O_2 isotopologues.

3. Ozone

Ozone is of great importance for the chemistry of the atmosphere, and its pronounced isotopic signature affects that of a host of other trace constituents. The gas-phase reaction that leads to the formation of the ozone molecule shows a large and unique kinetic isotope effect. After a short introduction into the atmospheric chemistry of ozone, we will first present laboratory and theoretical work on isotope fractionation in ozone formation and dissociation processes and then review atmospheric observations of isotope enrichments in ozone. It has been attempted to completely cover relevant atmospheric, laboratory, and theoretical investigations. However, experiments on ozone decomposition, which involve condensed phases of ozone or thermal decomposition, are not in the context of this review. Also, very early theoretical explanations for the origin of the ozone isotope effect are not reviewed. In the text and tables, experimental uncertainties are cited at a 95% level of confidence.

3.1. Kinetic Considerations

The first evidence for an anomalous isotope composition of ozone came from stratospheric observations,[24] and—as will be reviewed later—it is now firmly established that atmospheric ozone indeed carries a unique isotope signature. Atmospheric processes which could possibly lead to the redistribution of oxygen isotopes in ozone thus deserve special attention.

Chapman[25] suggested that ozone in the atmosphere is formed in the three-body recombination reaction,

$$O + O_2 + M \rightarrow O_3 + M \quad (1)$$

This is the principal ozone-forming reaction at nearly all altitudes up to 50 km, above which electronically excited oxygen or ion−molecule reactions may contribute.[26] It is commonly assumed that reaction 1 proceeds according to the energy-transfer mechanism, which consists of three elementary steps:

$$O + O_2 \rightarrow (O_3)^* \quad (1a)$$

$$(O_3)^* \rightarrow O + O_2 \quad (1b)$$

$$(O_3)^* + M \rightarrow O_3 + M \quad (1c)$$

In an association step (1a), a vibrationally excited molecule $(O_3)^*$ is formed which may either dissociate back to the reactants (1b) or, by collision with an inert molecule (1c), form stable ozone. In the presence of isotopes, the above scheme needs to be modified inasmuch that an excited XYZ* molecule may decompose into several product channels, such as XY + Z, X + YZ, and Y + XZ. Experimental evidence shows[27,28] that the third channel may be neglected. Since ozone formation kinetics under atmospheric and most laboratory conditions is well in the low-pressure range,[29] the isotope association (1a) and dissociation (1b) dynamics lead to oxygen isotope-exchange reactions, e.g.,

$$^{18}O + {}^{16}O_2 \leftrightarrow {}^{16}O + {}^{16}O^{18}O \quad (2)$$

$$^{17}O + {}^{16}O_2 \leftrightarrow {}^{16}O + {}^{16}O^{17}O \quad (3)$$

which are rapid compared to ozone formation. These isotope exchange reactions contribute to the observed isotope enrichments in ozone, because they determine the relative abundance of O atoms with ^{17}O and ^{18}O being always lower than statistically expected.[30,31] Apart from these atom abundance effects, which are governed by equilibrium thermodynamics,[32,33] the isotope abundance in ozone is additionally determined by the kinetic isotope effects of ozone formation. These will be reflected by isotope-dependent

third-order rate coefficients for individual formation reactions, e.g.,

$$^{16}O + ^{16}O_2 + M \rightarrow ^{16}O_3 + M \quad (4)$$

$$^{18}O + ^{16}O_2 + M \rightarrow ^{16}O_2{}^{18}O + M \quad (5)$$

$$^{16}O + ^{18}O_2 + M \rightarrow ^{16}O^{18}O_2 + M \quad (6)$$

$$^{18}O + ^{18}O_2 + M \rightarrow ^{18}O_3 + M \quad (7)$$

Besides ozone formation, ozone decomposition processes may also influence the isotopic composition of atmospheric ozone, and the study of isotope effects in the decomposition pathways may add insight into ozone chemistry. The relative importance of formation and decomposition processes for the isotopic composition of ozone may be readily inferred from considering the essentials of stratospheric ozone chemistry.

Ozone formation in the stratosphere is due to photolysis of O_2. Product atoms then react with O_2 to form ozone according reaction (1). Within typical time scales of less than 1000 s, ozone is photolyzed[34] into singlet or triplet oxygen species:

$$O_3 + h\nu \rightarrow O(^1D) + O_2(^1\Delta_g) \quad (8)$$

$$O_3 + h\nu \rightarrow O(^3P) + O_2(^3\Sigma_g) \quad (9)$$

Since the main fate of $O(^1D)$ is immediate quenching by N_2 or O_2, photolysis of ozone essentially leads to $O(^3P)$ product atoms which again recombine with O_2 via reaction (1). While these rapid interconversion reactions in the stratosphere do equilibrate $O(^3P)$ with O_3, the ozone budget is fixed by the following direct sink reaction for odd oxygen, $O_x = (O(^3P), O_3)$,

$$O + O_3 \rightarrow 2O_2 \quad (10)$$

and other catalytic reactions, which convert odd into even oxygen. In the middle and upper stratosphere, 10−20% of the total ozone loss rate is due to reaction (10), and the remaining part is due to three other processes, commonly referred to as the ClO_x, NO_x, and HO_x cycles.[35]

The fact that cycling within the O_x reservoir is fast as compared to source or sink reactions for the odd-oxygen species[35] severely limits the reaction pathways that are able to produce significant isotope fractionation in ozone. Compared to fractionation in ozone formation (1) or photolysis (8, 9), kinetic fractionation in the odd-oxygen sink reactions will contribute little to the isotopic composition of ozone because the rates of these processes are at least 1 or 2 orders smaller than the rate of the odd-oxygen cycling reactions: typical ratios for odd-oxygen loss rates over ozone photolysis rates are between 1/50 and 1/400.[36]

As was recognized already in 1983, the photolysis of molecular oxygen may be ruled out as a source of fractionation in ozone. The rapidity of the $O + O_2$ isotope exchange (2, 3) will dilute any such isotope effect on the oxygen atoms within the large reservoir of oxygen molecules.[30] Isotopic fractionation of excited species $O(^1D)$ and $O_2(^1\Delta_g)$ with respect to $O_2(^3\Sigma_g)$ will also not affect the ozone isotope composition. The rates of reaction with ozone are too slow under stratospheric conditions.[37,38]

On the basis of the commonly accepted atmospheric kinetic processes, only the formation (1) and the destruction reactions (8) and (9) can have a significant impact on the isotope composition of ozone. Consequently, both formation and dissociation processes have been studied intensively in the laboratory.

3.2. Laboratory Studies on Ozone Formation

A large variety of laboratory experiments to study the isotope composition of ozone after production from molecular oxygen have been reported. In the first generation of experiments, ozone was converted into molecular oxygen for mass spectrometric analysis.[39−45] Investigations focused on the different kinds of ozone formation techniques (electric and microwave discharge, UV dissociation of oxygen, visible light recycling of ozone) as well as on the effects of pressure and temperature.[39−47] Later, multi-isotope composition analysis of ozone became available through direct measurement of ozone isotopologues in molecular beam mass spectrometers.[48−50] This technique substantially extended the observations from three to ten isotopologues. Additional information about the process of ozone formation has been inferred from symmetry-selective detection techniques, which comprise mid-IR tunable diode laser absorption spectroscopy, microwave spectroscopy, and far-IR Fourier transform spectroscopy.[27,28,51−55]

A new era in ozone isotopomer research started when the attempt was made to investigate individual reaction channels.[56−58] These experiments have been extended to a set of 15 out of 36 possible rate coefficients,[31] and their dependence on pressure,[59] third-body collision partner,[60] and temperature[61] has been investigated such that detailed comparison with recent theoretical modeling[62−73] has become possible.

3.2.1. Ozone Formation—Natural Oxygen

As was only recognized several years later,[74] the laboratory experiment to study the isotope effect in ozone formation was given in two simultaneous papers[12,39] by Heidenreich and Thiemens in 1983. Ozone was produced by an electric discharge in oxygen, with part of the reactor being immersed into liquid N_2, and both $\delta^{17}O$ and $\delta^{18}O$ values were measured for different degrees of oxygen-to-ozone conversion. Maximum ozone enrichments, corresponding to conversion degrees <30%, were 3.90 ± 0.06% and 4.00 ± 0.02% for ^{17}O and ^{18}O, respectively. In a three-isotope plot ($\delta^{17}O$ vs $\delta^{18}O$), a slope of 1.00 ± 0.02 is reported for the oxygen isotope composition of product ozone together with leftover oxygen. This dataset provided the first and fundamental observation that ^{17}O and ^{18}O isotopes may have equal enrichments within a chemical setting. It has been attempted to explain these data on the basis of a single kinetic fractionation mechanism.[4] The lack of a tight correlation between reaction

extent and fractionation data,[39] however, renders this approach questionable.

In a follow-up study, the pressure dependence of this effect in pure oxygen and in an oxygen−helium mixture was investigated.[40] Again, ozone formation was initiated by electron impact dissociation of oxygen, and the product ozone was immediately condensed. The δ values of ozone were reported relative to the residual oxygen reservoir for degrees of oxygen-to-ozone conversion varying between 1.5% and 25%. They agree in magnitude with the first results[39] at sufficiently high pressures. For oxygen pressures below 3 Torr, ozone was found to be depleted, and the corresponding $\delta^{17}O$ and $\delta^{18}O$ values showed deviations from the 1:1 correlation.

An explanation was provided by Bains-Sahota and Thiemens,[41] who extended the database to an even lower pressure range (20 mTorr $\leq p \leq$ 62 Torr) using a microwave discharge flow reactor experiment. Between 0.216 and 5.0 Torr, a pressure-independent depletion of ^{17}O and ^{18}O of ca. −4.0% and −7.0%, respectively, was observed. Toward lower pressures, the depletion became less pronounced, whereas at higher pressures, ^{17}O and ^{18}O in ozone were enriched by as much as 8.2% and 10.1%, respectively. Heterogeneous wall reactions have been suggested to explain the isotope signature of depletion, and it was argued that oxygen atom diffusion could be the rate-limiting step in ozone formation at low pressures, because the diffusional time constants for ^{18}O vs ^{16}O would differ by about 6% and therefore could almost account for the observation of heavy isotope depletion by −7.0%.[41] While later experiments have added support to the hypothesis of a heterogeneous ozone formation reaction,[28,45] the details of this process have not yet been firmly established. In particular, O atom diffusion may only account for −2%, since it must be expected that about one-third of heavy ozone ($^{16}O_2{}^{18}O$) will be formed in the heavy-atom reaction $^{18}O + {}^{16}O_2$, whereas two-thirds of the heavy molecules come from $^{16}O + {}^{16}O{}^{18}O$.

Using UV dissociation of molecular oxygen, Thiemens and Jackson investigated the isotope signature of ozone in a series of experiments.[42−44] In the first set of these experiments,[42] small reaction volumes were employed (3 cm diameter). The samples were kept at liquid N_2 temperatures, with the exception of a region close to a MgF_2 window. Comparison with room-temperature data obtained in the second set of experiments, performed in a spherical 5-L volume,[43] shows that the high-pressure data of the first series, with $\delta^{18}O \approx 9.0\%$, presumably resulted from oxygen photolysis close to the entrance window. The low-pressure regime is characterized by decreasing enrichment values with decreasing pressure and indicates contribution from wall reactions.[43] In the 5-L experiment, the pressure was varied between 2.1 and 760 Torr, and the reaction chamber was either kept at liquid N_2 temperatures or was not cooled at all.[43] Fractionation values for the cooled reactor were typically 1−2% lower than those for the room-temperature reactor. The high-temperature data are reproduced in Figure 2. In an intermediate range between 160 and 450 Torr, one finds $\delta^{17}O \approx 9\%$ and $\delta^{18}O \approx 10\%$. Above 450 Torr, a modest decrease in enrichments is observed, but at pressures smaller than 160 Torr an increase in the δ values is found. From a three-isotope plot, secondary isotope effects are inferred for this low-pressure region.[43] The slope of 0.515 in this data subset could indicate either photolytic ozone decomposition[43] or evaporative fractionation effects, which should become more pronounced at small sample sizes. Possibly the combination of both effects could have led to the peak value of $\delta^{18}O = 14.3\%$. Since no active temperature control mechanism is mentioned in this and the follow-up study,[43,44] it is unclear how much the oxygen gas and parts of the reaction chamber were heated by the incident radiation. In the final series of experiments, the pressure range was significantly extended toward the high-pressure region.[44] Oxygen photolysis was carried out at pressures between 0.8 and 87 atm. The key observation of this study was that the isotope enrichment disappeared at pressures around 55 atm, well below the falloff pressure of ozone formation.[29]

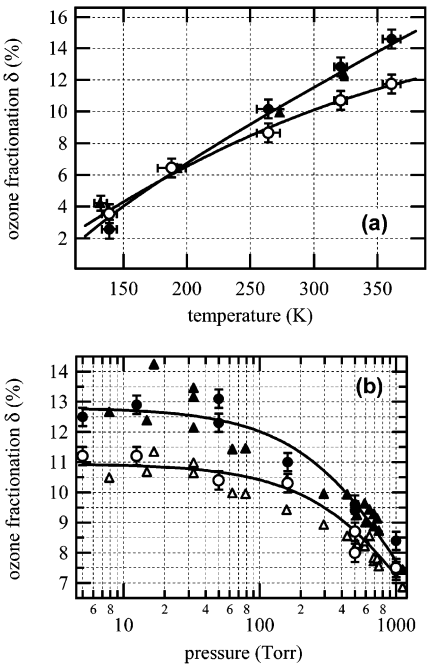

Figure 2. Temperature and pressure dependence of oxygen fractionation in $^{16}O_2{}^{17}O$ (open symbols) and $^{16}O_2{}^{18}O$ (solid symbols) which is formed in pure oxygen or air. (a) δ values for temperatures between 130 and 360 K. Circles from ref 45 at a constant oxygen pressure of 50 Torr, triangles from ref 61 at 45 Torr. Values were obtained by reading data points in Figure 3,[45] and dividing them into five groups, which were then averaged. The error bars denote 2σ statistical uncertainties, which are consistent with the scatter of the data points. Best-fit curves are from ref 61. (b) δ values between 5 and 1000 Torr. Circles represent data from ref 45 at a constant temperature of 321 K with 2σ uncertainty as reported. Best-fit curves to the data of ref 45 are obtained by using the model suggested in ref 59. Triangles are measurements performed under room-temperature conditions from refs 43 and 44. No error bars were added to the latter data since the scatter seems to be larger than the reported precision of 0.10%.

Morton et al.[45] designed a photolysis recycling experiment to measure oxygen isotope fractionation in the ozone formation process under temperature and pressure control. Visible light photolysis of ozone

in an oxygen bath gas of known isotopic composition served as the source of oxygen atoms. Through rapid isotope exchange reactions (2, 3), the atoms equilibrate with the molecular oxygen and re-form ozone molecules according to reaction (1). In this way, ozone is photolytically recycled and acquires an isotopic composition which depends only on the bath gas composition and the isotope fractionation mechanisms in the formation as well as in the photolytic destruction of ozone.

Large temperature-dependent enrichments at a constant oxygen pressure of 50 Torr were observed. Delta values increase from $\delta^{17}O = 3.6 \pm 0.6\%$ and $\delta^{18}O = 2.6 \pm 0.6\%$ at 130 K to $\delta^{17}O = 11.7 \pm 0.6\%$ and $\delta^{18}O = 14.6 \pm 0.6\%$ at 361 K. The pressure dependence has been characterized at 321 K between 5.0 and 1000 Torr. Enrichment values of $\delta^{17}O = 11.2 \pm 0.6\%$ and $\delta^{18}O = 12.9 \pm 0.6\%$ have been found in the low-pressure regime, and they decrease to $\delta^{17}O = 7.5 \pm 0.6\%$ and $\delta^{18}O = 7.9 \pm 0.6\%$ at 1000 Torr. Results of these measurements are reproduced in Figure 2. They agree with earlier measurements[43] of the pressure dependence using UV photolysis of oxygen as an atomic oxygen source. Further, a rationale is given for why the first experiment of Heidenreich and Thiemens[39] resulted in $\delta^{17}O/\delta^{18}O = 1$, with a maximum $\delta^{18}O$ value of only 4%. The combination of liquid N_2 cooling along with the glowing discharge has most likely led to effective gas temperatures between 150 and 200 K, where $\delta^{18}O$ values almost equal $\delta^{17}O$ values and fall between 3.8% and 6%.

The most important aspect is perhaps that large enrichments of ^{17}O and ^{18}O in ozone were observed in an experiment in which the oxygen chemistry involved constituents exclusively in their electronic ground states. The anomalous fractionation must therefore be attributed to the elementary kinetic process of ozone formation. Blank experiments assured that wall and other possible interfering reactions had minor effects. A direct measurement of the fractionation factor of visible light photolysis was not performed, but the authors checked whether the combined effect of ozone photolysis, $O_3 + h\nu \rightarrow O_2 + O$ and $O + O_3 \rightarrow 2O_2$, would change the isotopic composition of ozone. No such effect was found.

The dataset of Morton et al.[45] is a useful reference for atmospheric and laboratory studies, because with the exception of possible fractionation effects in the broadband photolysis of ozone, all chemical and physical parameters like pressure and temperature are well characterized. Because of the reference temperature of 321 K in the pressure dependence study, a correction for atmospheric temperatures needs to be applied. Since the temperature dependence (Figure 2a) has been measured at 50 Torr, the values in the low-pressure plateau may be easily corrected using this curve. For higher pressures, the same correction should still apply, at least for $^{16}O_2{}^{18}O$. This is due to the observation that the pressure dependence[59] of the enrichment is determined by the rate of reaction $^{16}O + {}^{16}O^{18}O$, whereas the temperature dependence[61] of the enrichment comes from the isotope exchange equilibrium (2) and from the pressure-independent rate $^{18}O + {}^{16}O_2$ (see section 3.4). Assuming the same correction for ^{17}O-containing ozone, $\delta^{17}O = 7.2 \pm 0.6\%$ and $\delta^{18}O = 7.6 \pm 0.6\%$ are predicted for 298 K and 760 Torr. It may be observed that the experiments of Thiemens and Jackson[43,44] predict higher enrichments for room-temperature and normal-pressure conditions. The exact gas temperature in these measurements, however, may significantly deviate from the stated value for two reasons. First, there is good agreement with the Morton et al. data,[45] which were measured at 321 K (see Figure 2b), and second—similar to the Morton et al. experiment—a strong light source has been used which most likely has led to additional heating.

3.2.2. Ozone Formation—Enriched Oxygen

It was recognized early on that additional information about the unusual isotope effect in ozone might be obtained from the study of ozone formation in heavily enriched oxygen,[46,47] because not virtually exclusively singly substituted ozone isotopologues, such as $^{16}O_2{}^{17}O$ and $^{16}O_2{}^{18}O$, would be formed. The first attempt to study this was described by Yang and Epstein, who formed ozone from oxygen with varying isotope compositions. An electric discharge in a fused silica container immersed in liquid N_2 was used to generate the ozone.[46] Isotope analysis was done on molecular oxygen which has been obtained from the product ozone after chemical conversion. While the measurements on atmospheric oxygen produced results similar to those of the experiment of Heidenreich and Thiemens,[39] it was observed that the results depended on the isotope composition of the oxygen bath. Ozone from highly enriched oxygen gas was depleted in the heavy isotopes, and a shift from 1 to 0.5 in the slope in a three-isotope diagram was observed.[46] It is, however, not commonly recognized[4,46,47,62] that conversion of ozone into oxygen destroys the desired information. While for a small fraction of heavy isotopes, mass balance requires to a high degree of approximation that, e.g., $\delta^{18}O(O_3) = \delta^{18}O(O_2$ after conversion from $O_3)$, a similar one-to-one relation cannot hold for ozone from heavily enriched oxygen, because ten ozone isotopologues are converted into only seven isotopologues of molecular oxygen.

A successful measurement of ozone isotopologue formation from heavy oxygen therefore requires direct analysis of ozone. Using a molecular beam mass spectrometer,[75] Morton et al.[48] measured ozone which has been formed in an electric discharge experiment. Later, Mauersberger et al.[49] improved the measurement by using a more refined calibration technique in combination with photolysis recycling of ozone. The isotopologue fractionation E in multi-substituted molecules is commonly expressed as

$$1 + E = \frac{([^{16}O_l\ {}^{17}O_m\ {}^{18}O_n]/[^{16}O_3])_{obs}}{([^{16}O_l\ {}^{17}O_m\ {}^{18}O_n]/[^{16}O_3])_{stat}}, \quad l + m + n = 3 \quad (11)$$

where the index "obs" stands for the observed isotopologue ratio in ozone and "stat" means the same ratio as statistically calculated from the composition

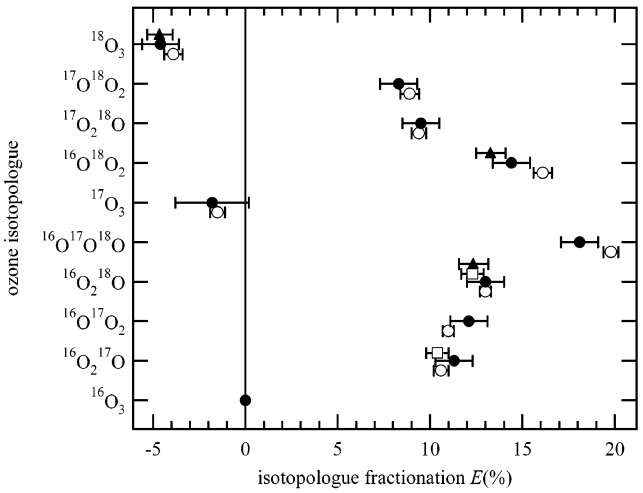

Figure 3. Multi-isotopologue fractionation in ozone around room temperature. Shown are the results from photolysis recycling experiments. Open circles, Mauersberger[49] at 321 K; solid circles, Wolf et al.[50] at 300.5 K; open squares, Morton et al.[45] at 321 K; and filled squares, Janssen et al.[61] at 320 K.

the scrambled oxygen gas. Assuming that o, p, and q are the fractions of ^{16}O, ^{17}O, and ^{18}O in molecular oxygen, then $o + p + q = 1$, and the statistical ratio can be calculated according to

$$([^{16}O_l\,{}^{17}O_m\,{}^{18}O_n]/[^{16}O_3])_{\mathrm{stat}} = \frac{6}{l!m!n!}\,o^{l-3}p^m q^n \quad (12)$$

The results of these investigations are displayed in Figure 3 and may be summarized as follows. Homonuclear ozone isotopologues are depleted in a standard fashion, with $^{18}O_3$ being depleted most (−4.6%). Heteronuclear molecules are strongly enriched, and the highest enrichment of about 18% resides in $^{16}O^{17}O^{18}O$. All other isotopologues are about two-thirds as much enriched as $^{16}O^{17}O^{18}O$. The data on $^{16}O_2{}^{17}O$ and $^{16}O_2{}^{18}O$ agree particularly well with measurements in natural oxygen[45] and thus confirm that the ozone isotope effect is independent of the isotope composition of the oxygen.[49] These earlier measurements have now been substantiated,[50,61] even though it appears that the particular multi-isotope study by Wolf et al.[50] shows a tendency toward higher values when compared to the temperature-dependent measurements using natural[45] and ^{18}O-enriched[61] oxygen (Figure 3). It is noteworthy here that the depletion of the homonuclear molecules almost follows the prediction[30] from isotope equilibrium thermodynamics (compare section 3.1), whereas the strong enrichments of the heteronuclear species require a kinetic effect.

The multi-isotope measurements have suggested that molecular symmetry could play the dominating role in ozone isotopologue formation,[76] which was later shown to be misleading.[58] Interestingly, though, the results may provide a qualitative explanation for the observations of Yang and Epstein when the contributions of equilibrium and kinetic effects in ozone formation are considered separately:[46] assuming that the conversion of ozone into molecular oxygen occurs in a statistical manner, and noting that the ozone isotopomer distribution due to kinetic fractionation is almost symmetric under complete isotope substitution ($E(^{16}O^{18}O_2) \approx E(^{16}O_2{}^{18}O)$, $E(^{18}O_3) \approx 0$ etc.), it may be observed that, for ozone from a ^{16}O:^{18}O = 1:1 mixture, $^{16}O^{18}O$ will not be enriched over $^{16}O_2$. To a first-order approximation, the kinetic effect shown in Figure 3 will therefore be annihilated in the molecular oxygen. Since the original experiments have been performed at low temperatures, however, the effect of the isotope exchange, favoring the formation of light ozone molecules in a standard mass-dependent way, was more pronounced than depicted in Figure 3. Consequently, a shift toward depletion in $^{16}O^{18}O$ and decreasing slope values are expected when ozone from heavily enriched oxygen mixtures is analyzed after conversion into molecular oxygen.

3.2.3. Symmetry-Selective Detection

To explore the aforementioned role of symmetry in the ozone formation process, both mid- and far-IR absorption spectroscopic techniques have been used. Branching ratios in individual ozone formation reactions as well as the relative abundance of asymmetric vs symmetric species of a single ozone isotopologue, e.g., $r_{50} = [^{16}O^{16}O^{18}O]/[^{16}O^{18}O^{16}O]$ from scrambled oxygen could thus be studied. Anderson et al.[51] employed tunable diode laser absorption spectroscopy (TDLAS) in the ν_3 band to measure r_{50} in ozone that had been formed from slightly enriched ($^{18}O/^{16}O \approx$ 3%) oxygen at two different temperatures: $r_{50} = 2.187 \pm 0.022$ and 2.274 ± 0.031 were found for low- and high-temperature ozone, respectively. Due to the rather large and systematic uncertainty in individual line strengths, the indicated statistical uncertainties may severely underestimate the experimental accuracy. Therefore, a differential technique was developed, which relies on the change of symmetry-specific enrichments,

$$1 + a = \frac{([^{16}O^{16}O^{18}O]/[^{16}O_3])_{\mathrm{obs}}}{([^{16}O^{16}O^{18}O]/[^{16}O_3])_{\mathrm{stat}}} \quad \text{and}$$

$$1 + s = \frac{([^{16}O^{18}O^{16}O]/[^{16}O_3])_{\mathrm{obs}}}{([^{16}O^{18}O^{16}O]/[^{16}O_3])_{\mathrm{stat}}}$$

with temperature. With temperature increasing from low (l) to high (h), robust changes in a and s were obtained: $\Delta a = a_{\mathrm{h}} - a_{\mathrm{l}} = 0.084 \pm 0.013$, and $\Delta s = s_{\mathrm{h}} - s_{\mathrm{l}} = 0.035 \pm 0.016$. Interestingly, the results seem to imply that some enrichment resides in the symmetric species and that the asymmetric isotopomer carries an enrichment that is about $\Delta a/\Delta s = 2.4 \pm 1.2$ as large as the enrichment in the symmetric molecule.

In another series of experiments, Larsen and coworkers employed far-IR spectroscopic techniques to obtain the branching ratios for the $^{18}O + {}^{16}O_2$ and $^{16}O + {}^{18}O_2$ reaction,[27,54] as well as the ratios r_{50} and $r_{52} = [^{16}O^{18}O^{18}O]/[^{18}O^{16}O^{18}O]$.[27,52−55] The results of a microwave study of ozone isotopomers after photolysis of $^{16}O_3$ in a bath of $^{18}O_2$ could be compared with kinetic modeling. In this way, an upper limit of 5% was derived for the fraction γ of symmetric molecules

from the reactions $^{16}O + {}^{18}O_2$ and $^{18}O + {}^{16}O_2$.[27,54] This demonstrates that ozone is predominantly formed in end-on association reactions that preserve the symmetry of the intermediate. Later, these observations were confirmed by TDLAS, and more accurate values of $\gamma_{8+66} = 0.7 \pm 1.0\%$ and $\gamma_{6+88} = 1.8 \pm 0.8\%$ were reported for reactions $^{18}O + {}^{16}O_2$ and $^{16}O + {}^{18}O_2$, respectively.[28]

Far-IR experiments were successively improved[52,53,55] to find significant deviations in r_{50} from the value of 2. The most recent and accurate values, however, are $r_{50} = 1.99 \pm 0.02$ and $r_{52} = 2.51 \pm 0.04$ for ozone that was formed by an electric discharge in an $^{16}O-{}^{18}O$ mixture in a small reactor cooled by liquid N_2.[55] While the large value of r_{52} was found to agree with the results of kinetic measurements,[58,77] the statistical ratio between $^{16}O^{16}O^{18}O$ and $^{16}O^{18}O^{16}O$ was interpreted to be in conflict with earlier experiments[28,77] which imply $r_{50} > 2$. The ozone of the seemingly conflicting TDLAS measurements[28] which indeed did have a larger value ($r_{50} = 2.128 \pm 0.020$) was, however, generated around 360 K.[78]

Because of the large differences in the ozone formation temperatures, the results for r_{50} do not actually imply a discrepancy between the mid- and far-IR measurements. The measurements reported by Anderson et al.[51] already showed that r_{50} decreases with decreasing temperatures. Qualitatively, this behavior is also expected from temperature-dependent mass spectrometric studies[61] and from the temperature dependence of the isotope exchange reactions.[57] More quantitative experiments that monitor both the relative isotopomer abundances and the temperature and pressure conditions of ozone formation are clearly desirable to substantiate the degree of agreement between the different experimental techniques.

Isotope transfer into other atmospheric oxygen-containing compounds, such as $O(^1D)$, is most likely determined by the asymmetric ozone species,[79] rather than by the total heavy ozone. The knowledge of the intramolecular isotope distribution, therefore, appears to be a preferred measure for the source strength of the isotope anomaly, which is crucial for the understanding of these transfer processes. Especially in light of the unusual isotope composition of stratospheric CO_2 (section 5), symmetry-dependent studies on $^{16}O_2{}^{17}O$, which are completely lacking at the present time, are urgently required.

3.2.4. Kinetic Experiments

The importance of a kinetic description of the ozone isotope effect is evident from the fact that the isotope anomaly is an intrinsic kinetic feature, not covered by equilibrium thermodynamics. However, only recently were corresponding experiments undertaken. The first measurement was carried out by Sehested et al.,[56] who used pulse radiolysis of carbon dioxide as a source of atomic oxygen. Subsequent ozone formation from different $^{16}O-{}^{18}O$ mixtures in a CO_2 bath gas at 1 atm was monitored by UV absorption spectroscopy, leading to absolute values for rate coefficients of the ozone forming reactions (4) and (7) as well as of the combination of $^{16}O + {}^{18}O_2$ and $^{18}O + {}^{16}O_2$ and of $^{16}O + {}^{16}O^{18}O$ and $^{18}O + {}^{16}O^{18}O$. Later the experiment was repeated using argon as a buffer gas.[57]

Table 1. Reaction Channels of All Possible Oxygen Isotope Combinations Leading to Ozone Molecules

mass (u)	reaction	rate coefficient ratio[a]
48	$^{16}O + {}^{16}O_2 \rightarrow {}^{16}O_3$	1.00
49	$^{17}O + {}^{16}O_2 \rightarrow {}^{16}O_2{}^{17}O$	1.03[b]
50	$^{16}O + {}^{17}O^{17}O \rightarrow {}^{16}O^{17}O_2$	1.23[b]
	$^{16}O + {}^{16}O^{18}O \rightarrow {}^{16}O^{16}O^{18}O$	1.45[c]
	$\rightarrow {}^{16}O^{18}O^{16}O$	1.08[c]
	$^{18}O + {}^{16}O_2 \rightarrow {}^{18}O^{16}O^{16}O$	0.92
	$\rightarrow {}^{16}O^{18}O^{16}O$	0.006
51	$^{17}O + {}^{17}O_2 \rightarrow {}^{17}O_3$	1.02
52	$^{16}O + {}^{18}O_2 \rightarrow {}^{16}O^{18}O_2$	1.50
	$\rightarrow {}^{18}O^{16}O^{18}O$	0.029
	$^{18}O + {}^{16}O^{18}O \rightarrow {}^{18}O^{16}O^{18}O$	1.04[c]
	$\rightarrow {}^{18}O^{18}O^{16}O$	0.92[c]
	$^{18}O + {}^{17}O_2 \rightarrow {}^{18}O^{17}O_2$	1.03[b]
53	$^{17}O + {}^{18}O_2 \rightarrow {}^{17}O^{18}O_2$	1.31[b]
54	$^{18}O + {}^{18}O_2 \rightarrow {}^{18}O_3$	1.03

[a] Rate coefficient ratios (refs 77 and 28) relative to the standard reaction of $^{16}O + {}^{16}O_2 + M$. Data were obtained in N_2/O_2 mixtures at 200 Torr and at room temperature. [b] These rates may contain small contributions from the subsequent symmetric molecules (ref 28). [c] For those reactions involving heteronuclear oxygen molecules, the relative reaction probability is shown. Rate coefficient ratios may be obtained by dividing the quoted numbers by 2.

For CO_2, reaction (7) was found to be $9.8 \pm 2.6\%$ faster than reaction (4), and the average enhancement of asymmetric ozone molecule formation from reactions with homonuclear oxygen was $14.7 \pm 2.8\%$, whereas ozone from reaction with heteronuclear oxygen was enhanced by only $3.6 \pm 2.4\%$. The corresponding measurements in argon provided different reaction rate enhancements of $-2.3 \pm 2.1\%$, $18.4 \pm 3.7\%$, and $15.5 \pm 6.2\%$ for the same reactions or combination of reactions.

Anderson et al.[58] used mass spectrometry to monitor ozone isotopologue formation from UV dissociation of unscrambled $^{16}O-{}^{18}O$ mixtures in order to isolate the individual rate coefficients of reactions (4)−(7). The surprising result was that formation of asymmetric ozone molecules did not guarantee a rate coefficient advantage. While reaction (6) indeed showed a very large rate coefficient of 1.48 ± 0.08 compared to reaction (4), reaction (8) had a rate coefficient of only 0.92 ± 0.02. The large variability of rate coefficient ratios for asymmetric ozone formation between 0.90 ± 0.04 and 1.50 ± 0.03, as depicted in Table 1, has since then been confirmed in improved relative rate measurements by Mauersberger et al.,[77] which included reactions with the ^{17}O isotope, and in measurements by Janssen et al.,[28] who quantified the reaction channels for heteronuclear molecule reactions in the binary $^{16}O-{}^{18}O$ system.

The pressure dependence of the ratios of the respective rate coefficient for reaction (5)/reaction (4) and reaction (6)/reaction (4) has been determined in a separate study.[59] It was found that the low-rate-coefficient reaction (5) has the same pressure dependence as reaction (4), whereas the high-rate-coefficient reaction (6) slows down with increasing pressure when compared to reaction (4). Most interestingly, the rate coefficient ratios from reactions (4)−(7) do

not change significantly when the buffer gas is varied from Ar, via Kr, Xe, N_2, to CH_4 and CO_2,[60] even though the absolute rates of formation change by a factor of 4 between Ar and CO_2. As discussed by Sehested et al.[57] and Guenther et al.,[60] the agreement between the pulse radiolysis and rate coefficient ratio measurements is satisfying, except for the high rate coefficient of reaction (7) in the pulse radiolysis experiments using CO_2 as a buffer gas. Resonance effects in the ozone stabilization reaction (1c) have been suggested by Sehested et al.[56] to explain the high value, but since agreement with the other available data is good,[60] it must be either a singular effect or a measurement artifact.

The observed independence of the ozone isotope effect on the third-body partner supports that the $O-O_2$ interaction is important for the ozone isotope effect rather than interaction between one of the reactants and the third body. This apparently confirms the suggestion[28] that zero-point energy (ZPE) differences in the $O + O_2$ isotope exchange reactions could be responsible for the observed rate coefficient variability. It has been shown that the rate coefficients leading to asymmetric ozone product molecules in Table 1 linearly correlate with the energy change in the associated isotope exchange reactions and span the range of observed values, whereas isotope effects in reactions with symmetric product molecules are small.[31] Interestingly, the correlation line for the asymmetric molecules has an offset of about 15% compared to the cluster of symmetric molecules. This supports the idea of Marcus and co-workers that, in addition to a large ZPE effect, an intrinsic symmetry effect is reflected in the reaction rates.[62−65]

The temperature dependence of rate coefficient ratios and heavy isotopologue fractionation values in the $^{16}O-^{18}O$ isotope system have been measured only recently.[61] The results agree with earlier measurements close to room temperature[45,49,59,60,77] and with the temperature dependence study of $^{16}O_2{}^{18}O$ by Morton et al.[45] The observation of large $^{18}O_3$ depletions, $E = -(16.4 \pm 1.5)\%$, at low temperatures demonstrates that the contribution of the isotope exchange equilibria becomes increasingly important with decreasing temperatures.

Similar to the study of the pressure dependence of rate coefficient ratios,[59] where only one channel has shown an extra pressure dependence, again only one of the reactions (5)−(7) shows an extra temperature dependence. Interestingly, it is reaction (5), with the low rate coefficient ratio that increases with increasing temperature when compared to reaction (4). This has an important implication for the temperature and pressure dependence of $\delta^{18}O$ of ozone. It predicts that the observed temperature dependence[45] of $\delta^{18}O$ can be extended from the low-pressure regime toward atmospheric and even higher pressures, because the pressure-dependent rate coefficient ratio is not temperature-dependent and vice versa (compare section 3.2.1).

3.3. Development of Theories

Since the discovery of the large and unusual ozone isotope effect,[24,39] numerous attempts have been undertaken to interpret the ever-increasing wealth of experimental observations within a theoretical framework. It is beyond the scope of this review to give a full account of the complete theoretical work which has been devoted to the ozone problem. Here, theoretical treatments are presented which are phrased in kinetic terms and thus can be compared to the results of the previous section. There is no theory yet that can, from first principles, predict the ozone isotope effect.

Gellene and co-workers have developed a group theoretical analysis that treats symmetry restrictions in ion−molecule clustering reactions and successfully explains large symmetry-induced kinetic isotope effects (SIKIE), which have experimentally been observed in these reactions.[80−83] When this approach was then applied to the association step (1a) of the ozone formation scheme, the seemingly symmetry-dependent enrichments in the heteronuclear ozone molecules could be reproduced.[67] Predictions from the same theory for the individual rate coefficients, however, contradict experimental evidence, since symmetry restrictions apply to all reactions with homonuclear oxygen molecules as compared to heteronuclear molecule reactions. The large and unexpected rate coefficient variations within the homonuclear oxygen reactions (4)−(7) thus cannot be explained.

In a series of publications, Marcus and co-workers propose a modified Rice−Ramsperger−Kassel−Marcus (RRKM) theory to model the unusual ozone isotope effect.[62−65] The calculations successfully describe isotope kinetic[31,59] as well as abundance[45,49] data. Two different physical mechanisms contribute to the observed isotope effect. The first has been introduced into the theory as an ad hoc factor to describe possible nonstatistical effects, which affects symmetric and asymmetric molecule formation differently. The second is treated within the RRKM theory and relates to differences in ZPE[62,84,85] between competing dissociation channels of the reaction intermediate $(O_3)^*$ in ozone formation. Part of the agreement between experimental and theoretical values is due to the use of two yet unknown, temperature-dependent parameters: the nonstatistical factor and a parameter which describes the efficiency of energy transfer in the stabilization reactions (1c). Both have been fitted to reproduce the rate coefficient ratios $^{16}O + {}^{18}O_2/{}^{16}O + {}^{16}O_2$ and $^{18}O + {}^{16}O_2/{}^{16}O + {}^{16}O_2$ and their temperature dependence.[62] While the modified RRKM theory is successful in the quantitative description of the isotope effect in ozone formation, two questions remain unresolved, mainly because of the lack of independent data: Does molecular symmetry cause the apparent difference between asymmetric and symmetric molecules? And if so, does symmetry selection in ozone formation appear in the association/dissociation dynamics (1a) and (1b) of ozone formation or is it, perhaps, due to the stabilization process (1c)?[62,67] Independent information on both of the yet unknown parameters in this theory would be helpful to confirm the non-RRKM approach and to understand the true nature of the ozone isotope effect.

Robert and Camy-Peyret propose a phenomenological model to account for the different reaction rates and abundance effects.[69] In their model, quantum mechanical symmetry restrictions in identical particle collisions are transferred to the three-atom association/dissociation dynamics of ozone in a classical way. The experimental observations of multi-isotope enrichments[49] as well as of the kinetic studies[28,77] can be reproduced by the adjustment of five different parameters. One limitation of this model is to impose quantum mechanical symmetry restrictions to only two out of three atoms, and, as the authors state, the validity of this approach remains to be tested by a more rigorous quantum mechanical calculation.

Miklavc and Peyerimhoff suggest that the isotope selectivity in ozone formation arises primarily from the transfer of excess kinetic energy of the relative $O + O_2$ motion into O_2 vibration, and no attempt is made to account for the re-dissociation (1b) or stabilization (1c) steps.[70] Any conclusive comparison between experimental and theoretical values therefore seems to be premature. The same applies to a quantum mechanical approach from Charlo and Clary, who studied isotope effects in the energy-transfer step (1c) for homonuclear and asymmetric ozone molecules.[71]

The basis for a theoretical treatment of the ozone anomaly on an ab initio level has recently been improved by new calculations of the potential energy surface of the ground electronic state of ozone. Siebert et al.[86,87] constructed a new global potential energy surface (PES) which has been modified to agree with higher level of theory calculations[86,88,89] along the $O + O_2$ minimum energy path. A particular feature of the ozone potential appears to be a barrier toward ozone dissociation slightly (10−15 meV) below the $O + O_2$ asymptote, which separates the ozone wells from van der Waals minima.

Rosmus et al., however, pointed out that the near electronic degeneracy of 27 $O + O_2$ asymptotic states may prevent a realistic description of ozone-forming $O + O_2$ collisions in terms of the singlet electronic ground-state surface alone.[90] In particular, the neglect of non-adiabatic transitions between the ground state and repulsive PESs could well be responsible for the discrepancy between the calculated[88] and observed rates[91,92] of isotope exchange. Nevertheless, a recent isotope-dependent classical trajectory study of the same reaction by Fleurat-Lessard et al.[93] has indicated that this neglect may have no effect on the isotope dependence and thus lends some credit to approaches which are based on the ground-state potential only.

First results from fully quantum mechanical calculations using the improved ground-state PES have only recently been published. Babikov and colleagues calculated $O + O_2$ scattering resonances for different $^{16}O-^{18}O$ isotope combinations and zero angular momentum. The calculations reveal an increased number of long-lived metastable vibrational states of ozone just at the dissociation threshold of asymmetric ozone species.[94,95] The increased number of scattering resonances is attributed to the ZPE differences of the possible dissociation pathways of the asymmetric molecule,[94,95] and it is further suggested[94] that the energy transfer could be symmetry-selective. Employing a simple energy-transfer model, semiquantitative agreement is found with two experimental ratios of rate coefficients.[72] A more quantitative analysis, including higher angular momentum collisions and other rate coefficient ratios, is clearly needed in order to establish the connection to the measurements. Furthermore, the influence of the van der Waals minima needs to be identified. Grebenshchikov et al. suggest that these van der Waals minima actually lead to the observed increase in number of states close to the dissociation threshold.[96] Presently it is not clear how these states could contribute to ozone formation and its associated fractionation effects.

Classical trajectory calculations such as the ongoing studies of Gellene and co-workers[68] can complement the understanding of the $O + O_2$ collision dynamics. By incorporating zero-point energies in a phenomenological way, Schinke et al.[73] found isotope-dependent lifetimes of $O + O_2$ collision complexes which indicate the importance of the experimentally observed role of ZPE differences for the isotope selectivity in ozone formation.

The further development of these different theoretical approaches may finally lead to a complete understanding of the ozone isotope effect. This unique effect may then be identified either as a general model case for other molecular systems, or eventually as being in fact exotic and peculiar.

3.4. Photodissociation of Ozone

Knowledge of the effect of photoinduced dissociation on the isotopic composition of ozone is presently inadequate. Application to atmospheric chemistry is limited by the experimental difficulty in separating the photolysis steps (8) or (9) from subsequent ozone-destroying reactions of the photoproducts, like reaction (10). Also, most of the photolysis data rely on narrow-band or resonance light sources to initiate ozone decomposition, which impedes quantitative predictions for atmospheric ozone.

Bhattacharya and Thiemens[97] first investigated the effect of UV radiation on ozone using a microwave-driven Hg resonance lamp. From the data, mass-dependent fractionation factors $\alpha = 1.019$ for ^{18}O and $\alpha = 1.010$ for ^{17}O can be derived. Morton et al.[45] gave the first report on the effect of visible light photolysis on ozone isotopic composition. When a tungsten lamp with a cutoff toward low wavelengths was used to photodissociate 80% of the initial ozone in the Chappuis band, no significant ($|\delta^{18}(O)| < 0.6\%$) change in the ozone isotopic composition was observed. Using a frequency-doubled Nd:YAG laser at 532 nm to irradiate ozone at low pressures, Wen and Thiemens[98] found a mass-dependent enrichment of the residual ozone which corresponds to an enrichment factor of roughly $\alpha = 1.017$ for ^{18}O. A similar value of $\alpha = 1.016$ for Hg-resonance lamp-induced photodissociation in the Hartley band was observed, together with a corresponding ^{17}O fractionation factor $\alpha = 1.011$. In a recent study, Chakraborty and

Bhattacharya[99] found almost the same values for ozone photolysis by using a Hg-resonance lamp (1.011 and 1.017 for ^{17}O and ^{18}O, respectively). The accuracy of the α values in the latter work may have been compromised by the use of a simple Rayleigh model for the analysis which does not account for the slight curvature in most of the $\ln(R/R_0)$ vs $\ln(f)$ data. When the UV dissociation experiments are performed at relatively high nitrogen pressures ($p(N_2) \geq 40$ Torr, initial $p(O_3) \leq 1$ Torr), fractionation factors are reduced to $\alpha = 1.007$ for both ^{17}O and ^{18}O. These values are exclusively attributed to the dissociation reactions (8) and (9).[99] This conclusion appears to be premature, because the possible influence of photoproduct reactions is neglected. Product atoms from reactions (8) and (9)—the former after rapid quenching—inevitably will react according to (10) and therefore contribute to the observed ozone decomposition. Within the experimental setting, $O(^3P)$ may even form new ozone when a substantial amount of the initial ozone already has been converted into molecular oxygen. This obviously can have a major impact on the observed isotope signatures.

Chakraborty and Bhattacharya[99] further report $\alpha = 1.015$ and 1.008 for ^{18}O and ^{17}O, respectively, when ozone is photolyzed at both 520 and 630 nm. It is unclear, however, whether these measurements have been affected by heterogeneous loss of ozone at the walls of the spherical 5-L reactor, which was initially filled with 0.2 Torr of ozone. Irradiation times of up to 25 h (as compared to UV dissociation irradiation times of up to 12 min only) are on the high-end side for this type of experiment and may well allow heterogeneous decomposition to play a role. The result for ozone photodissociation with the unfiltered light from a tungsten lamp is in apparent contrast with the above-mentioned result from Morton et al.[45] In a single measurement where about 70% of the initial ozone was decomposed, the isotopic composition changed by 2.2% and 1.2% for ^{18}O and ^{17}O, respectively.[99]

Given the likely effect of photodissociation on the isotopic composition of ozone, the current status is not satisfactory. There is considerable uncertainty in the visible light experiments, the database is small, and the only two comparable experiments have led to conflicting results. While narrow-band irradiation in the visible light region seems to favor a decomposition-related effect of about 2%, the extremely small photolysis rate in the corresponding measurements[99] may have suffered from interfering heterogeneous ozone loss at the walls. This could have produced a similar fractionation, and the measurement results therefore may not be taken as conclusive evidence. In contrast, UV light from Hg-resonance lamp emission is known to produce an effect in the Hartley band ozone dissociation of the order of 1.8%. As in the case of visible light photolysis, however, the role of the secondary kinetics of the photoproducts is yet completely unknown.

That secondary chemistry indeed plays an important role can be inferred from the ozone dissociation experiments of Chakraborty and Bhattacharya[99] with or without nitrogen buffer gas present. Upon addition of the buffer gas, which efficiently quenches atomic excited states and thus changes ozone decomposition kinetics, fractionation factors for ^{18}O decrease from 1.018 to 1.007. Interestingly, ^{17}O fractionation does not change very much in the same experiments.

The current experimental results thus may be interpreted as an indication that decomposition effects will be significantly smaller in magnitude than isotope fractionation during ozone formation. Nevertheless, ozone photodissociation may add to the observed isotope fractionations in the atmosphere. Any quantitative prediction, however, is prevented by the fact that laboratory experiments have not yet been able to single out the fractionation factors which are associated with the individual steps of photodissociation, (8) or (9). In addition to this handicap, most reported fractionation factors for ozone dissociation rely on measurements with narrow-band light sources only; experiments with simulated solar radiation are yet sparse and need to be carried out in the future.

3.5. Photodissociation-Related Fractionation Processes

While the very photodissociation process of ozone may have an impact on its isotopic composition, there have been more reaction pathways proposed that can have—through isotope-selective secondary chemistry of photodissociation products—an impact on the isotopic ozone budget in the stratosphere. Even though some aspects and kinetic steps in the following models are based on solid experimental evidence, so far we are not aware of a definite link between the suggested mechanisms and ozone enrichments in laboratory and atmospheric settings.

Valentini et al.[100] were the first to observe and explain a symmetry-related oxygen fractionation process in O_3 dissociation. Coherent anti-Stokes Raman scattering (CARS) spectroscopy was used to investigate $O_2(^1\Delta_g)$ photoproducts from Hartley band photodissociation of ozone between 230 and 311 nm. Photoexcitation to the upper electronic states (1^1B_2 and 2^1A_1) leads to primary dissociation not only to the excited exit channel (9) but also to the ground-state exit channel (8) due to a curve-crossing with a repulsive state, which is thought to occur at already extended $O-O_2$ distances. Valentini et al.[100] found anomalous rotational distributions for $O_2(^1\Delta_g)$ photoproducts, which are predominantly in even-J rotational states when $^{16}O_3$ is dissociated. This predominance is not observed in $^{16}O^{18}O(^1\Delta_g)$ from photolysis of $^{16}O_2{}^{18}O$, where odd and even J states are about equally populated. This effect has successfully been explained by parity restriction in the curve-crossing process to the $O_2(^3\Sigma_g) + O(^3P)$ exit channel. Since homonuclear $^{16}O_2(^3\Sigma_g)$ allows only odd-J rotational states, only those rotational states from the excited species can undergo the curve-crossing, which leads to a quantum-selective depletion of odd-J rotational states in $^{16}O_2(^1\Delta_g)$. The same restriction, however, does not apply to heteronuclear oxygen molecules, such as $^{16}O^{18}O$ or $^{16}O^{17}O$, which therefore do not show this anomalous behavior. This was indeed demonstrated in the case of $^{16}O^{18}O$.

Since this selection mechanism guarantees a symmetry- rather than a mass-dependent isotope frac-

tionation of $O_2(^1\Delta_g)$ against $O_2(^3\Sigma_g)$, Valentini et al.[101] extended the above scheme to more generally treat isotope fractionation in non-adiabatic molecular collisions, which could possibly lead to anomalous isotope enrichment in ozone, as observed in electric discharge experiments and in the atmosphere. The starting point of Valentini's[101] argument is that the origin of $O_2(^1\Delta_g)$ from UV ozone photolysis is of no importance for the mechanism of isotope fractionation that is solely due to the quantum restrictions, which govern the curve-crossing process between the excited and ground electronic states of oxygen. Therefore, the same quantum symmetry restrictions should hold in the general $O_2(^1\Delta_g) + M \rightarrow O_2(^3\Sigma_g) + M$ quenching reaction as well as in the special case of near-resonant energy-transfer reactions, e.g.,

$$^{16}O^{18}O(^1\Delta_g) + {}^{16}O_2(^3\Sigma_g) \leftrightarrow {}^{16}O_2(^1\Delta_g) + {}^{16}O^{18}O(^3\Sigma_g) \quad (5)$$

These reactions are generally so rapid that they control isotopic partitioning between $O_2(^3\Sigma_g)$ and $O_2(^1\Delta_g)$. Symmetry restrictions are such that—apart for small standard mass-dependent effects—the forward reaction is twice as fast as the backward reaction, which depletes $O_2(^1\Delta_g)$ in the heavy isotopes while these are enriched in $O_2(^3\Sigma_g)$. The magnitude of the isotope effect in $O_2(^3\Sigma_g)$ will be simply determined by mass balance.

For $[O_2(^1\Delta_g)]/[O_2(^3\Sigma_g)] \leq 0.1$ (the upper limit can be reached under electric discharge conditions), $O_2(^3\Sigma_g)$ will be enriched in both the heavy isotopes by about $[O_2(^1\Delta_g)]/[O_2(^3\Sigma_g)] \times 50\%$. Ozone formation from the enriched $O_2(^3\Sigma_g)$ will subsequently lead to isotope enrichment in ozone, which itself—apart from the isotope exchange effect—is not fractionated against the $O_2(^3\Sigma_g)$ reservoir, however. It is thus clear that this effect needs consideration in experiments involving quantitative amounts of singlet oxygen. While the proposed mechanism predicts a fractionation of ^{17}O and ^{18}O isotopes in singlet as compared to ground-state oxygen, it does not predict heavy isotope fractionation in ozone against ground-state oxygen as is observed in the atmosphere. Therefore, application of this mechanism in the atmosphere seems to be precluded. Furthermore, steady-state mixing ratios in the middle stratosphere are low, such that direct application of the above scheme would predict unmeasurable isotope effects. Only when speculative steady removal of $O_2(^1\Delta_g)$ into other long-lived oxygen-containing compounds without (or with very slow) return to the molecular oxygen reservoir occurs, a measurable shift in the isotopic composition of molecular oxygen can be expected.[101]

The observation of highly vibrationally excited $O_2(^3\Sigma_g, v \geq 26)$ in the photodissociation of O_3 at 226 nm led Miller et al.[102] to suggest an alternative pathway for additional heavy isotope enrichment in ozone. Their proposal relies on the observation of Valentini et al.[100] that $O_2(^3\Sigma_g)$ from UV ozone photodissociation (9) is enriched in the heavy isotopes and consequently $O_2(^3\Sigma_g, v \geq 26)$ from 226-nm photolysis. This vibrationally excited oxygen molecule could then, as suggested by Rogaski et al.,[103] form ozone via the hypothesized reaction

$$O_2(^3\Sigma_g, v \geq 26) + O_2(^3\Sigma_g) \rightarrow O(^3P) + O_3(^1A_1) \quad (11)$$

It should be noted, however, that there is no direct experimental evidence for reaction (11). The reaction was rather indirectly inferred as a dark channel to explain a sharp increase in the rate of disappearance of vibrationally excited oxygen. Vibrational excitation of oxygen beyond a threshold value of $v \geq 26$ led to an increased disappearance in a relaxation experiment. Since this level of vibrational excitation roughly corresponds to the thermodynamic threshold of reaction (11), the observation was taken as evidence for occurrence of this reaction. Theoretical studies on reaction (11) or its reverse, however, could not confirm this process.[104] Despite missing evidence, the suggested scheme implies that one out of three oxygen atoms will return to the ozone pool without undergoing isotope exchange with molecular oxygen. Since this prevention of isotope exchange occurs in favor of the heavy molecules, ozone will subsequently be enriched in the heavy isotopes when compared to the molecular oxygen reservoir. Houston et al.[36] have improved the original calculations of Miller et al.[102] and predict a maximum enrichment of about 3% in equatorial regions at around 42 km.

Recently, the reaction of $O(^1D)$ with O_3 has been suggested as an alternative pathway to induce additional fractionation in ozone. The suggestion is based on the observation of strongly enriched ozone samples ($\delta^{18}O$ up to 18%) from UV photolysis of an oxygen or combined oxygen/nitrogen bath gas at low pressures in the 10−20 Torr range.[105] As pointed out in a comment,[105] however, the above proposition needs to be rejected for a number of reasons. Due to the sample treatment, the observed high enrichment data are of questionable integrity. Furthermore, the $O(^1D) + O_3$ reaction is insignificant under the experimental conditions, and it is even less significant under stratospheric conditions.

3.6. Atmospheric Observations

3.6.1. Stratosphere

The isotopic composition of stratospheric ozone has been investigated by various techniques conducted from ground and in-flight measurement platforms, the latter mostly being balloons. Mass spectrometers (MS) have been employed either for in situ detection of $^{16}O_2{}^{18}O$ by a molecular beam technique[24,106] or for the analysis of oxygen samples that were obtained by cryogenic sampling (CS) of ozone on-board balloon gondolas.[49,107,108] The latter method is especially favorable for precision measurements even at low concentrations and thus permits analysis of both rare isotopologues $^{16}O_2{}^{18}O$ and $^{16}O_2{}^{17}O$.[109] It further extends the specificity of the system through cryogenic trapping, which reduces the number of gases that are admitted to the MS. Spectroscopic techniques such as mid-infrared absorption (MIRAS) or far-infrared emission spectroscopy (FIRES), which further allow for the selective detection of even the isomeric species

$^{16}O^{18}O^{16}O$ and $^{16}O^{16}O^{18}O$, have been applied as complementary methods. While MIRAS of ozone isotopomers has been performed with ground-based Fourier transform instruments[110−112] and with balloon-borne or Space Shuttle-operated spectrometers,[112,113] FIRES has been exclusively applied from balloon platforms.[114−116] In the most recent of these investigations, IR spectroscopy has been used to investigate also the rare ^{17}O-containing isotopomers. Almost all of the measurements undertaken have probed stratospheric ozone in the northern hemisphere, with the majority of the data from around 30°N. Some of the measurements provide data from northern polar regions between 60°N and 80°N.[108,111,112,116,117] Only the data from the ATMOS experiment[112] cover both hemispheres between 80°S and 80°N. The different measurements are summarized in Table 2.

The first measurement[24] of the ^{18}O isotopic composition of stratospheric ozone did trigger several remote sensing[110,113−115] and in situ[106] studies. These experiments from the first decade of ozone isotope research report a rather large range of $\delta^{18}O$ enrichments (between 0% and 41%) and suffer from comparatively low precision (2σ errors of up to 30%). None of the improved precision ($2\sigma < 10\%$) experiments from the next two decades[49,107,108,111,112,116,117] could confirm the very high ^{18}O enrichments in stratospheric ozone, which were occasionally reported in the earlier measurements. The later experiments rather showed a trend toward decreasing $\delta^{18}O$ values, which are close to the laboratory predictions (section 3.2.1). This supports the conclusion of Mauersberger et al.[117] that the early measurements probably have to be disregarded, even though the source of the errors has not been clearly identified. For this reason, only the more recent measurements are discussed.

Schueler et al.[107] developed a two-stage cryosampler[109] to be flown on balloons. They reported the first simultaneous measurements of $\delta^{18}O$ and $\delta^{17}O$ from three balloon flights where samples cover the altitude range 27.5−34 km. Later, the result of a fourth flight with the same sampling system was added to extend the altitude range up to 37 km.[49] The nine samples returned from all four flights demonstrated that the $\delta^{18}O$ and $\delta^{17}O$ enrichment values around 30 km are in the 8−10% range, which is very close to the laboratory predictions by Morton et al.[45] A systematic departure, however, from these values may be observed at higher altitudes, where enrichments of ^{18}O and ^{17}O in ozone up to 23 ± 5% and 13 ± 4%, respectively, were measured at about 37 km in the last flight.

In 1996, the observational database was greatly extended. Meier and Notholt[111] reported the results of 27 ground-based solar and lunar mid-infrared absorption spectra in the Arctic (79°N) covering the period from April 1994 to August 1995. The $\delta^{18}O$ column enrichments of $^{16}O_2{}^{18}O$, $^{16}O^{16}O^{18}O$, and $^{16}O^{18}O^{16}O$ show almost constant values of 14.0 ± 1.5%, 15.4 ± 1.8%, and 11.2 ± 2.8%, respectively, in the period ranging from spring to fall. A strong preference for the abundance of the asymmetric isotopomer is indicated. Though less significant, this preference is also clear from the lunar spectra which cover the period of the polar night. Averages during the winter period are 8.8 ± 4.7%, 9.0 ± 6.6%, and 8.5 ± 5.0% for $\delta^{18}O$ in $^{16}O_2{}^{18}O$, $^{16}O^{16}O^{18}O$, and $^{16}O^{18}O^{16}O$, respectively. Both lower enrichment values and a decreased enrichment of asymmetric over symmetric species at lower temperatures seem to comply with the observed temperature dependencies from laboratory experiments[45,51] (sections 3.2.1 and 3.2.3). One issue inherent in all MIRAS measurements is that line intensities, which are used to determine the isotopomer abundances of the heteronuclear species, are subject to systematic error. This error arises from experimentally yet unverified assumptions in the calibration procedure of the reference measurements, which is discussed in some detail by Flaud and Bacis.[118] Presently, this calibration error is difficult to quantify but could well be in the few percent range. The value $\delta^{18}O = 14.0 \pm 1.5\%$ in ozone, as observed in the solar spectra by Meier and Notholt,[111] therefore cannot be interpreted as a profound deviation from the laboratory predictions, which are closer to the 7−11% range.

Another time series of ground-based MIRAS column measurements, comprising a set of 48 individual spectra, was provided by operation of the ATMOS Fourier transform instrument at Table Mountain (34°N) for a period of about 5 years. The time series did not show a significant seasonal variability in the column enrichment of $^{16}O^{16}O^{18}O$, which had an average value of $\delta^{18}O = 17 \pm 8\%$, in good agreement with the solar absorption measurements of Meier and Notholt. No ground-based column $\delta^{18}O$ values for $^{16}O^{18}O^{16}O$ have been reported in this study. The operation of the same instrument aboard the Space Shuttle in four flights provided vertical profiles for the enrichments of both isotopomers between 25 and 41 km, covering both hemispheres between 80°S and 80°N. Mission (latitude) averaged profiles of $\delta^{18}O$ in $^{16}O^{16}O^{18}O$ and $^{16}O^{18}O^{16}O$ have 2σ standard errors of 16% and 20%, respectively. Within these rather large uncertainties, no variation with altitude or latitude could be determined. The observed column enrichments were 13 ± 10%, 15 ± 12%, and 10 ± 14% for $^{16}O_2{}^{18}O$, $^{16}O^{16}O^{18}O$, and $^{16}O^{18}O^{16}O$, respectively.

In a more recent FIRES study, which includes seven balloon flights between 1989 and 1997, Johnson et al.[116] reported the first δ values for both ^{17}O- and ^{18}O-containing ozone isotopomers obtained by spectroscopy. While the uncertainty in individual data points is very large, averages over 25−35 km result in enrichments of 10.2 ± 8.6%, 12.2 ± 8.6%, and 6.1 ± 9.1% for $^{16}O_2{}^{18}O$, $^{16}O^{16}O^{18}O$, and $^{16}O^{18}O^{16}O$, as well as in enrichments of 7.3 ± 12.0%, 8.0 ± 13.4%, and 1.6 ± 17.4% for $^{16}O_2{}^{17}O$, $^{16}O^{16}O^{17}O$, and $^{16}O^{17}O^{16}O$.

The most recent stratospheric observations were obtained by a second generation of cryosamplers. A total of 19 samples from five balloon flights either from Aire-sur-l'Adour (44°N) or from Kiruna (68°N) were collected from an altitude range between 21 and 38 km.[108,117] Both $\delta^{17}O$ and $\delta^{18}O$ values were measured with improved precision when compared to the earlier campaigns.[49,107] Enrichments between 6.69 ± 0.35% and 9.55 ± 0.56% for $\delta^{17}O$ and between 6.59 ± 56% and 10.78 ± 0.35% for $\delta^{18}O$ have been

Table 2. Comparison of Heavy Ozone Isotopomer Measurements in the Stratosphere: Technique, Experimental Platform, Geographical/Altitude Parameters, and Number of Independent Measurements[a]

technique	instrument platform	location	altitude range, resolution	measurements and data points	column enrichment, $\delta^{18}O$ (%)	average or typical enrichments, $\delta^{18}O$ (%)	comment	$\delta^{18}O$ (%) in $^{16}O^{16}O^{18}O$	$\delta^{18}O$ (%) in $^{16}O^{18}O^{16}O$	ref
MBMS	balloon	31°N	20−38 km, 1-km res.	1 flight		0 ± 30 to 40 ± 30	maximum enrichment at 32 km			24
MBMS	balloon	31°N	27−43 km, <2-km res.	2 flights, 20 points		13 ± 10 to 41 ± 14	variable, minima around 35 km, maxima at low and high altitudes			106
CSMS	balloon	31°N/ 34°N	27.5−37.1 km	4 flights, 9 samples		8.1 ± 1.5 to 23.0 ± 5.0, $\delta^{17}O$ = 8.1 ± 1.8 to 13.0 ± 4.0				49, 107
CSMS	balloon	44°N/ 68°N	21−38 km	5 flights, 19 samples		6.59 ± 0.56 to 10.86 ± 34, $\delta^{17}O$ = 6.69 ± 0.36 to 9.24 ± 0.5	only statistical measurement uncertainty is reported			108, 117
MIRAS	ground	32°N	column	3 spectra	9 ± 15		solar	11 ± 22	5 ± 14	110
MIRAS	ground/ balloon	34°N/ 31°N	column column >37 km	1 flight 2 spectra	<20 ± 20 26 ± 14		solar	− 30 ± 20	− 17 ± 14	113
MIRAS	ground	79°N	column	17 spectra 10 spectra	14.0 ± 1.5 8.8 ± 4.7		solar lunar	15.4 ± 1.8 9.0 ± 6.6	11.2 ± 2.8 8.5 ± 5.0	111
MIRAS	ground shuttle	32°N 80°S/ 80°N	column 25−41 km, 1-km res.	48 spectra 4 flights	− 13 ± 10	 no significant lat. + alt. variation	solar, no seasonal variation	17 ± 8 15 ± 12	− 10 ± 14	112
FIRES	balloon	34°N/ 31°N	25−37 km	1 flight, 5 values	34 ± 20	(13−45) ± 28		23 ± 20	56 ± 24	114
FIRES	balloon	32°N	28−38 km	1 flight, 3 values	10 ± 20	no significant variation with altitude		equal within errors		115
FIRES	balloon/ aircraft	30−35°N/ 68°N	25−35 km, 1-km res.	7 flights	10.2 ± 8.6 $\delta^{17}O$ = 7.3 ± 12.0	as above		12.2 ± 8.6 $\delta^{17}O$ = 8.0 ± 13.3	6.1 ± 9.1 $\delta^{17}O$ = 5.9 ± 17.4	116

[a] If reported in the original literature, column values are given. Profile data are characterized by the range of observation with remarks about the altitude dependence. If available, δ values for isotopomers are listed as column values. If not noted otherwise, 2σ estimated total uncertainty is given.

reported, with errors indicating the statistical uncertainty on a 95% level of confidence.

It is interesting to note that this most accurate and recent dataset of 19 samples, obtained by cryogenic sampling, shows within 1−2% perfect agreement with the laboratory measurements[43,45] when reasonable stratospheric temperatures are assumed. Furthermore, in a three-isotope plot, the data form a line with a slope of 0.62 ± 0.11, which is in very good agreement with the characteristics of temperature-dependent ozone formation. It was well recognized[116,117] that the first generation of CS measurements from Schueler et al.[107] and Mauersberger[49] exhibited a variability which could not be explained solely on the basis of stratospheric temperature variations. When compared to the second series of measurements, it is the data of only the first and the fourth flights which exceed the $\delta^{18}O$ range of all others, reaching a maximum $\delta^{18}O = 23 \pm 5\%$. Until now, the cause for these high values has not been identified.[117] It must be noted, however, that the highest enrichment coincides with the highest sampling altitude and the smallest sample size. Apparatus effects such as fractionation during sample collection or treatment may explain why enrichments were high and why, in a three-isotope plot, these data seem to fall below the line as defined from the most recent dataset.

Despite numerous experimental efforts to study isotope effects in ozone formation and decomposition processes, there are presently no known fractionation mechanisms which could operate under stratospheric conditions and lead to such large effects as to explain enrichments significantly higher than 10−11%, or even as high as 18%. This view, however, has recently been challenged by Bhattacharya et al.[119] The authors claim that ozone destruction via $O(^1D) + O_3$ should cause "significant" fractionations, which could possibly explain very high enrichments of 45 ± 28%, as observed by Abbas et al.[114] As already discussed in section 3.1, however, the proposed dissociation pathway is unimportant under stratospheric conditions, which makes this proposition untenable.[105]

Only very recently have accurate and reliable stratospheric data become available[108,117] which show satisfying agreement with laboratory predictions on ozone formation, leaving room for small 1−2% extra effects on ozone photodissociation. This is about the size of the effect which can well be expected from photolysis (section 3.4) or from bimolecular reactions. Future studies with similar or improved accuracy may actually quantify these effects and processes.

Generally, remote sensing adds an extra dimension to the investigation of stratospheric isotopes by its isotopomer specificity. Presently, however, the data are not yet accurate enough to aid in the investigation into possible ozone decomposition pathways. Within the precision of the IR techniques, however, variations in altitude, longitude, and time have been monitored and support the view that the very high enrichments observed in the first decade of observations should be disregarded. Given the still not quantified errors in MIRAS due to the systematic uncertainty in ozone isotopomer line strengths, all of the more recent IR data agree with the most recent cryogenic sampling mass spectrometry (CSMS) dataset. Significant differences in the enrichments of symmetric and asymmetric species have not yet been resolved in individual measurements. The entire dataset, however, agrees with the laboratory findings that the asymmetric species is more strongly enriched than the symmetric one.

3.6.2. Troposphere

Isotope analysis of tropospheric ozone is particularly challenging due to the low $[O_3]/[O_2]$ ratio (up to ~20 nmol/mol). Krankowsky et al.[120] were the first to collect and analyze tropospheric O_3. They sampled at the outskirts of Heidelberg (49°N), from July to September 1994. Collection and immediate sample analysis were performed with a two-stage cryosampler/magnetic mass spectrometer combination. Following the cryogenic removal of water and CO_2, ozone together with xenon was frozen out. After conversion to molecular oxygen and subsequent xenon removal, the oxygen gas was immediately admitted to the MS. No correlation between $\delta^{17}O$ and $\delta^{18}O$ was found, and averages of $\delta^{17}O = 7.1 \pm 0.3\%$ and $\delta^{18}O = 9.1 \pm 0.2\%$ were reported, with errors representing 2 standard deviations of the mean. Laboratory predictions from ozone formation for the average pressure and temperature conditions, however, are $\delta^{17}O = 7.2 \pm 0.6\%$ and $\delta^{18}O = 7.6 \pm 0.6\%$ (see section 3.2.1).

While $\delta^{17}O$ agrees well with this prediction, there is a discrepancy in $\delta^{18}O$ of about 1.5%. Given the large $\delta^{18}O$ value, this number is certainly small enough to conclude that atmospheric observations essentially reflect the isotope effect observed in the process of ozone formation. The small discrepancy, however, might indicate extra fractionation effects in tropospheric ozone, but systematic errors in both the laboratory and atmospheric studies may also be responsible. Systematic uncertainties in the laboratory prediction include the possible fractionation effect due to visible light photolysis of ozone, which could not yet be quantified (see section 3.4). The possible influence of this effect was found to be smaller than 0.6%,[45] but this error limit has uncertainties depending on the unknown fractionation in the simultaneously occurring $O + O_3$ reaction. The common but yet arbitrary assumption that the latter is negligible would increase the error interval for $\delta^{18}O$, which is based on statistical analysis, by a factor of 2. This would almost imply agreement between tropospheric and laboratory experiments.

Johnston and Thiemens[121] used a similar technique to collect and analyze samples between January 1995 and April 1996. Collection efficiencies were between 4% and 19%, with 10% being a typical value.[122] Twenty-nine, six, and seven different samples were taken at the three different locations: La Jolla, CA; White Sands Missile Range (WSMR), NM; and Pasadena, CA, respectively. Average $\delta^{17}O$ and $\delta^{18}O$ values varied between 6.6 ± 0.3% and 7.8 ± 0.2% and between 8.2 ± 0.2% and 9.0 ± 0.3%, respectively. Table 3 lists all of the tropospheric data.

A comparison between the Heidelberg and the combined La Jolla and Pasadena datasets shows that

Table 3. Tropospheric Ozone Measurements: Total Number of Samples on Each Sampling Site, Mean Meteorological Parameters, and Sample Averages

location	period	no.	mean pressure (hPa)	mean temp (K)	average[a] $\delta^{17}O$ (%)	average[a] $\delta^{18}O$ (%)	ref
Heidelberg (49°N, 9°E)	7/94−9/94	47	975	298	7.1 ± 0.3	9.1 ± 0.2	120
La Jolla (33°N, 117°W)	1/95−4/96	29	1015	292	6.9 ± 0.2	8.2 ± 0.2	121
WSMR (32°N, 106°W)	3/95	6	874	290	7.8 ± 0.2	9.0 ± 0.3	
Pasadena (34°N, 108°W)	9/95	7	−	301	6.6 ± 0.3	8.6 ± 0.4	

[a] At 2σ total estimated uncertainty.

there is agreement between the $\delta^{17}O$ averages but disagreement between the $\delta^{18}O$ values. At first glance, the La Jolla/Pasadena dataset seems to be more compliant with the laboratory data. But the observed variability of $\delta^{18}O$ well exceeds the stated measurement precision, as well as exceeds effects from pressure and temperature variations on ozone formation. This makes the agreement with laboratory data on ozone formation accidental. Indeed, Johnston and Thiemens[121] conclude that the observed variability reflects the influence of atmospheric ozone decomposition processes, and—on the basis of a linear regression analysis of the three isotope data—they infer that differences in variability between the three U.S. sampling sites might indicate different ozone decomposition pathways. Presently this proposition remains speculative, because the differences in the derived regression parameters are not significant at the 95% level of confidence.

Correlations between $\delta^{17}O$ and $\delta^{18}O$ could also indicate that experimental deficiencies in the collection system or analysis procedure exists. Generally, the measurements of Johnston and Thiemens[121] seem to be more susceptible to systematic errors when compared to the measurements of Krankowsky et al.[120] This is due to the low collection efficiency, the admission of xenon together with the sample into the mass spectrometer, and up to 8 days storage time for sample sizes ranging from 20 to 210 nmol.[122]

Given the possibility of small, undetected or underestimated systematic errors in both experiments—due to differences in sampling efficiency, interferences, sample storage prior to analysis, etc.—or given that small isotope effects in the ozone decomposition chemistry may exist, the agreement for these difficult measurements is encouraging. The agreement in the $\Delta^{17}O$ values is especially good. Taking aside the WSMR data, which due to the elevation of this site are at significantly lower pressures, the average of the Pasadena and La Jolla data, $\Delta^{17}O = 2.54 \pm 0.16\%$, compares well with the corresponding value $\Delta^{17}O = 2.37 \pm 0.32\%$ from Heidelberg.

The precision of the existing measurements nevertheless demonstrates either that ozone decomposition reactions have a small but significant impact on the isotope composition of tropospheric ozone or that problems still exist in the measurements. Both areas need more investigation, and laboratory experiments, such as the isotopic investigation of the $O_3 + NO$ reaction and the study of isolated ozone photolysis reactions, would be particularly useful to fully understand the isotope chemistry of ozone.

4. Methane, CH_4

CH_4 has been measured most extensively (apart from tropospheric H_2O and CO_2) and does offer a clear example of the application of isotope variations in a conventional sense. In this review, neither the processes that lead to the isotopic composition of methane from the various source, nor fractionation due to soil process, will be considered. For recent reviews concerning atmospheric methane that also include isotopic data, we refer the reader to works by Khalil,[123] Wubbels and Hayoe,[124] and to Bréas et al.[125] Isotope effects in CH_4 have been reviewed by Gros et al.[126] Conny and Currie[127] have conducted a largely theoretical study of the isotopic characterization of CH_4 and the products of its photochemically driven removal from the atmosphere.

4.1. Measurement and Laboratory Studies

A main point of progress on CH_4 isotope analysis and its application to atmospheric chemistry is fueled by the development of GC−IRMS. Measurement of ^{13}C so far has been mainly based on combustion of CH_4, followed by mass spectrometry of CO_2. Alternatively, tunable diode laser absorption spectroscopy (TDLAS) has been used, which allows determination of both $^{13}C/^{12}C$ and D/H ratios, albeit on large air samples from which CH_4 has to be preconcentrated considerably. The TDLAS is, however, a rather specialized technique, and not available commercially. For mass spectrometric determination of deuterium, the CH_4 sample was burned to yield H_2O, which subsequently was reduced to H_2 and analyzed mass spectrometrically. This cumbersome MS procedure for deuterium, using large samples (a few hundred liters of air), has been almost totally superseded by GC−IRMS. By the use of GC−IRMS, nanomole amounts can be assayed by pyrolysis of CH_4 to H_2. In fact, GC−IRMS for deuterium not only uses small samples and is less elaborate, but most likely can match the precision of the conventional method. However, achieving the highest accuracy for ^{13}C by GC−IRMS is still difficult. Pyrolysis of CH_4 is difficult due to the high temperatures required. Nevertheless, in general, GC−IRMS determinations of both ^{13}C and deuterium appear to be possible routinely.[128,129] Because isotope variations for ^{13}C in atmospheric methane are small, the precision and accuracy of the mass spectrometry measurements have to be high. Also, for the comparison of time series obtained by several laboratories, the problem of standardization is substantial. For laboratory experiments where sufficient compound is available to study reaction kinetics, Fourier transform infrared

Table 4. Kinetic Fractionation Factors (α or KIE) for Methane

reaction	$k(^{12}C)/k(^{13}C)$	$k(H)/k(D)$	ref
$CH_4 + OH$	1.0039	1.294	284
	1.0054		285
		1.25	286
$CH_4 + Cl$	1.0621	1.474	287
		1.54	288
	1.066		289
	1.066		290
		1.508	291
$CH_4 + O(^1D)$	1.013	1.06	284
	1.001		292

spectroscopy (FTIR) has been used. In this case, isotopically enriched CH_4 can be used to alleviate the problem of the lower sensitivity.

Laboratory studies have focused on the three important chemical sink reactions, namely those with OH, Cl, and $O(^1D)$, for which the ^{13}C as well as the D KIEs have been measured. Table 4 lists the current status (for the actual temperature ranges we refer to the original publications), and agreement only exists for reaction with Cl. The difficulty of determining the fractionation in the reaction with $O(^1D)$, combined with the fact that the value for ^{13}C seems rather large for such a fast reaction, will continue to cast doubt on these findings until measurements are repeated. There have been attempts to calculate the isotope effect for Cl ab initio. It seems that the laboratory measurements will provide a good framework for testing improved and refined theoretical models. At this stage, calculation of the reaction $O(^1D)$ with CH_4 would already be beneficial.

As mentioned previously, laboratory studies have mostly dealt with the isotopic change of the reactant, and less is often known about the product. The main reason for this is that often the products react further, undergo isotopic exchange, or are more easily contaminated, in particular when H_2O and CO_2 are to be considered as end products. As a result, we do not yet know the precise rate difference between the reactions

$$CDH_3 + OH \rightarrow CDH_2 + H_2O \quad \text{and}$$
$$CDH_3 + OH \rightarrow CH_3 + HDO$$

Since only the first reaction can lead to HD, the difference in reaction rates between these two pathways should be studied.[130]

4.2. Atmospheric Applications

Atmospheric measurements are routinely carried out by several groups worldwide, and GC−IRMS is rapidly becoming the standard technique. It is expected that the GC−IRMS method will lead to an enormous increase in data. The NOAA/CMDL carbon cycle group[131] routinely measures ^{13}C in CH_4, and the datasets are sufficiently extensive for inverse modeling of tropospheric $^{13}CH_4$.

Concerning the stratosphere, great progress has been made recently by accurate analyses of large sample sets from the NASA ER2 aircraft for D and ^{13}C.[129] Two challenges result from this work. One is the investigation of the important role of transport and mixing, in particular at high latitudes. The other is that large differences between the ^{13}C fractionation factors for the reaction with OH and $O(^1D)$ persist. Further, carefully controlled experiments are clearly necessary, and a glance at the two equations above confirms that much work lies ahead if products are to be known as well.

The ^{13}C fractionation in the reaction with Cl atoms is large, and in the atmosphere evidence of the reaction has also been found by analyzing CO. Thus, both under ozone hole conditions[132] and during surface ozone loss events in the Arctic, evidence of CH_4 reaction with Cl has been found using ^{13}C measurements.[133] The concomitant impact on the ^{13}C value (and D) of the remaining CH_4 is very small.[134,135]

5. Carbon Dioxide, CO_2

Carbon dioxide is a most intensively studied trace gas, and its isotopic composition has also been well studied. The extremely high degree of precision and reproducibility that are required for atmospheric observations has contributed enormously to better understanding of the mass spectrometry itself. This has resulted in the most detailed understanding[18] of absolute isotope ratios in reference materials.

As pointed out in the Introduction, mass spectrometry of CO_2, using masses 44, 45, and 46, assumes a certain relationship between ^{17}O and ^{18}O variations. One way around this problem has been pioneered by Verkouteren,[136] who also measured mass 47, predominantly consisting of $^{13}C^{16}O^{18}O$. Precise measurement of this signal allows, in principle, one to obtain a set of equations of ion abundances that uniquely determines the CO_2 isotopic makeup, without a priori assumptions about the ^{17}O-to-^{18}O relationship. We further remark that it has generally been overlooked that, in the atmosphere, the abundance of $^{12}C^{18}O^{18}O$ does not necessarily exactly agree with that calculated for the same CO_2 sample on the basis of its $^{12}C^{18}OO$ abundance. Zyakun and Brenninkmeijer[137] noted that, when CO_2 from two different pools is mixed, e.g., from burning and respiration, this should indeed be the case. The principle can be demonstrated readily by assuming, for instance, no ^{18}O in CO_2 from respiration, and normal ^{18}O in CO_2 from combustion. The reason for this is that isotopic scrambling between CO_2 molecules in the atmosphere does not take place. To what degree this exceedingly small signal can be useful, and importantly whether it can be detected reliably (ultrapure CO_2 would be a prerequisite), remain to be seen. An experimental study of possible similar effects in stratospheric N_2O is reported in section 6.2.1.

The isotopic composition of tropospheric CO_2 varies mainly due to its sources and due to oxygen isotope exchange with water. In this exchange, leaf, soil, and ocean water dominate, whereas exchange with rainwater is insignificant. The ^{13}C and ^{18}O isotopic abundances of tropospheric CO_2 are sensitive gauges for its interaction with the biosphere and oceans, and for anthropogenic CO_2 emissions.[138−141] Unlike for any other atmospheric trace gas, isotope measurements on CO_2 with the highest precision are carried out by laboratories around the globe to quantify the

individual processes and improve our understanding of the global carbon cycle. The present review concentrates on isotope effects in atmospheric chemistry, where stratospheric CO_2 is at the center of one highly interesting isotope exchange process.

5.1. Measurements of Stratospheric CO_2

A few years after the discovery of the strong ^{18}O enrichment in stratospheric ozone,[24,106] a less extreme yet substantial enrichment was observed in stratospheric CO_2.[142,143] Thiemens et al.[144] clearly showed that the enrichment for CO_2 does not follow the conventional mass-dependent relationship $\delta^{17}O \approx 0.5(\delta^{18}O)$. Yung et al.[145] proposed isotope transfer from O_3 to CO_2 via the short-lived CO_3* intermediate in the stratosphere as a potential mechanism, and this mechanism has indeed been verified in the laboratory (see below).

Thiemens et al.[146] reported a correlation between the two heavy isotope signatures in stratospheric CO_2 according to $\delta^{17}O \approx 1.2(\delta^{18}O)$. Extrapolation of the linear fit through these data, obtained by rocket-based sampling, did not pass through the isotopic composition of tropospheric CO_2. On the other hand, very precise $\Delta^{17}O$ isotope measurements on CO_2 collected in the lowermost stratosphere between New Zealand and Antarctica[147] provided values only slightly enriched relative to tropospheric CO_2, indicating that the $\delta^{17}O-\delta^{18}O$ correlation should actually pass through the tropospheric isotope value. A tight correlation with ^{14}CO as a stratospheric tracer (not $^{14}CO_2$, as indicated by Weston[4]) also existed. The data from Thiemens et al.[147] were a selection of a larger dataset published in a NASA report,[148] and the data points not considered do better indicate that a linear fit should intersect the tropospheric value. A recent dataset reported by Lämmerzahl et al.[149] produced the very tight correlation $\delta^{17}O \approx 1.7(\delta^{18}O)$, which does pass through the tropospheric value. This finding is generally supported by new measurements by Alexander et al.[150] and data from the Zipf and Erdman[148] dataset. The slope of 1.7 is unusual in the sense that the enrichment for ^{17}O is much higher than that for ^{18}O, surpassing that of O_3 itself. All presently available data are shown in a three-isotope plot in Figure 4.

Nevertheless, the data in Figure 4 show that not all results fall on the line with slope 1.7. Lämmerzahl et al.[149] state that some of their data were rejected due to contamination, which was independently indicated by unstable pressure readings during extraction of these samples (supposedly due to water). Additionally, this contamination, if present, occurred for the first sample only, whereas the duplicate sample from the same altitude level fits exactly on the correlation line 1.7. No such checks may have been possible in earlier studies, whereas contamination with tropospheric H_2O remains a problem inherent in stratospheric sampling of CO_2 and, of course, H_2O as well. The points rejected by Lämmerzahl et al.[149] invariably fell below the fit line, and all of the points significantly below that line were rejected. In the early data from Thiemens et al.,[144] five of the six

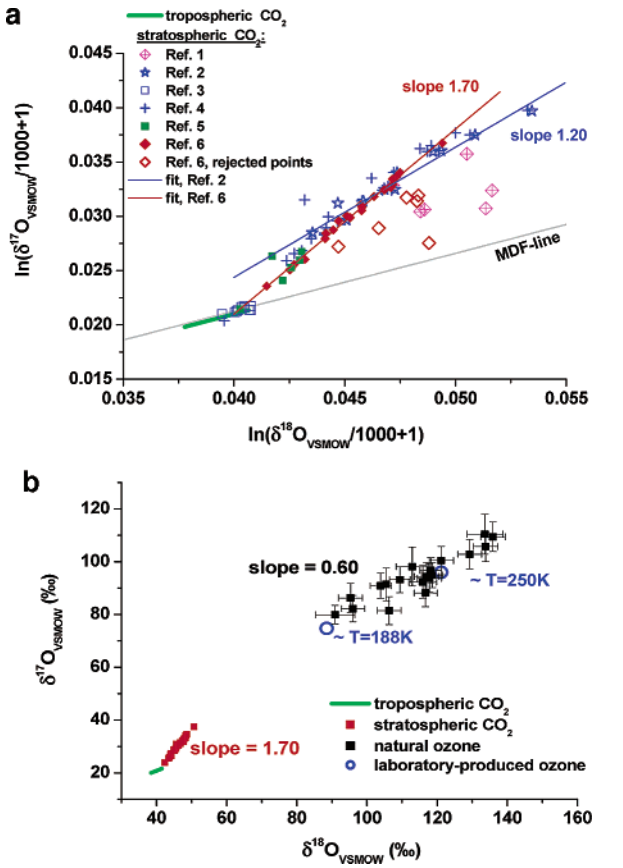

Figure 4. (a) All available $\delta^{17}O/\delta^{18}O$ (CO_2) data, shown on a ln/ln scale. The mass-dependent relationship, the early slope estimate of ~1.2 which invoked speculations about unknown processes, and the recent best fit with a slope of 1.7 are shown. This fit passes through the tropospheric data. Ref 1,[144] refs 2 and 3,[147] ref 4,[148] ref 5,[293] ref 6.[149] (b) The CO_2 data in relation to the ozone data.

data points were significantly below the fit line. Similarly, for the rocket data,[147,148] the two highest points clearly fell below the fit line. It is mainly these two data that caused the lower slope reported in early work.[147] Since these samples were from very high altitudes not covered by the Lämmerzahl et al.[149] dataset, one can certainly not exclude that, at these altitudes, other processes contribute. However, awareness of the contamination problem weakens evidence for such processes.

Thiemens has noted that CO_2 photolysis in the mesosphere may cause an additional isotopic signal. A striking ^{17}O enrichment in the photolysis products O_2 and CO has been reported for CO_2 photolysis at 185 nm, which disappears at 160 nm.[151] Such an effect would deplete the remaining CO_2 in ^{17}O and could cause lower values at high altitudes. Broadband photolysis experiments under relevant conditions are needed to assess the potential importance of this process for the upper atmosphere.

Only a limited number of data points are presently available for small isotope enrichments, representing the lower stratosphere. It has been shown that the seasonal cycle of the tropospheric CO_2 mixing ratio propagates to a certain degree into the stratosphere, in particular in the tropics but also extending to mid-latitudes.[152] This must also be the case, then, for the seasonal cycle of the isotope signatures. The effect

should be clearly measurable for $\delta^{18}O$ in the tropics if the precision is sufficient.

5.2. Laboratory Studies

Yung et al.[145] proposed a mechanism for the transfer of the mass-independent oxygen isotope signature from O_3 to CO_2. In their scheme, $O(^1D)$ radicals from UV photolysis of O_3 and CO_2 form a short-lived CO_3* intermediate, which pre-dissociates after about $10^{-11}-10^{-12}$ s to $CO_2 + O(^3P)$.[153] Isotope transfer is possible via formation of the CO_3* intermediate. Yung et al.[145] showed that, when included in a one-dimensional photochemical model, this mechanism could reproduce the then-available ^{18}O enrichments in stratospheric CO_2 which increase with altitude from the tropopause.

$$O_3 + h\nu \rightarrow O(^1D) + O_2 \qquad \lambda < 315 \text{ nm} \quad \text{(R1)}$$

$$CO_2 + O(^1D) \rightarrow CO_3^* \quad \text{(R2)}$$

$$CO_3^* \rightarrow CO_2 + O(^3P) \quad \text{(R3)}$$

Only two sets of laboratory experiments have been published to date that investigate this isotope-transfer process in detail. The first study[154] confirmed that isotope exchange occurs but concluded that additional fractionation processes associated with the CO_3* intermediate must contribute. These experiments investigated the transfer process in pure O_3-CO_2 mixtures according to R1−R3. As realized by Yung et al.,[155] it was not taken into account that the $O(^3P)$ formed in R3 can react with O_2 (which builds up in the course of the reaction) to re-form O_3, so that the oxygen atoms cycle several times through O_3 before ending up as O_2. The recycled O_3 clearly has an isotopic composition different from that of the initial O_3, owing to the strong isotope effect in its formation. Thus, the isotopic composition of the O_3 reactant changes during the experiment without being continuously monitored, limiting the use of the results to obtain detailed insight into the fractionation process.

The second set of experiments[156] started with O_2-CO_2 mixtures. Photolysis of O_2 was used to produce O_3, which was then photolyzed again to exchange heavy isotopes with CO_2. The measurements revealed the temporal evolution and the final equilibrium value of the CO_2 and O_2 reservoirs. Similarly to case in the atmosphere, in these experiments O_3 was in isotopic equilibrium with O_2, and thus changes in O_2 reflected those in O_3. The results indicate that the isotope-transfer process shows many features of the two-component mixing proposed by Yung et al.,[155] but that other factors also contribute, as witnessed by a dependence on total pressure and CO_2 mixing ratio in the experiments. It appears that a systematic investigation of the full parameter space is necessary to understand the process in more detail.

The major challenge both laboratory investigations pose is that they produce a $\delta^{17}O-\delta^{18}O$ slope of approximately 1, rather than the 1.7 observed in the stratosphere. The reason for this large difference is not yet clear. Important parameters may be temperature and photolysis wavelength (both studies used Hg lamps and room temperature) and the isotopic composition of the initial O_2 (O_3) and CO_2 reservoirs. A new study is presently under review in which slopes similar to the ones in the stratosphere have been obtained (Chakraborty and Bhattacharia, personal communication), but the origin of the differences from the previous laboratory experiments and what exactly causes the preferential transfer of ^{17}O into CO_2 remain unknown at present.

5.3. The Isotope Exchange Process at the Molecular Level

To date, at least four different mechanisms have been proposed to explain the oxygen isotope transfer from O_3 to CO_2:

(1) Simple statistical mixing between the CO_2 and the $O(^1D)$ reservoirs according to R1−R3.[145,155]

(2) Isotope transfer according to R1−R3, including an additional mass-dependent fractionation process in the CO_3* complex.[157]

(3) Isotope transfer according to R1−R3, including an additional mass-independent fractionation (MIF) process in the CO_3* complex.[154,156]

(4) An additional (e.g., mesospheric) source of the mass-independent anomaly in stratospheric CO_2.[147]

From the molecular perspective, isotope transfer according to R1−R3 is governed by two important effects: first, the isotopic composition of the $O(^1D)$ reactant, and second, possible fractionation mechanisms in the formation and/or dissociation of the CO_3* complex. If the former is known, the latter can be derived, and thus a decision can be made between mechanisms 1−3 above. Unfortunately, the isotope signature of the $O(^1D)$ reactant cannot be directly measured, and it is not clear how it is related to the isotopic composition of its source molecule, O_3. Several aspects have to be considered here. First, it is well-established that ^{18}O is not distributed randomly in the O_3 molecule but favors the terminal positions at ambient temperatures (see the section on ozone). No experimental evidence is yet available for ^{17}O, but the rate constants for the symmetric ozone isotopologue from the Gao−Marcus theory[63] imply a similar nonrandom distribution for ^{17}O. If $O(^1D)$ is preferentially formed from the terminal oxygen atoms in ozone,[158] it may have, at the outset, an isotope signature significantly different than that of the parent O_3 (also see Lyons[159]). The intramolecular distribution of heavy oxygen in ozone should be temperature-dependent, and thus different for the presently available laboratory measurements compared to stratospheric data. Furthermore, a possible fractionation in the UV photolysis of ozone would further modify the isotopic composition of the $O(^1D)$ product. Finally, isotope fractionation in the quenching of $O(^1D)$ with O_2 and other gases may alter the isotopic composition of the fraction of $O(^1D)$ that is available for reaction with CO_2.

Given the lack of information on $O(^1D)$, it is problematic to decide between mechanisms 1−3 above. For mechanism 1 to be true, the $O(^1D)$ from stratospheric ozone must lie on the extrapolated fit line through the stratospheric CO_2 data, since a

simple mixing process proceeds along a straight line between the mixing reservoirs. For mechanisms 2 and 3, $O(^1D)$ could lie anywhere in the $\delta^{17}O-\delta^{18}O$ plane in principle, but a fractionation mechanism in the CO_3* complex would bring it back to the extrapolated fit line (with slope ≈ 0.5 for mechanism 2 and other slopes for mechanism 3). Of course, a valid transfer mechanism must also be able to explain the laboratory data. Johnston et al.[156] present arguments against mechanisms 1 and 2 based on their laboratory work and detailed modeling results, in particular from the $\delta^{17}O-\delta^{18}O$ slopes. Since the difference between the stratospheric and laboratory slope values is not understood yet, and may involve other parameters that are not understood in detail (temperature, wavelength, etc.), mechanisms 2 and 3 cannot yet be totally dismissed.

Regarding mechanism 4, the fact that the extrapolation of the stratospheric data precisely intersects the tropospheric isotope value indicates that the mechanism actually involves tropospheric CO_2, which gets progressively enriched in the stratosphere. A possible contribution of a mesospheric source at high altitudes cannot yet be excluded.

The central question as to whether the chemistry involving CO_3* introduces MIF independently of that caused by O_3 chemistry cannot yet be answered. The interesting aspect in Figure 4 is that the range in $\delta^{17}O$ and $\delta^{18}O$ values of stratospheric O_3 is large, while CO_2 seems to alter its isotopic composition systematically toward one single end-member. The relatively large reservoir of CO_2 is gradually modified, and one would conclude that exchange with O_3 of a well-defined composition dominates. The simplest working hypothesis is to assume no additional process of MIF in CO_3. Molecular beam experiments[160] are bound to give the necessary insight.

5.4. Applications for Atmospheric Research

Despite the lack of a thorough understanding of the $CO_2-O(^1D)$ isotope exchange on a molecular level, this exchange has interesting atmospheric applications. The mass-independent anomaly in CO_2 is a true stratospheric tracer, and therefore provides information about stratosphere−troposphere exchange. Near the tropopause, it is an indicator for tropospheric or stratospheric air, although its use there is likely to be of minor importance since generally other tracers are used, which can be measured easily and with high temporal/spatial resolution.

The ^{17}O anomaly is removed in the troposphere by exchange with water and the biosphere. Therefore, the equilibrium level of the CO_2 isotope anomaly in the troposphere (which still has to be determined with high precision) links two important global quantities, namely cross-tropopause transport and gross exchange of CO_2 with water and the biosphere.

In the stratosphere itself, the value of the anomaly increases as CO_2 ascends to higher altitudes and can be regarded as an integrating tracer for the $CO_2-O(^1D)$ interaction (and thus for $O(^1D)$ levels). Even up to 60 km altitude, CO_2 is not more than about 15‰ enriched in ^{18}O and 20‰ in ^{17}O (Figure 4). Assuming the $O(^1D)$ enrichment (including additional fractionations) to be in the range of stratospheric ozone, the equilibrium enrichment for CO_2 would be expected to be 3−5 times higher than observed, which means that roughly only every second CO_2 molecule exchanges with $O(^1D)$ during its ascent to 60 km.

The furthest developed application of the heavy isotope transfer from O_3 to CO_2 is the effect on the isotopic composition of atmospheric O_2, as noted by Bender et al.[161] The strong isotope enrichment in O_3 formation implies that the remaining O_2 is correspondingly depleted. Without transfer of the isotope anomaly to CO_2, the heavy oxygen atoms would simply be cycled through the O_x reservoirs as part of the Chapman cycle. When the ^{17}O excess is transferred via $O(^1D)$ to CO_2, however, it is lost from the O_x reservoirs; i.e., the transfer process represents a constant small leak of excess ^{17}O from O_2 to CO_2 (and finally to the large H_2O reservoir via isotope exchange in the troposphere). Over a time scale of about 1000 years (the exchange time of the atmospheric O_2 reservoir with the biosphere), this ^{17}O leak produces a measurable ^{17}O deficiency in atmospheric O_2.[162] At equilibrium, the magnitude of this ^{17}O deficiency is controlled by the stratospheric leak and global biosphere productivity. Measurements of $\delta^{17}O$ and $\delta^{18}O$ in atmospheric O_2 from air trapped in ice cores have accordingly been used to estimate global productivity on large time scales.[163,162] It must be noted that not only transfer of MIF from molecular oxygen, via CO_2 to the H_2O reservoir, plays a role. For more on this point we refer the reader to the article by Lyons.[159]

6. Nitrous Oxide, N_2O

Like CO_2, N_2O is a greenhouse gas, is of importance in biological processes, and from an atmospheric chemistry point of view plays a major role in stratospheric chemistry. In the stratosphere it has its two chemical sinks, namely photolysis and reaction with $O(^1D)$. N_2O has been studied intensively, including isotope studies that date back several decades.[164,165] We will review the case of N_2O in detail because its intramolecular nitrogen isotope distribution has been measured recently for the first time using optical and mass spectrometric techniques. Thus, not only $\delta^{18}O$ and the overall $\delta^{15}N$ value characterize N_2O isotopically. The latter can now be replaced by $^1\delta^{15}N$ and $^2\delta^{15}N$. Apart from this, N_2O appears to exhibit a small but distinct degree of MIF. This is, as we will see below, of special interest in the hunt for photochemical sources of this interesting trace gas.

6.1. Measurement and Analytical Techniques

Mass spectrometric and infrared absorption spectroscopic techniques are used in N_2O isotopic analyis. Absorption spectroscopy is nondestructive, less laborious in sample preparation, and discriminates against isotopic composition as well as structure. Until recently, only isotopologues,[10] e.g., $^{14}N_2O$ and $^{15}N_2O$, were accessible to mass spectrometric analyses, but not the isotopomers $^{14}N^{15}NO$ and $^{15}N^{14}NO$. Nevertheless, mass spectrometry was and is used on a wider scale than optical methods, because small samples

can be rapidly measured with high precision. Moreover, recent analytical developments have made possible the mass spectrometric analysis of N_2O isotopomers, i.e., the determination of the position-dependent nitrogen isotopic composition.

Early studies of the isotopic composition of N_2O used mass spectrometry to measure the average $^{15}N/^{14}N$ ratio.[164,166−168] Following this, infrared absorption spectroscopy with tunable diode lasers was developed for $^{18}O/^{16}O$ analysis.[169,170] Later, the first mass spectrometric dual-element ($^{15}N/^{14}N$, $^{18}O/^{16}O$) studies appeared.[171,172] Cliff and Thiemens[22] pioneered the $^{17}O/^{16}O$ analysis. The early mass spectrometry measurements involved decomposition of N_2O with analysis of either N_2 and/or CO_2[164,167,171,172] or N_2 and O_2.[22] An alternative way to measure the $^{17}O/^{16}O$ ratio was demonstrated by Röckmann et al.,[173] who converted N_2O to CO_2 and then reduced CO_2 with H_2 to $CH_4 + H_2O$, and finally oxidized H_2O to O_2 applying F_2.[20] Large sample sizes (micromole quantities) were required in all cases.

Direct injection of N_2O into a mass spectrometer was avoided initially for fear of contamination by CO_2 (also at masses 44, 45, and 46), which can considerably corrupt the N_2O isotope results, even if present in trace amounts only. Kim and Craig[174] solved this problem by applying a preparatory GC step. However, Tanaka et al.[175] showed that trace amounts of CO_2 could persist and still lead to errors. The influence of residual CO_2 can be corrected for by measuring so-called "interfering masses" at mass-to-charge ratios (m/z) 12 or 22, arising from $^{12}C^+$ and $^{12}C^{16}O_2^{2+}$.[23,175] Furthermore, continuous-flow techniques have been introduced for N_2O.[176]

FTIR spectroscopy[177] and tunable-diode laser absorption spectroscopy[178] can be used to measure the position-dependent ^{15}N abundance. These optical techniques measure the individual N_2O species directly. Recently, mass spectrometric techniques have been developed for the position-dependent ^{15}N analysis.[179,180] Mass spectrometry of N_2O (m/z 44, 45, 46) is used to obtain the ^{18}O and mean ^{15}N abundance. The NO^+ fragment in the spectrum is mainly derived from the central N atom, with only about 8% scrambling.[17,23,179,180] Measurements of the ion−current ratios at m/z 30 and 31, therefore, give essentially the ^{15}N abundance at the central N site. The ^{15}N abundance at the terminal N site can then be calculated by difference from the mean ^{15}N abundance, provided the absolute ^{15}N distribution in the reference gas is known. The N_2^+ fragment (m/z 28, 29) can be useful to gauge the $^{17}O/^{16}O$ isotope ratio, as explained below.

Since isotope ratio mass spectrometry cannot distinguish between species of equal mass numbers, corrections have to be applied to the measured molecular ion−current ratios in order to obtain the elemental isotope ratios. A reference material of known absolute isotopic composition is required to correct for mass discrimination effects and to convert the measured ion current ratios to "molecular isotope ratios" (e.g., ^{45}R, ^{46}R). The following relations between "molecular isotope ratios" and elemental isotope ratios then hold:

$$^{45}R = {}^{15}R_1 + {}^{15}R_2 + {}^{17}R$$

$$^{46}R = {}^{18}R + ({}^{15}R_1 + {}^{15}R_2){}^{17}R + {}^{15}R_1{}^{15}R_2$$

where $^{15}R_1$ and $^{15}R_2$ stand for the $^{15}N/^{14}N$ isotope ratios at the terminal and central nitrogen sites,[179] respectively.

Clearly, it is not possible to derive the desired elemental isotope ratios from measurements of "molecular isotope ratios" alone. The conventional approach is to define a mean nitrogen isotope ratio $^{15}R = {}^1/_2({}^{15}R_1 + {}^{15}R_2)$ and to assume that the geometric mean $({}^{15}R_1{}^{15}R_2)^{1/2}$ is well-approximated by the arithmetic mean.[23] Furthermore, covariance of ^{17}R and ^{18}R is expressed by a power law: $^{17}R = A(^{18}R)^{\beta}$. The three-isotope exponent β has to be determined by independent experiments. The coefficient A can be calculated from β and the isotope ratios of VSMOW. If β is close to 0.5, this is considered to be a mass-dependent relationship. On the basis of data from Cliff and Thiemens,[181] Kaiser[23] calculated a value of $\beta = 0.516$ for mass-dependently fractionated N_2O and a value of $A = 0.00937035$. However, atmospheric N_2O has an oxygen isotope anomaly (section 4.2.3) which, strictly speaking, has to be taken into account. The modified system of equations can then be solved numerically for ^{15}R and ^{18}R.

The NO^+ fragment is used to determine position-dependent ^{15}N isotope ratios. To account for the effect of scrambling in NO^+ formation, a scrambling coefficient s is introduced. s is the fraction of terminal N atoms ending up in NO^+:[17,23]

$$^{31}R_s = s\,{}^{15}R_1 + (1-s){}^{15}R_2 + {}^{17}R - \frac{s(1-s)({}^{15}R_1 - {}^{15}R_2)^2}{1 + s\,{}^{15}R_2 + (1-s){}^{15}R_1}$$

Toyoda and Yoshida[180] overlooked the last term in $^{31}R_s$. The isotopic composition of the N_2^+ fragment is given by

$$^{29}R = {}^{15}R_1 + {}^{15}R_2$$

Since the difference between the ratios ^{45}R and ^{29}R is equal to ^{17}R, the N_2^+ fragment can be used to measure the ^{17}O abundance.

With the four "molecular isotope ratios" ^{45}R, ^{46}R, $^{31}R_s$, and ^{29}R, it is possible to solve unambiguously for $^{15}R_1$, $^{15}R_2$, ^{17}R, and ^{18}R. Unfortunately, the precision of ^{29}R is limited to 0.025‰, which restricts the precision of ^{17}R to >0.5‰.[23] Conversion of N_2O to O_2 is therefore the preferred analytical technique to measure the $^{17}O/^{16}O$ isotope ratio of atmospheric N_2O.[181,182]

6.2. Atmospheric Applications

The available information on the isotopic composition of N_2O sources is limited. For a recent overview, see Gros et al.[126]

6.2.1. The Stratosphere and Photochemical Removal

Stratospheric N_2O is enriched in heavy isotopes due to isotopic fractionation in the stratospheric N_2O

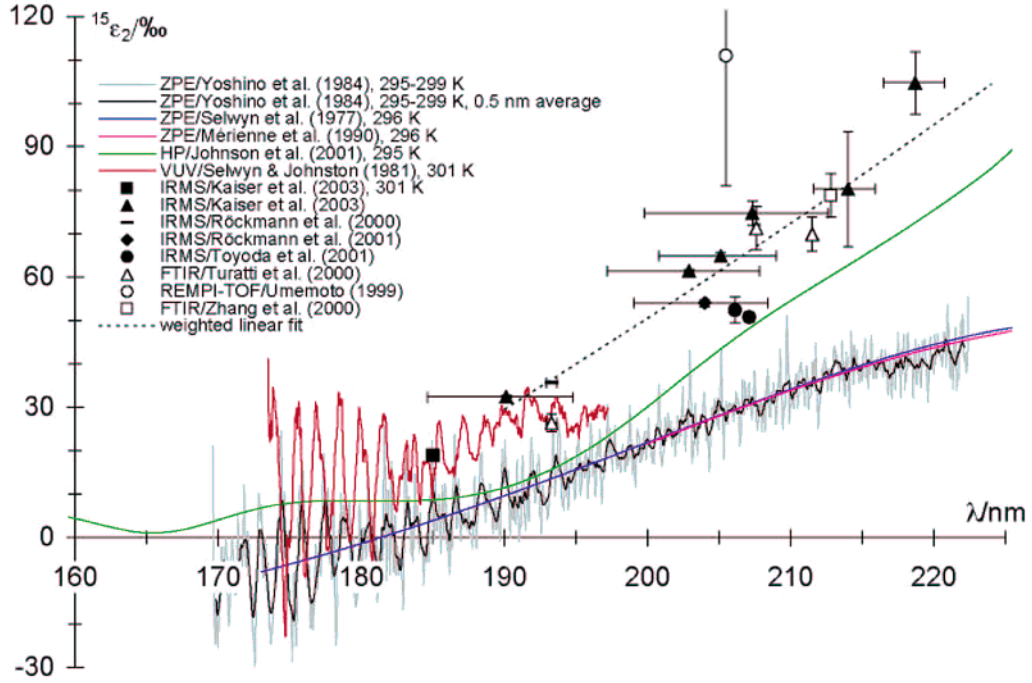

Figure 5. Wavelength dependence of $^{15}\epsilon_2$ (fractionation constant for the central nitrogen site) in N_2O at or about at room temperature. The curves labeled "ZPE" refer to predictions by the zero-point energy theory,[195] using high-resolution N_2O spectra from Yoshino et al. (1984)[294] or polynomial interpolations by Selwyn et al. (1977)[295] and Mérienne et al. (1990).[296] The "HP" curve is based on the hermite propagator theory from Johnson et al. (2001).[197] Experimental vacuum ultraviolet (VUV) measurements from Selwyn and Johnston (1981)[186] between 173 and 197 nm are also shown. Experimental results from photodissociation experiments with mercury lamps or lasers at "single" wavelengths and with broadband lamps over wider wavelength ranges are represented by individual symbols. The results from broadband irradiations are shown at the median photodissociation wavelength (calculated from the overlap of lamp spectrum and N_2O absorption cross sections), where "x-errors" indicate the first and last quartile of the integrated photolysis rates. Measurements by isotope ratio mass spectrometry (IRMS) are from Kaiser et al. (2003),[203] Röckmann et al. (2000 and 2001),[173,190] and Toyoda et al. (2001).[191] Fourier transform infrared spectroscopic (FTIR) analyses were made by Turatti et al. (2000)[192] and Zhang et al. (2000),[194] whereas Umemoto (1999)[193] used resonance-enhanced multiphoton ionization time-of-flight mass spectrometry (REMPI-TOF) of the $O(^1D)$ product to measure the $^{15}\epsilon_2$ fractionation constant.

sink reactions, photolysis (R1), and reaction with $O(^1D)$ (R2 and R3).

$$N_2O + h\nu \rightarrow N_2 + O(^1D) \quad (185\ \text{nm} < \lambda < 230\ \text{nm}) \quad (90\%) \quad \text{(R1)}$$

$$N_2O + O(^1D) \rightarrow 2\ NO \quad (6\%) \quad \text{(R2)}$$

$$N_2O + O(^1D) \rightarrow N_2 + O_2 \quad (4\%) \quad \text{(R3)}$$

The percentages in parentheses give the relative importance of each loss process.[183] Maximum N_2O photolysis rates occur at 195−205 nm, but, depending on altitude and latitude, there are contributions down to 185 nm and up to 230 nm. Reaction R2 is the major source of stratospheric nitrogen oxides (NO_x) and plays a key role in ozone cycling.[184,185]

Isotopic enrichment of stratospheric N_2O was noted early by Moore.[164] Laboratory measurements of absorption cross sections of N_2O isotopologues by Selwyn and Johnston,[186] as well as direct photolysis experiments by Yoshida,[187] showed that stratospheric N_2O photolysis could cause this enrichment. Thus, Kim and Craig[174] concluded that the isotopic enrichment of tropospheric N_2O relative to its surface sources is caused by the back-mixing flux of heavy stratospheric N_2O. The subsequent laboratory measurements by Johnston et al.[188] then came as a surprise, because they showed no significant isotopic fractionation due to N_2O photolysis at 185 nm, and only negligible fractionation by the second N_2O sink, reaction with $O(^1D)$. The observed oxygen fractionation constants (ϵ) in the latter case were $^{18}\epsilon = k(N_2{}^{16}O)/k(N_2{}^{18}O) - 1 \approx 6‰$ and $^{17}\epsilon = k(N_2{}^{16}O)/k(N_2{}^{17}O) - 1 \approx 3‰$, with k being the reaction rate coefficient of $O(^1D)$ with the individual N_2O isotopologues.

Later, both experimental[173,189−194] and theoretical work[195−198] demonstrated that N_2O photolysis does cause wavelength-dependent fractionation. Since photolysis (R1) comprises approximately 90% of the global N_2O sink, it is also the major cause of isotopic fractionation. Measurements of stratospheric samples obtained from balloon platforms[173,199−201] and by remote sensing (FTIR spectroscopy)[202] confirmed the heavy isotope enrichment of stratospheric N_2O.

Most laboratory studies (results are compiled in Figure 5) used specific wavelengths. Röckmann et al.[173] first used a broadband ultraviolet lamp with a photolysis spectrum similar to stratospheric actinic flux. Kaiser et al.[203] acquired additional data both with broadband light sources and at 185 nm, and reviewed the available experimental data and theoretical predictions to compile an overview of the wavelength dependence of isotopic fractionation by N_2O photolysis, including the position-dependent ^{15}N fractionation. The isotopic enrichment in the residual

N_2O was always highest at the central nitrogen site, followed by oxygen and the terminal nitrogen site. This pattern extended over the entire wavelength region that had been subject to experimental studies (namely from 185 to about 220 nm). The isotopic enrichment was largest at the longest wavelengths (with highest ϵ values of 105‰ for the central nitrogen atom at 219 nm), qualitatively in agreement with predictions from zero-point energy (ZPE) theory, which explains the isotopic fractionation in N_2O photolysis by small shifts in the ZPE upon isotopic substitution. Only at 185 nm was a small isotopic depletion found for ^{15}N at the terminal nitrogen site ($^{15}\epsilon_1 = -10.3 \pm 0.3$‰) and for ^{18}O ($^{18}\epsilon = -3.7 \pm 0.1$‰). The small discrepancy between these results and the previous measurements for ^{18}O was explained by analytical artifacts in the study by Johnston et al.[188] The measurements at the "single wavelengths" of 185 and 193 nm were in striking agreement with the vacuum ultraviolet (VUV) spectroscopic measurements reported by Selwyn and Johnston.[186] Unfortunately, the latter study only measured the absorption of nitrogen isotopologues of N_2O and only covered the wavelength region between 173 and 197 nm. New VUV spectroscopic measurements of the entire stratospherically relevant wavelength interval are currently underway (P. von Hessberg, personal communication, 2003).

Kaiser et al.[204] performed experiments at stratospherically relevant temperatures down to 193 K. Fractionation increased toward lower temperatures. The relative changes were in the order $^{14}N^{15}N^{16}O > {}^{14}N_2{}^{18}O > {}^{15}N^{14}N^{16}O$, the same as for the absolute values. In this study, a previously overlooked artifact in laboratory measurements was also discovered. At high degrees of conversion, N_2O loss by reaction with $O(^1D)$ becomes important, presumably due to the photochemical production and subsequent photolysis of NO_2 in the reactor. The effect increased with N_2O concentration and reduced the absolute value of the measured fractionation constants, requiring corrections for initial N_2O mixing ratios of 4 mmol/mol. Subsequent work on double-substituted $^{15}N_2{}^{16}O$ by the same authors[205] and at least one previous study[189] showed similar artifacts.

Fractionation of $^{15}N_2{}^{16}O$ was even larger than that for $^{14}N^{15}N^{16}O$. The pertinent fractionation constant (designated $^{15}\epsilon_{1+2}$) matched the sum of individual ^{15}N fractionation constants at the terminal ($^{15}\epsilon_1$) and central nitrogen sites ($^{15}\epsilon_2$). This corresponds to a statistical relationship between isotopic fractionation of $^{15}N^{14}N^{16}O$, $^{14}N^{15}N^{16}O$, and $^{15}N_2{}^{16}O$. On the basis of theoretical considerations, Kaiser et al.[205] concluded that other polysubstituted N_2O isotopologues and isotopomers should also be fractionated by photolysis, in line with a statistical rule. Therefore, $^{15}N_2O$ is likely to be present at its statistically predicted abundance.

Further quantum-theoretical work by Johnson et al.[197] included effects other than ZPE which are influenced by isotopic substitution, such as contributions of vibrationally excited N_2O in the ground state, the shape of the ground-state wave function, the transition dipole moment, and the dynamics of the excited state. The experimental oxygen isotope fractionation constants were reproduced nearly quantitatively; better agreement was achieved than with the ZPE theory for $^{14}N^{15}N^{16}O$, but the disagreement was equal or worse for $^{15}N^{14}N^{16}O$ and $^{15}N_2{}^{16}O$. The discrepancies were attributed to the two-dimensional potential energy surface used for the calculations, which only considers the NN−O distance and the bending angle, but no changes in the N−NO distance.[206] The simulated spectra therefore lacked the "fine structure" seen in the ZPE predictions and VUV spectroscopic measurements. Blake et al.[198] pursued a simpler semiempirical approach that dealt with some of the deficiencies of the ZPE theory and achieved good agreement with the experimental data, including the $^{15}N^{14}N^{16}O$ isotopomer, without resorting to full-fledged quantum chemistry.

Isotopic fractionation in the second stratospheric N_2O sink, reaction with $O(^1D)$, was investigated by Kaiser et al.[207] No dependence of the fractionation constants on temperature, pressure, mixing ratio, or reactor type was observed. The pattern of fractionation constants was clearly distinct from photolysis, with the largest fractionation occurring for ^{18}O ($^{18}\epsilon = -12$‰), followed by the terminal ($^{15}\epsilon_1 = -9$‰) and the central ($^{15}\epsilon_2 = -2$‰) nitrogen atoms. This opens up the possibility of distinguishing N_2O sinks using position-dependent ^{15}N isotope measurements of N_2O (see below).

Isotopic analysis of stratospheric N_2O[173,174,199−202] showed enrichments of all heavy isotopes toward higher latitudes and altitudes, along with the progressive degree of destruction of N_2O. The relative enrichments were in the same order as for N_2O photolysis ($^{14}N^{15}N^{16}O > {}^{14}N_2{}^{18}O > {}^{15}N^{14}N^{16}O$), confirming the view that photolysis is mainly responsible for the isotopic enrichment. Maximum enrichments (vs air N_2 and V-SMOW, respectively) were $^1\delta^{15}N \approx 40$‰ (terminal nitrogen atom), $^2\delta^{15}N \approx 140$‰ (central N atom), and $\delta^{18}O \approx 120$‰. The trend could be described by a Rayleigh fractionation pattern in which the isotopic composition of the remaining substrate is described by $\delta = y^{-\epsilon/(1+\epsilon)} - 1$, with y being the ratio of stratospheric to tropospheric $^{14}N_2{}^{16}O$ (i.e., only the lightest isotopologue). To derive the fractionation constant ϵ, a linearized plot of $\ln(1 + \delta)$ versus $\ln y$ is often used, and y can be very well approximated by the ratio of stratospheric to tropospheric N_2O.[207] The apparent fractionation constants calculated from stratospheric observations have consistently been smaller than the values measured in the laboratory, with the exception of the FTIR measurements by Griffith et al.[202] This can be attributed to the interplay between transport, mixing, and chemistry. Current reanalyses of the FTIR spectra do, however, yield a smaller fractionation constant (D. Griffith, personal communication).

To give an example, the apparent fractionation constants (ϵ_{app}) in a regime consisting of a chemical reaction combined with one-dimensional diffusion are expected to vary between $(1 + \epsilon)^{1/2} - 1 \approx {}^1/_2\epsilon$ (diffusion-limited) and ϵ (reaction-limited), with ϵ being the fractionation constant for the reaction alone (the

derivation by Rahn et al.[189] is flawed). More generally, a value of

$$\epsilon_{app} = \frac{1 - \sqrt{1+Q}}{1 - \sqrt{1+Q+Q\epsilon}} - 1$$

can be derived, with the parameter $Q = 4H_{av}^2k/K_z$, where H_{av} is the scale height, K_z is the diffusion coefficient, and k is the reaction rate constant for the isotopically light N_2O species.[23] In the latter work, the effect of linear mixing on the apparent fractionation constant was also investigated. In the case of mixing between tropospheric (non-photolyzed) and stratospheric (photolyzed) air masses, ϵ_{app} was shown to fall into an interval between $-y_B\delta_B/[1 - y_B(1 + \delta_B)]$ and ϵ, where y_B is the ratio of the stratospheric to the tropospheric mixing and δ_B represents the isotopic composition of stratospheric N_2O.

Intercomparisons of the data on stratospheric N_2O isotopes were published by Kaiser[23] and McLinden et al.[206] Kaiser[23] re-evaluated some of the data, as in the original studies ϵ values were often derived approximately from plots of δ versus ln y rather than ln$(1 + \delta)$ versus ln y,[199,202] or used another definition of ϵ[173] (such as the alternative $\epsilon' = -\epsilon/(1 + \epsilon)$). In all data sets, the magnitude of lower stratospheric ϵ_{app} is smaller than its middle stratospheric value, due to the aforementioned effects of mixing and diffusion. However, ratios of apparent fractionation constants also change between the middle and lower stratosphere.[173,201] Such changes cannot be caused by transport processes, but must be attributed to changes in photochemistry.[207] Two diagnostic values have been defined in order to detect changes in photochemistry, free from the influence of transport effects: $\eta = {}^{15}\epsilon_2/{}^{15}\epsilon_1$ and $\psi = {}^{18}\epsilon/{}^{15}\epsilon$. ψ_{app} showed only minor variations, but η_{app} was clearly higher in the middle stratosphere than in the lower stratosphere.[23] Changes in photolysis wavelength or temperature would not lead to the observed change in η_{app}; the most likely cause is the contribution of $O(^1D)$, which is much larger in the lower than in the middle stratosphere. Kaiser[23] estimated the contribution of the $O(^1D)$ sink to be 10% for the middle stratosphere, and 40% in the lower stratosphere. The former value is in agreement with the integrated value for the total stratosphere.

6.2.2. Tropospheric N_2O

Rahn and Wahlen[208] tried to establish a trend in $\delta^{15}N$ and $\delta^{18}O$ from historic N_2O isotope measurements, but the available data had insufficient precision and accuracy. There is no certified reference material for isotopic analysis of N_2O gas, and so each laboratory relies on its own calibration of a reference gas relative to atmospheric N_2 and VSMOW. Recent studies report values for $\delta^{15}N$ of 7.0 ± 0.6‰[200] and 6.7 ± 0.1‰,[17,23] and values for $\delta^{18}O$ of 43.7 ± 0.9‰ and 44.6 ± 0.2‰, in both cases for mixing ratios of 316 ± 2 nmol/mol. The agreement within errors is all the more noteworthy, because both studies relied on independent calibrations of their working reference gas and used different techniques.

Regrettably, the data on the position-dependent ^{15}N isotope signature of tropospheric N_2O reported by Yoshida and Toyoda[200] and Kaiser[17,23] are clearly different. Whereas the former study reports ${}^1\delta^{15}N = -2.35‰$ and ${}^2\delta^{15}N = 16.35‰$ for the terminal and central nitrogen atoms, respectively, the latter study finds a much larger "site preference" $({}^2\delta^{15}N - {}^1\delta^{15}N)$ of 45.8 ± 1.1‰. This large deviation from the former study's value of 18.7 ± 2.2‰[200] must be a consequence of the position-dependent isotopic calibration of the reference gas,[23] since the position-dependent isotopic composition of N_2O is nearly constant throughout the troposphere. The position-dependent calibrations in both studies were based on entirely different approaches: Yoshida and Toyoda prepared N_2O from ammonium nitrate (NH_4NO_3) of known isotopic composition and assumed that the NH_4^+−N transfers to the terminal N atom in N_2O and the NO_3^-−N to the central N atom. In contrast, Kaiser et al.'s approach was based on a mass spectrometric technique using $^{15}N_2{}^{16}O$-enriched samples of their reference gas and measuring ${}^{31}\delta$ and ${}^{46}\delta$ values of the enriched samples relative to the reference gas. The reference gases of Yoshida−Toyoda and Kaiser also differ in the average $\delta^{15}N$ (−1.9‰ vs 1.0‰) and $\delta^{18}O$ (23.3‰ vs 38.5‰), so that differences in the position-dependent ^{15}N values seem plausible, but nevertheless the results for tropospheric N_2O should be the same. It should also be noted that the approach by Kaiser et al. does depend on the correctness of the absolute isotope ratios of VSMOW and air N_2.

The $\delta^{18}O$ values for tropospheric N_2O reported by Cliff et al.[181] are lower than in any other published study and show a rather large variability, although no significant variations in the N_2O mixing ratios were reported. This study used a method based on conversion of N_2O to N_2 and O_2 and subsequent cryogenic separation of N_2 and O_2. The discrepancy might point to both calibration and analytical problems, since a laboratory study on isotopic fractionation in N_2O photolysis[188] which used the same analytical procedure to measure $\delta^{17}O$ and $\delta^{18}O$ seems to have suffered from similar difficulties, as discussed by Kaiser.[23]

6.2.3. MIF in N_2O

A rigorous definition of MIF, which does not involve any approximation in its derivation from the basic mass-dependent fractionation law for fractionation constants (e.g., ${}^{17}\alpha = {}^{18}\alpha^{\beta}$), is given by $\Delta^{17}O \equiv (1 + \delta^{17}O)/(1 + \delta^{18}O)^{\beta} - 1$.[16,23] β is the three-isotope exponent for mass-dependently fractionated N_2O, and equals 0.516.[23,181] δ values must be expressed relative to VSMOW. If $\delta^{17}O$ is expressed relative to another reference gas (e.g., air-O_2) which lies on another mass-dependent fractionation line with VSMOW (e.g., 0.510 in the case of air-O_2), a correction factor has to be included in the definition of $\Delta^{17}O$:

$$\Delta^{17}O = \frac{1 + \delta^{17}O_{air}}{(1 + \delta^{18}O_{air})^{\beta}}[1 + \delta^{18}O_{VSMOW}(air)]^{0.510-0.516} - 1$$

In light of the new definition and the discovery that a correction to $\Delta^{17}O$ is required if it is measured

relative to air-O_2, Kaiser[23] re-evaluated the results of Cliff and Thiemens[181] and Röckmann et al.,[182] and obtained ^{17}O excesses of $\Delta^{17}O = 0.85 \pm 0.19‰$ and $0.93 \pm 0.08‰$.

A number of reactions have been proposed to explain the origin of the ^{17}O excess, including $N_2 + NO_2^*/NO_3^*$,[209] $N_2 + CO_3^*$,[210] $N_2 + O_3^*$,[211,212] UV photolysis,[196,197] and $N_2 + O(^1D)$.[213] Subsequent experiments have partly ruled out the importance of some of these sources, such as $N_2 + NO_2^*$,[214] $N_2 + CO_2^*$,[215] $N_2 + OO_3^*$,[213] and photolysis.[23,182,188] Röckmann et al.[182] proposed the reaction of $NH_2 + NO_2$ as a source due to the fact that the strong coupling between O_3 and NO_x in the atmosphere is expected to impart a fraction of the ^{17}O excess in O_3 to NO_2, which then transfers it to N_2O. Initially, the reaction of $NH_2 + NO_2$ alone was believed to be sufficient to explain most of the oxygen isotope anomaly in N_2O (0.8‰ out of 0.9‰), as it was assumed to contribute between 2% and 7% to the global N_2O source strength, with a best estimate of 3.4%.[216] However, measurements of the branching ratio of the $NH_2 + NO_2$ reaction[217−220] found contributions of only 19−24% for the N_2O product channel, compared to previous estimates of 95%.[37] This indicates a smaller contribution (∼0.2‰) of this source to the ^{17}O excess of atmospheric N_2O. Estupiñán et al.[213] estimated the contribution of their proposed $N_2 + O(^1D)$ source to the total N_2O emissions to be 1.4%, and suggested that this reaction would account for 0.4‰ of the ^{17}O excess in N_2O, assuming $\Delta^{17}O(O_3) = 30‰$. Another source of excess ^{17}O in N_2O may be denitrification of atmospheric nitrate, which owes its oxygen isotope anomaly to NO_x and ultimately O_3.[221] Since some denitrifiers are slow to exchange oxygen with water (a characteristic that was exploited in a method to measure the oxygen isotopic composition of nitrates[222]), even some biologically produced N_2O is expected to have an oxygen isotope anomaly, although biological processes in general are expected to fractionate isotopes in line with a mass-dependent fractionation law.[223]

6.2.4. The Global N_2O Isotope Budget

Early budget calculations[174,200,224] attempted to close the N_2O budget, assuming steady-state conditions. The return flux of isotopically enriched N_2O from the stratosphere was assumed to balance the isotopically light emission from microbial N_2O at the earth's surface. However, due to the growth in N_2O, a small trend is expected in the isotope ratio as well, although this effect has not yet been verified directly. Data from Antarctic firn air samples allow us to infer current trends of $0.041^{+0.05}_{-0.03}‰/a$ in $\delta^{15}N$ and $0.025^{+0.06}_{-0.04}‰/a$ in $\delta^{18}O$.[225] Sowers et al.[226] performed similar measurements. The derived changes in $\delta^{15}N$ and $\delta^{18}O$ over the past century were in agreement in the two studies, although the work of Röckmann et al. involved an extrapolation, since the mean age of the firn air did not exceed 35 years. From Röckmann et al.,[225] changes of $1.8 \pm 0.2‰$ and $1.0 \pm 0.3‰$ could be derived, whereas Sowers et al.[226] gave $1.7 \pm 0.3‰$ and $0.9 \pm 0.4‰$ for $\delta^{15}N$ and $\delta^{18}O$, respectively.

Model predictions are in relatively good agreement with the measured trends. On the basis of the available information on N_2O sources, Rahn and Wahlen[208] estimated the present trends in both $\delta^{15}N$ and $\delta^{18}O$ to be $0.03‰/a$. Pérez et al.[227] performed new measurements of the isotopic composition of N_2O emissions from fertilized tropical soils and updated the prediction for $\delta^{15}N$ to $0.04-0.06‰/a$. McLinden et al.[206] used an atmospheric chemistry transport model to calculate the isotopic fractionation in the stratospheric sinks (rather than in situ measurements of the isotopic composition of lower stratospheric N_2O) and arrived at trends of $0.04-0.06‰/a$ for $\delta^{15}N$ and $0.01-0.02‰/a$ for $\delta^{18}O$, depending on the assumed isotopic fractionation in stratospheric photolysis.

Concluding the overview of the exciting progress on N_2O, we remark that although the isotope measurements are in agreement with budget calculations as far as the partitioning between ocean/terrestrial sources is concerned, future work will have to show to what degree isotope measurements can constrain budget estimates indeed.

7. Carbon Monoxide, CO

The situation for CO is similar to that of CH_4, with four exceptions. Foremost, CO has in situ sources which makes it necessary to determine their isotopic signatures. Weston[228] tackled the problem of calculating the ^{18}O isotopic composition of CO from CH_4 oxidation by OH. Second, atmospheric CO displays MIF,[229−231] and interestingly the origin of its "mass-independent" composition has two causes, as we will see further along. Anyway, it means that there are three independent isotopic signals in CO, namely for ^{13}C, ^{17}O, and ^{18}O. The third difference from CH_4 is that the study of ^{14}CO, which is an ultratrace gas with a source (mainly cosmogenic ^{14}C) that is largely decoupled from the common CO sources, has great merit because ^{14}CO is a tracer for assessing global OH. Yet, even though neither the application nor the detection of ^{14}CO is based on its radioactivity, we will not consider it in this review. We merely note its uniqueness and that isotopic analysis of CO compared to CH_4 has this extra dimension. The fourth distinction between CO and CH_4 is that the signals of isotope variation of tropospheric CO are large. This obviously reflects its shorter lifetime, in the presence of fairly large KIEs. For reviews of the isotopic composition of CO, we refer the reader to Brenninkmeijer et al.[232] and Gros et al.[126]

7.1. Measurement and Laboratory Studies

Isotopic analysis used to be solely based on the oxidation of CO to CO_2, followed by mass spectrometric analysis. By using acidified I_2O_5 as oxidant, merely an O atom is added to the CO molecule without the formed CO_2 undergoing isotopic exchange. The principle of this method has been implemented in GC−IRMS systems,[233] and in any case the system has to be calibrated for the isotopic change due to the I_2O_5. Alternatively, but also using GC−IRMS, CO is separated from air, followed by

direct analysis of mass 28, 29, and 30 of the CO.[234] After the pioneering work by Stevens et al.[235] on the KIEs for ^{13}C and ^{18}O in the reaction of CO with OH, which constitutes the main loss process, these values have been confirmed in later work. For ^{13}C, the KIE ranges from 6‰ (at 1 bar) to about −3‰ at 0.2 bar. Thus, at lower pressures the isotope effect changes from the usual fractionation into inverse fractionation. Upon ^{18}O substitution, $C^{18}O$ reacts about 10‰ faster than $C^{16}O$, with little pressure dependence ($\alpha = 0.99$). This also is an inverse isotope effect (note, however, the two opposite conventions for defining α).

A theoretical explanation for the inverse fractionation for ^{18}O has not been given yet. A renewed interest in the reaction CO + OH, which is one of the most studied gas-phase reactions, arose after ^{17}O analyses. The analysis of CO extracted from air samples collected in New Zealand[229] established that the fractionation for ^{17}O was not half of that for ^{18}O, as confirmed later in more detail.[230,236] One cause for MIF in tropospheric CO could be identified, i.e., the formation of CO from the reaction of O_3 with unsaturated hydrocarbons. Given the presence of MIF in O_3, the transfer of an oxygen (via ozonolysis) from O_3 to product CO constitutes a small source of CO that acquires MIF from O_3.[237] The strength of this source, however, did not explain the magnitude measured in atmospheric samples.

Although it is highly plausible that CO from combustion sources does not possess MIF due to high temperatures, it has not been experimentally excluded that the production of CO from the oxidation of CH_4 produces MIF. Notwithstanding, by investigating the sink reaction CO + OH in the laboratory,[238] it could be established that MIF occurs (tropospheric fractionation ($\Delta^{17}O$) about 4‰), and the magnitude was sufficient to explain the atmospheric signal (Figure 1). The challenge is that there is no theory yet that explains why the frequently studied reaction CO + OH causes MIF. Theoretical work is in progress (R. Marcus, private communication, 2002). It is noted that, in the complex reaction CO + OH, the unstable intermediate HOCO, which can be de-energized through collision with a third body, plays a central role. It introduces the pressure dependence in the reaction rate and forms an ideal playground for studying the hitherto unrecognized isotopic behavior. The laboratory studies and the atmospheric observations in Spitsbergen of the annual cycle of all CO isotopes confirm the picture that during summer, when the CO inventory declines due to reaction with OH, ^{18}O declines strongly whereas ^{17}O does not follow suit.

7.2. Atmospheric Applications

The general features of isotope variations in CO[232] can be compiled as follows: ^{13}C shows a very clear annual cycle, with low ^{13}C values in late summer, when the contribution of CO from CH_4 oxidation peaks. However, the effect of pollution, from biomass burning or from fossil fuel combustion, is surprisingly small. The ^{13}C data thus show little scatter on a clear seasonal cycle. The reason atmospheric CO has a ^{13}C composition close to that of combustion products, and not lower due to input of light CO from methane oxidation, is the kinetic isotope effect in the reaction with OH. This raises $\delta^{13}C$ again close to the value of combustion products. We note that the ^{13}C budget of CO in the SH could not be closed. Basically, the values measured in summer were not as low as expected on the basis of the relatively large contribution of light CO from CH_4 oxidation. A low yield had to be assumed.[239] Alternatively, fractionation occurs in the pathway from CH_4 via HCHO to CO. This is a strong impetus to do laboratory work.

^{18}O in CO reflects clearly the input of CO from combustion sources, which input CO with a $\delta^{18}O$ value close to that of atmospheric O_2 (+23.8‰ V-SMOW). As such, ^{18}O is an excellent indicator of input of CO from pollution. However, with increasing distance from the source, $\delta^{18}O$ rapidly drops ($\epsilon = -10‰$) due to CO + OH. Again, $\delta^{18}O$ of CO from CH_4 oxidation or of other reduced precursors is not known yet.[228]

Bergamaschi et al.[240] have used the existing atmospheric CO isotope measurement results in inverse modeling, which has led to useful constraints on the CO budget. However, questions about the isotopic composition of various sources remain (their Table 3). With the advent of GC−IRMS, more CO isotope data will most probably become available, and continued modeling of the isotopes will indeed lead to quantitative results for this important trace gas.

8. Hydrogen, H_2

Following a spate of early work exploring the isotopic composition (including tritium) of atmospheric hydrogen, this gas has received relatively little attention in general. This has changed, in particular in view of the awareness of a changing chemistry in the stratosphere. Increasing methane leads to increasing stratospheric H_2O. Furthermore, H_2 is a potential future energy carrier and, when used on a large scale, may affect the atmospheric H_2 budget significantly.[241] From an isotopic point of view, H_2 being a light molecule, the substitution with deuterium strongly affects its main physical properties. Therefore, with the soil sink being important for the tropospheric budget, in particular in the northern hemisphere, fractionation which depends on the diffusion into the soil and the uptake by bacteria will be large. But the reaction with OH shows a very large KIE,[242] and the impact on the isotopic composition from the partitioning between the soil sink and photochemical removal will be strong.

8.1. Measurement and Isotope Effects

The elaborate method of separating H_2 from hundreds of liters of air via oxidation to H_2O, that subsequently had to be reduced again to H_2 for mass spectrometric analysis, has been abolished in favor of the GC−IRMS method that now allows D/H analysis of samples of less than 1 L of air.[243−245]

The largest sink of atmospheric H_2 is uptake in soils by microbial activity. The associated KIE has been reported by Gerst and Quay[245] and Rahn et al.[246]

as 1.060 ± 0.027 and 1.063 ± 0.012, respectively for soils in Washington and Alaska. Although these values suggest fairly constant fractionation, more measurements in different ecosystems are required.

The photochemical sink for H_2 is the reaction with OH. Two determinations came up with essentially the same result for the KIE of 1.65 ± 0.05 [242] and 1.68 ± 0.1. [247] In the stratosphere, H_2 reacts also with $O(^1D)$, with a fractionation factor of 1.0 ± 0.2,[248] and with Cl radicals. The KIE for Cl is 1.4 times that of OH at room temperature.[249] No experiments have been carried out yet for stratospheric temperatures.

8.2. Atmospheric Applications

Gerst and Quay[244] and Rahn et al.[243] report δD values for H_2 over the North Pacific of ~120‰ (V-SMOW). Compared to earlier data, this may mean an increase of 35‰ over two decades, but the older data[250] may not have been of sufficient quality to allow firm conclusions. Gerst and Quay[244] observed that, in the southern hemisphere, δD values are 15 ± 8.5‰ enriched relative to the northern hemispheric values. Although this difference is statistically significant, it is premature to discuss the possible causes/implications without better knowing seasonal and spatial variations.

Considering the low δD values of the surface emissions of H_2 (biomass burning, fossil fuel combustion, bacterial processes, with low δ values from −800 to −250‰), it has been questioned why atmospheric H_2 is enriched in deuterium. Ehhalt et al.,[242] assuming the soil sink and OH sink strength to be about equal, attributed the enrichment to the kinetic isotope effect in the reaction with OH, but this analysis does not comply with the later work by Novelli[251] (the soil sink accounts for 75−80% of all losses). Gerst and Quay[245] speculated that photochemical production of H_2 from the precursors CH_4 and non-methane hydrocarbons would be enriched in deuterium by up to 130 ± 70‰.

Extreme deuterium enrichments are reported for the stratosphere. Measurements by Rahn et al.[252] and Röckmann et al.[253] reveal that, in the stratosphere, δD increases from 130‰ near the tropopause to over 400‰ at altitudes where the CH_4 concentration has dropped to about 700 nmol/mol. By this, the stratosphere has recently been identified as a source of isotopically heavy H_2, and the budget calculations could be reconciled accordingly. At the same time, the overall fractionation factor for the formation of H_2 from CH_4 under stratospheric conditions could be inferred to be 1.31.[252] Concerning future scenarios, model calculations have shown the effect of possible increased anthropogenic emissions of H_2 on the stratospheric H_2O budget.[241]

9. Water Vapor in the Stratosphere, H_2O

Isotopic information may help to solve issues related to transport and to the in situ source of stratospheric water vapor. The power of remote sensing for retrieving isotopic information cannot be better illustrated than by the studies of stratospheric water vapor using balloon-borne, satellite- and Space Shuttle-based spectrographs. It also allows the simultaneous measurements of CH_4 and water vapor, which is a logical combination with CH_4 oxidation being the in situ source of H_2O. Several studies, e.g., by Keith,[254] use the isotopic composition of H_2O for solving the difficult problem of transport of tropospheric H_2O into the stratosphere. Basically, δD of H_2O vapor entering the stratosphere is measured to be about −650‰,[255,256] whereas a value of almost −900‰ is calculated from the depletion due to precipitation formation and the kinetic isotope effect during transport through the cold upper troposphere. Excluding the kinetic effect ($\delta^{18}O$ does not support a kinetic effect) still leaves a discrepancy. A final answer, and the question to what degree evaporation from lofted ice particles plays a role, cannot be given yet.

Ridal et al.[257] give a 1D model, involving H_2 and CH_4 oxidation, for calculating HDO in the tropical stratosphere and indicate that they also would like to model ^{18}O in future work. Comparison with ATMOS data shows a reasonable agreement, and both model and measurements show a wave pattern due to the annual tropospheric changes. A 2D simulation of upper atmospheric water vapor (deuterium only) is given by Ridal.[130] Simulations at polar latitudes remain problematic, and there appears to be uncertainty about which fractionation factors in CH_4 with OH, $O(^1D)$, and Cl should be used. A thorough analysis of the isotopic composition of stratospheric water vapor is given by Bechtel and Zahn.[258]

Because of the great difficulty of collecting stratospheric water vapor without contamination or isotopic exchange, and the spatial limitation of such datasets, it seems that remote sensing and further improved modeling will continue to help to better understand the important water budget of the stratosphere. Nonetheless, one cannot escape the impression that it is the challenge of sampling stratospheric water vapor without isotopic contamination and/or exchange for accurate isotopic assay that needs to be taken on, sooner rather than later.

10. Hydrogen Peroxide, H_2O_2

Seeking information on the oxidation pathway of sulfur dioxide, the existing techniques were based on degassed rainwater treated with $KMnO_4$ to convert H_2O_2,without isotopic alteration, into O_2. Because this O_2 was isotopically normally assayed after conversion to CO_2, information on ^{17}O was lost. Savarino and Thiemens[259] refined this technique, omitting however the conversion to CO_2, and discovered MIF in H_2O_2 in over 30 rainwater samples precipitating from mostly air masses from the Pacific reaching La Jolla winter 1997−1998. The $\delta^{18}O$ values range from about 21.9‰ to over 51.5‰, and thus reflect enrichments of about 0−25‰ over atmospheric oxygen ($\delta^{18}O$ = 23.8‰). The values of $\Delta^{17}O$ are significant and range from 1.2‰ to 2.4‰, whereas nonenvironmental H_2O_2 was clearly shown to be mass-dependently fractionated, with a slope of 0.511 over a range of almost 60‰ in $\delta^{18}O$. The offset relative to the mass-dependent fractionation line for the laboratory/industry-produced H_2O_2 samples is

almost constant. It seems that the constant offset under a wide range of $\delta^{18}O$ values in H_2O_2 from rain suggests large mass-dependent fractionation of H_2O_2 that initially possesses a modest but significant degree of MIF. Using laboratory experiments reacting $H + O_2$, Savarino and Thiemens[260] demonstrated that MIF could be formed in O_2 and H_2O_2. A $\delta^{17}O/\delta^{18}O$ slope of 0.84 was derived with $\delta^{18}O$ values spanning about 100‰. The preliminary conclusion was that this indicated the origin of MIF in atmospheric H_2O_2.

Lyons[159] shows (by assuming rather high values for ^{18}O in O_3) that two-thirds of MIF measured in H_2O_2 can probably be explained by $OH + O_3 \rightarrow HO_2 + O_2$. Thus, upon the demise of an O_3 molecule due to reaction with OH, part of its MIF is inherited by HO_2, leading to MIF in H_2O_2. We note the strong effect of MIF in the asymmetric O_3 molecule. No MIF in HO_2 appears if there is assumed to be exchange between either OH or HO_2 and molecular oxygen. This is not so likely, however. Therefore, a small MIF signal in H_2O_2 can probably be explained via $OH + O_3$, which unambiguously links MIF in H_2O_2 to that of O_3. It seems that the values detected in rainwater are somewhat higher. We tend to note that, because of the small signal in H_2O_2 compared to O_3, extreme care has to be taken in experiments. Any trace of O_2 produced during the treatment of rainwater samples with $KMnO_4$ related to O_3, or nitrates, could affect these difficult experiments.

The laboratory experiments in which HO_2 was produced from $H + O_2$ show a strong degree of MIF. The only caveat again is that any type of O_3 chemistry must be totally excluded from having been possible. The authors checked the absence of ozone, as traces of it should have been visible by a blue color. The possible formation of atomic oxygen via $H + HO_2 \rightarrow H_2O + O$, possibly leading to O_3, has not yet been considered.

11. Formaldehyde, HCHO

The rapid turnover of this most abundant carbonyl component leads to low concentrations, which renders even its concentration measurements difficult. Basically, when trace gas measurements are relatively rare due to low abundance, one would not easily contemplate isotopic analysis. However, isotope measurements can, at times, give direct experimental evidence otherwise not available. This insight has inspired Johnson and Dawson[261] to undertake isotope measurements of formaldehyde. They reported $\delta^{13}C$ values of −17‰ (remote continental NH) to −28.3‰ (Baring Head, New Zealand). The difference was supposed to reflect the different contributions of HCHO derived from CH_4 (cf. Manning et al.[239]), which has $\delta^{13}C$ values of about −47‰, i.e., much lower than that of hydrocarbons. Tanner et al.[262] collected samples from the coastal region of Nova Scotia, obtaining −18.0‰ to −24.3‰, with an average of −22.8‰. Knowing that the $\delta^{13}C$ value of nonmethane hydrocarbons[263,264] is around −26 ‰ and that the KIEs for NMHCs with OH range from 0.5‰ to 12‰,[265] thus leading to depletion of the HCHO reservoir, and taking the low $\delta^{13}C$ value of CH_4 into account, leads us to consider that there must be isotope fractionation for ^{13}C in the removal processes of HCHO.

Concerning controlled experiments, Stone at al.[266] performed photolysis experiments using sunlight and found a KIE of 1.025. Beukes et al.[267] monitored the concentrations of HCHO isotopomers using FTIR spectroscopy during the reaction with halogen atoms. Recently, D'Anna et al.[268] reported KIEs for ^{13}C and D in the reaction with OH and NO_3 radicals (also using doubly deuterated formaldehyde). Interestingly, little fractionation was reported in the reaction with OH.[268] Since this radical removes half of all HCHO, it must be the photolysis of HCHO that causes isotopic fractionation for carbon. It is concluded that there is a strong and urgent need for laboratory experiments involving the photolysis HCHO under different conditions. Atmospheric measurements remain a major challenge, but in particular when measurement of deuterium would be feasible, this would certainly offer interesting insights.

12. Carbonylsulfide, OCS

Adequately quantifying the role of OCS in the formation of the Junge layer remains a test case for atmospheric scientists. In the lower troposphere, OCS behaves similarly to CO_2; i.e., during increased photosynthesis at the mid and higher latitudes, more COS is taken up by vegetation via the stomata. OCS that is not removed this way, or via chemical removal, will find its way into the stratosphere, where its role as supplier of sulfur for the sulfate aerosol layer in relation to other sources still has to be defined. It has been possible to detect $OC^{34}S$ using high-resolution balloon-borne and ground-based infrared solar absorption spectra.[269] Leung et al.[297] used the abundance and ^{34}S measurements from a large number of balloon flights at different latitudes to infer an average apparent fractionation constant of −68.7‰ (their Table 1). This fractionation constant of −68.7‰ indicates a strong depletion of OCS by photolysis. The authors point out that, consequently, stratospheric sulfate should have δ values around 80‰. This is in conflict with fairly old SSA data from Castleman et al.[270] Either OCS contributes very little to stratospheric sulfate, even at times of little volcanic influence, or the fraction of OCS destroyed in the stratosphere is in error. In conclusion, there is much uncertainty about an important trace gas. When one, at this point, briefly contemplates that OCS has 24 isotopomers (three oxygen isotopes, four sulfur isotopes, and two stable carbon isotopes), the door to the laboratory seems to be wide open (although $^{17}O^{13}C^{36}S$ is pretty rare).

13. Sulfate, SO_4^{2-}

Isotopic measurements of airborne sulfate have been carried out for several decades, with the anthropogenic contribution to the sulfur cycle being a main point of focus. Tropospheric SO_2 is not expected to exhibit MIF because its oxygen readily exchanges with that of H_2O. The basis for interest in ^{17}O and ^{18}O in sulfates is that oxidation of SO_2 in the atmosphere in the aqueous phase can transfer oxygen

from both O_3 and H_2O_2 to the product sulfate.[271,272] Thus, sulfates may show MIF, and its measurement may reveal something about the oxidation pathway in the liquid phase. Bearing in mind that sulfates are retained in ice cores and do not exchange oxygen, there are important applications.[3] Several interesting papers by Thiemens and co-workers have been published, and a powerful GC−IRMS technique for sulfur and oxygen isotopes has been developed.[273]

The oxidation of SO_2 via OH is not expected to induce MIF, because tropospheric OH, although it acquires MIF via $O(^1D)$, exchanges rapidly with H_2O. The absence of MIF was confirmed by Savarino et al.[274] This study reports ^{17}O values from a systematic series of experiments. The measurement of sulfate oxygen is difficult and requires several preparative steps. Savarino et al. do show that, when H_2O_2 with MIF is used as oxidant, about half of the MIF reappears in the sulfate. Thus, two of the four oxygen atoms are from this oxidant. For oxidation by O_3, one-fourth of the original MIF appears. A final test concerning oxidation by O_2, catalyzed by metal ions, shows a mass-dependent behavior. Thus, despite the complexity of the oxidation pathways of SO_2, two sources of MIF were clearly identified.

La Jolla rainwater and aerosol sulfate show $\delta^{18}O$ values from 5‰ to 15‰, with $\Delta^{17}O$ increasing from near zero to approximately 1.5‰. Sulfate extracted from the Vostok ice core[150] allowed reconstruction of $\Delta^{17}O$ during glacial times. The authors correct for primary sulfates, neglect the minor contribution to ^{17}O from H_2O_2-based oxidation, and propose that the changes in $\Delta^{17}O$ from 1.3‰ to 4.8‰ between glacial and interglacial periods reflect changes in the oxidation pathway in the troposphere. The sulfate signals are generally small[275] yet provide unique information. Of the two sources of MIF in sulfate, i.e., O_3 and H_2O_2, the former strongly dominates. Whereas primary sulfate from combustion is mass-dependently fractionated in oxygen and sulfur isotopes,[276] the photolysis of SO_2 produces MIF,[277] and sulfates from several origins (e.g., desert varnishes)[278,279] have been found to exhibit a very small degree of MIF.

14. Nitrate, NO_3^-

There has been interest in the isotopic analysis of ^{15}N and ^{18}O of nitrate for over two decades, and the awareness that, through the reaction of NO + O_3, NO_2 and ultimately atmospheric nitrate obtains MIF has sparked off exciting work using ^{17}O analysis. Because of the important role of NO in the oxidative cycle of the troposphere and its role with respect to stratospheric ozone and denitrification, there understandably is strong interest in isotope signals.

Michalski et al.[221] report a robust method for measuring the isotopic composition, including ^{17}O of nitrate. After application of several preparative chemical conversions, ^{17}O, ^{18}O, and ^{15}N can be analyzed. Applying the above technique, Michalski and Hernandez et al.[280,281] could demonstrate a substantial and rather constant MIF ($\Delta^{17}O \approx 23‰$) in atmospheric nitrate, based on aerosol collected on filters. This signal is fairly high compared to that of tropospheric O_3 but agrees well with a value of 22‰ derived by Lyons,[159] by assuming that $\Delta^{17}O(HNO_3) = {}^2/_3\Delta^{17}O(NO_2)$. Essential is the assumption that, in NO + O_3, a terminal oxygen atom from O_3 is transferred to NO_2 without scrambling. Michalski et al.[282] report a time series of $\Delta^{17}O$ for nitrate aerosols collected in La Jolla, showing a seasonal change from between about 23‰ in June to about 29‰ in January. Using a photochemical box model for polluted marine boundary layer air and the transfer of MIF from O_3, the values could be reproduced. Hastings et al.[283] used a denitrifier method to reduce rainwater nitrate to N_2O, which allows imultaneous measurements of the oxygen and nitrogen isotope composition of nitrate, although $\Delta^{17}O$ values are obtained with limited precision only. Seasonal variations of the $\delta^{15}N$ and $\delta^{18}O$ values of rainwater nitrate were interpreted as source- and chemistry-driven signals, respectively.

Finally, we reiterate that Lyons also calculated an extreme scenario in which MIF in H_2O_2, NO, and NO_2 in the troposphere is very low. This was achieved by assuming the oxygen isotopic exchange between HO_2 and OH with O_2 to be at the upper limit of published values. Realizing the difficulty of measuring these exceedingly small rate constants, it is probable that these two processes do not play a role. This scenario also contradicts the presence of MIF in H_2O_2 and is unlikely because of the detection of MIF in H_2O_2. Therefore, it is safe to assume that MIF in nitrate is (almost) entirely due to MIF in O_3, and that further experiments to confirm or deny this are necessary.

15. Prospects

For refining our understanding of the chemistry of atmospheric trace compounds, their tropospheric and stratospheric budgets, and their physical and chemical links, isotopic analyses will play an appreciable role. The increase in the number of observations in recent times shows a massive acceleration, thanks to GC−IRMS becoming commonplace. Along with careful experiments in the laboratory, isotope analysis of atmospheric constituents has quite suddenly reached the necessary critical mass. It has harvested the beneficial interest from those who develop and apply 2D and 3D mathematical models of the transport and chemistry of the atmosphere. We witness how this field, that once heavily relied on qualitative interpretations, has also gained solid support from laboratory kineticists. Concomitantly, the calculation of isotope effects in chemical reactions has been given a strong impetus, and the complexity of the ozone system forms a worthy challenge.

Concerning ozone—the most intensively studied atmospheric trace gas—one can say that its complex isotopic makeup has been revealed after decades of experiments and theoretical work by many researchers, and much credit goes to Konrad Mauersberger and co-workers, in Minnesota and later in Heidelberg, for the relentless hunt with the finest of tools for catching the true isotopic character of this intriguing molecule.

Concerning MIF, and the story is far from complete yet, work has to be done toward guiding this science from discussing "slopes" (MIF as "missing information on fractionation") to delivering improved, quan-

titative understanding at the process level. In particular, gas-phase reactions lend themselves to this excellently. The quest for hitherto unknown fractionation effects is valuable, and the findings have several applications—not only in the atmosphere—and inspire young scientists. Much credit goes to the prolific work by the group of Mark Thiemens at UCSD. Each occurrence of MIF of the oxygen isotopes, however, has to be viewed critically against the large effect in ozone, a molecule with extensive chemical links which we truly start to appreciate by tracing its isotopic signature to several trace gases, particulate species, and radicals in the atmosphere. In the end, the future will show how many, or how few, reaction schemes in the atmosphere do induce MIF, independent of that of ozone.

16. Note Added in Proof

Results for crossed molecular beam experiments for $O(^1D) + CO_2$ have now become available.[298]

17. References

(1) Kaye, J. A. *Rev. Geophys.* **1987**, *25*, 1609.
(2) Johnson, M. S. F., K. L.; von Hessberg, P.; Nielsen, O. J. *Chem. Soc. Rev.* **2002**, *31*, 313.
(3) Thiemens, M. H. *Science* **1999**, *283*, 341.
(4) Weston, R. E., Jr. *Chem. Rev.* **1999**, *99*, 2115.
(5) Mauersberger, K.; Krankowsky, D.; Janssen, C. *Space Sci. Rev.* **2003**, *106*, 265.
(6) Coplen, T. B.; Krouse, H. R.; Böhlke, J. K. *Pure Appl. Chem.* **1992**, *64*, 907.
(7) Coplen, T. B. *Geochim. Cosmochim. Acta* **1996**, *60*, 3359.
(8) Coplen, T. B.; Krouse, H. R. *Nature* **1998**, *392*, 32.
(9) Coplen, T. B. *Compilation of Minimum and Maximum Isotope Ratios of Selected Elements in Naturally Occurring Terrestrial Materials and Reagents*; U.S. Geological Survey: Washington, DC, 2002.
(10) Müller, P. *Pure Appl. Chem.* **1994**, *66*, 1077.
(11) Clayton, R. N.; Grossman, L.; Mayeda, T. K. *Science* **1973**, *182*, 485.
(12) Thiemens, M. H.; Heidenreich, J. E. *Science* **1983**, *219*, 1073.
(13) Li, W. J.; Meijer, H. A. J. *Isot. Environ. Health Stud.* **1998**, *34*, 349.
(14) Young, E. D.; Galy, A.; Nagahara, H. *Geochim. Cosmochim. Acta* **2002**, *66*, 1095.
(15) Matsuhisa, Y.; Goldsmith, J. R.; Clayton, R. N. *Geochim. Cosmochim. Acta* **1978**, *42*, 173.
(16) Miller, M. F. *Geochim. Cosmochim. Acta* **2002**, *66*, 1881.
(17) Kaiser, J.; Park, S.; Boering, K. A.; Brenninkmeijer, C. A. M.; Hilkert, A. W.; Röckmann, T. *Anal. Bioanal. Chem.* **2003**, in press.
(18) Assonov, S. S.; Brenninkmeijer, C. A. M. *Rapid Commun. Mass Spectrom.* **2003**, *17*, 1007.
(19) Angert, A.; Rachmilevitch, S.; Barkan, E.; Luz, B. *Global Biogeochem. Cycles* **2003**, *17*, 10.1029/2002GB001933.
(20) Brenninkmeijer, C. A. M.; Röckmann, T. *Rapid Commun. Mass Spectrom.* **1998**, *12*, 479.
(21) Assonov, S. S.; Brenninkmeijer, C. A. M. *Rapid Commun. Mass Spectrom.* **2001**, *15*, 2426.
(22) Cliff, S. S.; Thiemens, M. H. *Anal. Chem.* **1994**, *66*, 2791.
(23) Kaiser, J. Ph.D. thesis, Johannes Gutenberg-Universität Mainz, 2002.
(24) Mauersberger, K. *Geophys. Res. Lett.* **1981**, *8*, 935.
(25) Chapman, S. *Mem. R. Met. Soc.* **1930**, *3*, 103.
(26) Steinfeld, J. I.; Adler-Golden, S. M.; Gallagher, J. W. *J. Phys. Chem. Ref. Data* **1987**, *16*, 911.
(27) Larsen, N. W.; Pedersen, T.; Sehested, J. *Int. J. Chem. Kinet.* **1991**, *23*, 331.
(28) Janssen, C.; Guenther, J.; Krankowsky, D.; Mauersberger, K. *J. Chem. Phys.* **1999**, *111*, 7179.
(29) Hippler, H.; Rahn, R.; Troe, J. *J. Chem. Phys.* **1990**, *93*, 6560.
(30) Kaye, J. A.; Strobel, D. F. *J. Geophys. Res.—Oceans Atmos.* **1983**, *88*, 8447.
(31) Janssen, C.; Guenther, J.; Mauersberger, K.; Krankowsky, D. *Phys. Chem. Chem. Phys.* **2001**, *3*, 4718.
(32) Urey, H. C. *J. Chem. Soc. (London)* **1947**, 562.
(33) Bigeleisen, J.; Goeppert-Mayer, M. *J. Chem. Phys.* **1947**, *15*, 261.
(34) Brasseur, G.; Solomon, S. *Aeronomy of the Middle Atmosphere*; Reidel Publ. Co.: Dordrecht, The Netherlands, 1984.
(35) *Scientific Assessment of Ozone Depletion: 1998*; Ennis, C. A., Ed.; WMO: Geneva, 1999.
(36) Houston, P. L.; Suits, A. G.; Toumi, R. *J. Geophys. Res.—Atmos.* **1996**, *101*, 18829.
(37) DeMore, W. B.; Sander, S. P.; Golden, D. M.; Hampson, R. F.; Kurylo, M. J.; Howard, C. J.; Ravishankara, A. R.; Kolb, C. E.; Molina, M. J. *Chemical kinetics and photochemical data for use in stratospheric modeling*; Evaluation No. 12; Jet Propulsion Laboratory, California Institute of Technology, 1997.
(38) Anderson, S. M.; Morton, J.; Mauersberger, K.; Yung, Y. L.; Demore, W. B. *Chem. Phys. Lett.* **1992**, *189*, 581.
(39) Heidenreich, J. E.; Thiemens, M. H. *J. Chem. Phys.* **1983**, *78*, 892.
(40) Heidenreich, J. E.; Thiemens, M. H. *J. Chem. Phys.* **1986**, *84*, 2129.
(41) Bains-Sahota, S. K.; Thiemens, M. H. *J. Chem. Phys.* **1987**, *91*, 4370.
(42) Thiemens, M. H.; Jackson, T. *Geophys. Res. Lett.* **1987**, *14*, 624.
(43) Thiemens, M. H.; Jackson, T. *Geophys. Res. Lett.* **1988**, *15*, 639.
(44) Thiemens, M. H.; Jackson, T. *Geophys. Res. Lett.* **1990**, *17*, 717.
(45) Morton, J.; Barnes, J.; Schueler, B.; Mauersberger, K. *J. Geophys. Res.—Atmos.* **1990**, *95*, 901.
(46) Yang, J. M.; Epstein, S. *Geochim. Cosmochim. Acta* **1987**, *51*, 2011.
(47) Yang, J. M.; Epstein, S. *Geochim. Cosmochim. Acta* **1987**, *51*, 2019.
(48) Morton, J.; Schueler, B.; Mauersberger, K. *Chem. Phys. Lett.* **1989**, *154*, 143.
(49) Mauersberger, K.; Morton, J.; Schueler, B.; Stehr, J.; Anderson, S. M. *Geophys. Res. Lett.* **1993**, *20*, 1031.
(50) Wolf, S.; Bitter, M.; Krankowsky, D.; Mauersberger, K. *J. Chem. Phys.* **2000**, *113*, 2684.
(51) Anderson, S. M.; Morton, J.; Mauersberger, K. *Chem. Phys. Lett.* **1989**, *156*, 175.
(52) Christensen, L. K.; Larsen, N. W.; Nicolaisen, F. M.; Pedersen, T.; Sørensen, G. O.; Egsgaard, H. *J. Mol. Spectrosc.* **1996**, *175*, 220.
(53) Larsen, N. W.; Pedersen, T. *J. Mol. Spectrosc.* **1994**, *166*, 372.
(54) Larsen, N. W.; Pedersen, T.; Sehested, J. In *Isotope Effects in Gas-Phase Chemistry*; Kaye, J. A., Ed.; ACS Symposium Series 502; American Chemical Society: Washington, DC, 1992.
(55) Larsen, R. W.; Larsen, N. W.; Nicolaisen, F. M.; Sørensen, G. O.; Beukes, J. A. *J. Mol. Spectrosc.* **2000**, *200*, 235.
(56) Sehested, J.; Nielsen, O.; Egsgaard, H. *J. Geophys. Res.—Atmos.* **1995**, *100*, 20979.
(57) Sehested, J.; Nielsen, O.; Egsgaard, H.; Larsen, N. W.; Andersen, T. S.; Pedersen, T. *J. Geophys. Res.—Atmos.* **1998**, *103*, 3545.
(58) Anderson, S. M.; Hülsebusch, D.; Mauersberger, K. *J. Chem. Phys.* **1997**, *107*, 5385.
(59) Guenther, J.; Erbacher, B.; Krankowsky, D.; Mauersberger, K. *Chem. Phys. Lett.* **1999**, *306*, 209.
(60) Guenther, J.; Krankowsky, D.; Mauersberger, K. *Chem. Phys. Lett.* **2000**, *324*, 31.
(61) Janssen, C.; Guenther, J.; Krankowsky, D.; Mauersberger, K. *Chem. Phys. Lett.* **2003**, *367*, 34.
(62) Gao, Y. Q.; Marcus, R. A. *J. Chem. Phys.* **2002**, *116*, 137.
(63) Gao, Y. Q.; Marcus, R. A. *Science* **2001**, *293*, 259.
(64) Hathorn, B. C.; Marcus, R. A. *J. Chem. Phys.* **1999**, *111*, 4087.
(65) Hathorn, B. C.; Marcus, R. A. *J. Chem. Phys.* **2000**, *113*, 9497.
(66) Gross, A.; Billing, G. D. *Chem. Phys.* **1997**, *217*, 1.
(67) Gellene, G. I. *Science* **1996**, *274*, 1344.
(68) Baker, T. A.; Gellene, G. I. *J. Chem. Phys.* **2002**, *117*, 7603.
(69) Robert, F.; Camy-Peyret, C. *Ann. Geophys.* **2001**, *19*, 229.
(70) Miklavc, A.; Peyerimhoff, S. D. *Chem. Phys. Lett.* **2002**, *359*, 55.
(71) Charlo, D.; Clary, D. C. *J. Chem. Phys.* **2002**, *117*, 1660.
(72) Babikov, D.; Kendrick, B. K.; Walker, R. B.; Pack, R. T.; Fleurat-Lessard, P.; Schinke, R. *J. Chem. Phys.* **2003**, *119*, 2577.
(73) Schinke, R.; Fleurat-Lessard, P.; Grebenshchikov, S. Y. *Phys. Chem. Chem. Phys.* **2003**, *5*, 1966.
(74) Heidenreich, J. E.; Thiemens, M. H. *Geochim. Cosmochim. Acta* **1985**, *49*, 1303.
(75) Anderson, S.; Mauersberger, K. *Rev. Sci. Instrum.* **1981**, *52*, 1025.
(76) Anderson, S. M.; Mauersberger, K.; Morton, J.; Schueler, B. In *Isotope Effects in Gas-Phase Chemistry*; Kaye, J. A., Ed.; ACS Symposium Series 502; American Chemical Society: Washington, DC, 1992.
(77) Mauersberger, K.; Erbacher, B.; Krankowsky, D.; Gunther, J.; Nickel, R. *Science* **1999**, *283*, 370.
(78) Janssen, C. Ph.D. thesis, Ruprecht-Karls Universität Heidelberg, 1999.
(79) Sheppard, M. G.; Walker, R. B. *J. Chem. Phys.* **1983**, *78*, 7191.
(80) Gellene, G. I. *J. Chem. Phys.* **1991**, *96*, 4387.
(81) Griffith, K. S.; Gellene, G. I. *J. Chem. Phys.* **1991**, *96*, 4403.
(82) Yoo, R. K.; Gellene, G. I. *J. Chem. Phys.* **1995**, *102*, 3227.
(83) Yoo, R. K.; Gellene, G. I. *J. Chem. Phys.* **1996**, *105*, 177.
(84) Janssen, C. *Science* **2001**, *294*, 951A.

(85) Marcus, R. A. *Science* **2001**, *294*, 951A.
(86) Siebert, R.; Schinke, R.; Bittererova, M. *Phys. Chem. Chem. Phys.* **2001**, *3*, 1795.
(87) Siebert, R.; Fleurat-Lessard, P.; Schinke, R.; Bittererova, M.; Farantos, S. C. *J. Chem. Phys.* **2002**, *116*, 9749.
(88) Fleurat-Lessard, P.; Grebenshchikov, S. Y.; Siebert, R.; Schinke, R.; Halberstadt, N. *J. Chem. Phys.* **2003**, *118*, 610.
(89) Hernández-Lamoneda, R.; Salazar, M. R.; Pack, R. T. *Chem. Phys. Lett.* **2002**, *355*, 478.
(90) Rosmus, P.; Palmieri, P.; Schinke, R. *J. Chem. Phys.* **2002**, *117*, 4871.
(91) Anderson, S. M.; Klein, F. S.; Kaufman, F. *J. Chem. Phys.* **1985**, *83*, 1648.
(92) Wiegell, M. R.; Larsen, N. W.; Pedersen, T.; Egsgaard, H. *Int. J. Chem. Kinet.* **1997**, *29*, 745.
(93) Babikov, D.; Kendrick, B. K.; Walker, R. B.; Pack, R. T.; Fleurat-Lessard, P.; Schinke, R. *J. Chem. Phys.* **2003**, *119*, 2577.
(94) Babikov, D.; Kendrick, B. K.; Walker, R. B.; Schinke, R.; Pack, R. T. *Chem. Phys. Lett.* **2003**, *372*, 686.
(95) Babikov, D.; Kendrick, B. K.; Walker, R. B.; Pack, R. T.; Fleurat-Lesard, P.; Schinke, R. *J. Chem. Phys.* **2003**, *118*, 6298.
(96) Fleurat-Lessard, P.; Grebenshchikov, S. Y.; Schinke, R.; Janssen, C.; Krankowsky, D. *J. Chem. Phys.* **2003**, *119*, 4700.
(97) Bhattacharya, S., K.; Thiemens, M. H. *Geophys. Res. Lett.* **1988**, *15*, 9.
(98) Wen, J.; Thiemens, M. H. *Chem. Phys. Lett.* **1990**, *172*, 416.
(99) Chakraborty, S.; Bhattacharya, S. K. *J. Chem. Phys.* **2003**, *118*, 2164.
(100) Valentini, J. J. *J. Chem. Phys.* **1987**, *86*, 6757.
(101) Valentini, J. J.; Gerrity, D. P.; Phillips, D. L.; Jong-Chen, N.; Tabor, K. D. *J. Chem. Phys.* **1987**, *86*, 6745.
(102) Miller, R. L.; Suits, A. G.; Houston, P. L.; Toumi, R.; Mack, J. A.; Wodtke, A. M. *Science* **1994**, *265*, 1831.
(103) Rogaski, C. A.; Price, J. M.; Mack, J. A.; Wodtke, A. M. *Geophys. Res. Lett.* **1993**, *20*, 2885.
(104) Geiser, J. D.; Dylewski, S. M.; Mueller, J. A.; Wilson, R. J.; Toumi, R.; Houston, P. L. *J. Chem. Phys.* **2000**, *112*, 1279.
(105) Krankowsky, D.; Janssen, C.; Mauersberger, K. *J. Geophys. Res.−Atmos.* **2003**, *108*, doi 10.1029/2002JD003320.
(106) Mauersberger, K. *Geophys. Res. Lett.* **1987**, *14*, 80.
(107) Schueler, B.; Morton, J.; Mauersberger, K. *Geophys. Res. Lett.* **1990**, *17*, 1295.
(108) Krankowsky, D.; Lämmerzahl, P.; Mauersberger, K. *Geophys. Res. Lett.* **2000**, *27*, 2593.
(109) Stehr, J.; Krankowsky D.; Mauersberger, K. *J. Atmos. Chem.* **1996**, *24*, 317.
(110) Rinsland, C. P.; Malathy Devi, V.; Flaud, J.-M.; Camy-Peyret, C.; Smith, M. A.; Stokes, G. M. *J. Geophys. Res.* **1985**, *90*, 10719.
(111) Meier, A.; Notholt, J. *Geophys. Res. Lett.* **1996**, *23*, 551.
(112) Irion, F. W.; Gunson, M. R.; Rinsland, C. P.; Yung, Y. L.; Abrams, M. C.; Chang, A. Y.; Goldman, A. *Geophys. Res. Lett.* **1996**, *23*, 2377.
(113) Goldman, A.; Murray, F. J.; Murcray, D. G.; Kosters, J. J.; Rinsland, C. P.; Flaud, J.-M.; Camy-Peyret, C.; Barbe, A. *J. Geophys. Res.−Atmos.* **1989**, *94*, 8467.
(114) Abbas, M. M.; Guo, J.; Carli, B.; Mencaraglia, F.; Carlotti, M.; Nolt, I. G. *J. Geophys. Res.−Atmos.* **1987**, *92*, 13231.
(115) Carli, B.; Park, J. H. *J. Geophys. Res.−Atmos.* **1988**, *93*, 3851.
(116) Johnson, D. G.; Jucks, K. W.; Traub, W. A.; Chance, K. V. *J. Geophys. Res.−Atmos.* **2000**, *105*, 9025.
(117) Mauersberger, K.; Lämmerzahl, P.; Krankowsky, D. *Geophys. Res. Lett.* **2001**, *28*, 3155.
(118) Flaud, J.-M.; Bacis, R. *Spectrochim. Acta, Part A* **1998**, *54*, 3.
(119) Bhattacharya, S. K.; Chakraborty, S.; Savarino, J.; Thiemens, M. H. *J. Geophys. Res.−Atmos.* **2002**, *107*, art. no. 4675.
(120) Krankowsky, D.; Bartecki, F.; Klees, G. G.; Mauersberger, K.; Schellenbach, K.; Stehr, J. *Geophys. Res. Lett.* **1995**, *22*, 1713.
(121) Johnston, J. C.; Thiemens, M. H. *J. Geophys. Res.−Atmos.* **1997**, *102*, 25395.
(122) Johnston, J. C. Ph.D. thesis, University of California, San Diego, 1996.
(123) *Atmospheric Methane*; Khalil, M. A. K., Ed.; Springer: Berlin, 2000.
(124) Wuebbles, D. J.; Hayhoe, K. *Non-CO_2 Greenhouse Gases: Scientific Understanding, Control and Implementation*; Noordwijkerhout: The Netherlands, 2000; p 1.
(125) Bréas, O.; Guillou, C.; Reniero, F.; Wada, E. *Isot. Environ. Health Stud.* **2002**, *37*, 257.
(126) Gros, V.; Brenninkmeijer, C. A. M.; Jöckel, P.; Kaiser, J.; Lowry, D.; Nisbet, E. G.; O'Brien, P.; Röckmann, T.; Warwick, N. In *Emissions of chemical species and aerosols into the atmosphere*; Granier, C., Ed.; Kluwer: Dordrecht, The Netherlands, 2003.
(127) Conny, J. M.; Currie, L. A. *Atmos. Environ.* **1996**, *30*, 621.
(128) Rice, A. L.; Gotoh, A. A.; Ajie, H. O.; Tyler, S. C. *Anal. Chem.* **2001**, *73*, 4104.
(129) Rice, A. L.; Tyler, S. C.; McCarthy, M. C.; Boering, K. A.; Atlas, E. *J. Geophys. Res.−Atmos.* **2003**, *108*, doi 10.1029/2002JD003042.
(130) Ridal, M. *J. Geophys. Res.−Atmos.* **2002**, *107*, art. no. 4285.
(131) Miller, J. B.; Mack, K. A.; Dissly, R.; White, J. W. C.; Dlugokencky, E. J.; Tans, P. P. *J. Geophys. Res.* **2002**, *D13*, 10.1029/2001JD000630.
(132) Brenninkmeijer, C. A. M.; Müller, R.; Crutzen, P. J.; Lowe, D. C.; Manning, M. R.; Sparks, R. J.; van Velthoven, P. F. J. *Geophys. Res. Lett.* **1996**, *23*, 2125.
(133) Röckmann, T.; Brenninkmeijer, C. A. M.; Crutzen, P. J.; Platt, U. *J. Geophys. Res.−Atmos.* **1999**, *104*, 1691.
(134) McCarthy, M. C.; Connell, P.; Boering, K. A. *Geophys. Res. Lett.* **2001**, *28*, 3657.
(135) Wang, J. S.; McElroy, M. B.; Spivakovsky, C. M.; Jones, D. B. A. *Global Biogeochem. Cycles* **2002**, *16*, 1046 (doi: 10.1029/2001GB001572).
(136) Verkouteren, R. M.; Lee, J. N. *Fresenius J. Anal. Chem.* **2001**, *370*, 803.
(137) Zyakun, A. M.; Brenninkmeijer, C. A. M. International Conference on the Study of Environmental Change Using Isotope Techniques, Vienna, Austria, 2001.
(138) Ciais, P.; Tans, P. P.; White, J. W.; Trolier, M.; Francey, R. J.; Berry, J. A.; Randall, D. R.; Sellers, P. J.; Collnatz, J. G.; Schimel, D. S. *J. Geophys. Res.−Atmos.* **1995**, *100*, 5051.
(139) Levin, I.; Ciais, P.; Langenfelds, R.; Schmidt, M.; Ramonet, M.; Sidorov, K.; Tchebakova, N.; Gloor, M.; Heimann, M.; Schulze, E. D.; Vygodskaya, N. N.; Shibistova, O.; Lloyd, J. *Tellus* **2002**, *54B*, 696.
(140) Farquhar, G. D.; Lloyd, J.; Taylor, J. A.; Flanagan, L. B.; Syvertsen, J. P.; Hubick, K. T.; Wong, S. C.; Ehleringer, J. R. *Nature* **1993**, *363*, 439.
(141) Trolier, M.; White, J. W. C.; Tans, P. P.; Masarie, K. A.; Gemery, P. A. *J. Geophys. Res* **1996**, *101*, 25897.
(142) Gamo, T.; Tsutsumi, M.; Sakai, H.; Nakazawa, T.; Tanaka, M.; Honda, H.; Kubo, H.; Itoh, T. *Tellus* **1989**, *41B*, 127.
(143) Gamo, T.; Tsutsumi, M.; Sakai, H.; Nakazawa, T.; Machida, M.; Honda, H.; Itoh, T. *Geophys. Res. Lett.* **1995**, *22*, 397.
(144) Thiemens, M. H.; Jackson, T.; Mauersberger, K.; Schüler, B.; Morton, J. *Geophys. Res. Lett.* **1991**, *18*, 669.
(145) Yung, Y. L.; DeMore, W. B.; Pinto, J. P. *Geophys. Res. Lett.* **1991**, *18*, 13.
(146) Thiemens, M. H.; Jackson, T. L.; Brenninkmeijer, C. A. M. *Geophys. Res. Lett.* **1995**, *22*, 255.
(147) Thiemens, M. H.; Jackson, T.; Zipf, E. C.; Erdman, P. W.; van Egmond, C. *Science* **1995**, *270*, 969.
(148) Zipf, E. C.; Erdman, P. W. *Studies of trace constituents in the upper atmosphere and mesosphere using cryogenic whole air sampling techniques*; NASA's Upper Atmosphere Research Programme (UARP) and Atmospheric Chemistry Modeling and Analysis Programme (ACMAP) Research Summaries 1992−1993; NASA, 1994.
(149) Lämmerzahl, P.; Röckmann, T.; Brenninkmeijer, C. A. M.; Krankowsky, D.; Mauersberger, K. *Geophys. Res. Lett.* **2002**, *29*, 10.1029/2001GL014343.
(150) Alexander, B.; Savarino, J.; Barkov, N. I.; Delmas, R. J.; Thiemens, M. H. *Geophys. Res. Lett.* **2001**, *29*, 30.
(151) Bhattacharya, S. K.; Savarino, J.; Thiemens, M. H. *Geophys. Res. Lett.* **2000**, *27*, 1459.
(152) Boering, K. A.; Wofsy, S. C.; Daube, B. C.; Schneider, H. R.; Loewenstein, M.; Podolske, J. R. *Science* **1996**, *274*, 1340.
(153) DeMore, W. B.; Dede, C. *J. Phys. Chem.* **1970**, *74*, 2621.
(154) Wen, J.; Thiemens, M. H. *J. Geophys. Res.−Atmos.* **1993**, *98*, 12801.
(155) Yung, Y. L.; Lee, A. Y. T.; Irion, F. W.; DeMore, W. B.; Wen, J. *J. Geophys. Res.−Atmos.* **1997**, *102*, 10857.
(156) Johnston, J. C.; Röckmann, T.; Brenninkmeijer, C. A. M. *J. Geophys. Res.−Atmos.* **2000**, *105*, 15213.
(157) Barth, V.; Zahn, A. *J. Geophys. Res.−Atmos.* **1997**, *102*, 12995.
(158) Tannor, D. J. *J. Am. Chem. Soc.* **1988**, *111*, 2772.
(159) Lyons, J. R. *Geophys. Res. Lett.* **2001**, *28*, 3231.
(160) Boering, K. A. *EOS Trans. Suppl.* **2002**, *83* (47), Abstract B61D.
(161) Bender, M.; Sowers, T.; Labeyrie, L. *Global Biogeochem. Cycles* **1994**, *8*, 363.
(162) Luz, B.; Barkan, E.; Bender, M. L.; Thiemens, M. H.; Boering, K. A. *Nature* **1999**, *400*, 547.
(163) Blunier, T.; Barnett, B.; Bender, M. L.; Hendricks, M. B. *Global Biogeochem. Cycles* **2002**, *16*, 10.1029/2001GB001460.
(164) Moore, H. *Tellus* **1974**, *26*, 169.
(165) Heaton, T. H. E.; Collett, G. M. *The analysis of $^{15}N/^{14}N$ ratios in natural samples, with emphasis on nitrate and ammonium in precipitation*; National Physical Research Laboratory, Natural Isotopes Division, Council for Scientific and Industrial Research, 1985.
(166) Mariotti, A.; Germon, J. C.; Leclerc, A. *Can. J. Soil Sci.* **1982**, *62*, 227.
(167) Yoshida, N.; Matsuo, S. *Geochem. J.* **1983**, *17*, 231.
(168) Yoshida, N.; Hattori, A.; Saino, T.; Matsuo, S.; Wada, E. *Nature* **1984**, *307*, 442.
(169) Wahlen, M.; Yoshinari, T. *Nature* **1985**, *313*, 780.
(170) Yoshinari, T.; Wahlen, M. *Nature* **1985**, *317*, 349.
(171) Kim, K.-R.; Craig, H. *Nature* **1990**, *347*, 58.

(172) Yoshinari, T. In *Denitrification in Soil and Sediment*; Revsbech, N. P., Sørensen, J., Eds.; Plenum Press: New York, 1990.
(173) Röckmann, T.; Kaiser, J.; Brenninkmeijer, C. A. M.; Crowley, J. N.; Borchers, R.; Brand, W. A.; Crutzen, P. J. *J. Geophys. Res.−Atmos.* **2001**, *106*, 10403.
(174) Kim, K.-R.; Craig, H. *Science* **1993**, *262*, 1855.
(175) Tanaka, N.; Rye, D. M.; Rye, R.; Avak, H.; Yoshinari, T. *Int. J. Mass Spectrom. Ion Processes* **1995**, *142*, 163.
(176) Brand, W. A. *Isot. Environ. Health Stud.* **1995**, *31*, 277.
(177) Esler, M. B.; Griffith, D. W. T.; Turatti, F.; Wilson, S. R.; Rahn, T.; Zhang, H. *Chemosphere: Global Change Sci.* **2000**, *2*, 445.
(178) Uehara, K.; Yamamoto, K.; Kikugawa, T.; Yoshida, N. *Sens. Actuators B* **2001**, *74*, 173.
(179) Brenninkmeijer, C. A. M.; Röckmann, T. *Rapid Commun. Mass Spectrom.* **1999**, *13*, 2028.
(180) Toyoda, S.; Yoshida, N. *Anal. Chem.* **1999**, *71*, 4711.
(181) Cliff, S. S.; Thiemens, M. H. *Science* **1997**, *278*, 1774.
(182) Röckmann, T.; Kaiser, J.; Crowley, J. N.; Brenninkmeijer, C. A. M.; Crutzen, P. J. *Geophys. Res. Lett.* **2001**, *28*, 503.
(183) Minschwaner, K.; Salawitch, R. J.; McElroy, M. B. *J. Geophys. Res.−Atmos.* **1993**, *98*, 10543.
(184) McElroy, M.; McConnell, J. C. *J. Atmos. Sci.* **1971**, *28*, 1095.
(185) Crutzen, P. J. *Q. J. R. Met. Soc.* **1970**, *96*, 320.
(186) Selwyn, G. S.; Johnston, H. S. *J. Chem. Phys.* **1981**, *74*, 3791.
(187) Yoshida, N.; Morimoto, H.; Matsuo, S. *EOS* **1990**, *71*, 933.
(188) Johnston, J. C.; Cliff, S. S.; Thiemens, M. H. *J. Geophys. Res.−Atmos.* **1995**, *100*, 16801.
(189) Rahn, T.; Zhang, H.; Wahlen, M.; Blake, G. A. *Geophys. Res. Lett.* **1998**, *25*, 4489.
(190) Röckmann, T.; Brenninkmeijer, C. A. M.; Wollenhaupt, M.; Crowley, J. N.; Crutzen, P. J. *Geophys. Res. Lett.* **2000**, *27*, 1399.
(191) Toyoda, S.; Yoshida, N.; Suzuki, T.; Tsuji, K.; Shibuya, K. International Conference on the Study of Environmental Change Using Isotope Techniques, Vienna, Austria, 2001.
(192) Turatti, F.; Griffith, D. W. T.; Wilson, S. R.; Esler, M. B.; Rahn, T.; Zhang, H.; Blake, G. A. *Geophys. Res. Lett.* **2000**, *27*, 2489.
(193) Umemoto, H. *Chem. Phys. Lett.* **1999**, *314*, 267.
(194) Zhang, H.; Wennberg, P. O.; Wu, V. H.; Blake, G. A. *Geophys. Res. Lett.* **2000**, *27*, 2481.
(195) Yung, Y. L.; Miller, C. E. *Science* **1997**, *278*, 1778.
(196) Miller, C. E.; Yung, Y. L. *Chemosphere: Global Change Sci.* **2000**, *2*, 255.
(197) Johnson, M. S.; Billing, G. D.; Gruodis, A.; Janssen, M. H. M. *J. Phys. Chem. A* **2001**, *105*, 8672.
(198) Blake, G. A.; Liang, M. C.; Morgan, C. G.; Yung, Y. L. *EOS Trans. Suppl.* **2002**, *83*, Abstract B22D.
(199) Rahn, T.; Wahlen, M. *Science* **1997**, *278*, 1776.
(200) Yoshida, N.; Toyoda, S. *Nature* **2000**, *405*, 330.
(201) Toyoda, S.; Yoshida, N.; Urabe, T.; Aoki, S.; Nakazawa, T.; Sugawara, S.; Honda, H. *J. Geophys. Res.−Atmos.* **2001**, *106*, 7515.
(202) Griffith, D. W. T.; Toon, G. C.; Sen, B.; Blavier, J.-F.; Toth, R. A. *Geophys. Res. Lett.* **2000**, *27*, 2485.
(203) Kaiser, J.; Röckmann, T.; Brenninkmeijer, C. A. M.; Crutzen, P. J. *Atmos. Chem. Phys.* **2003**, *3*, 303 [online].
(204) Kaiser, J.; Röckmann, T.; Brenninkmeijer, C. A. M. *Phys. Chem. Chem. Phys.* **2002**, *4*, 4220.
(205) Kaiser, J.; Brenninkmeijer, C. A. M.; Röckmann, T. *Geophys. Res. Lett.* **2002**, *30*, 10.1029/2002GL016073.
(206) McLinden, C. A.; Prather, M. J.; Johnson, M. S. *J. Geophys. Res.−Atmos.* **2003**, *108*, doi 10.1029/2002JD002560.
(207) Kaiser, J.; Brenninkmeijer, C. A. M.; Röckmann, T. *J. Geophys. Res.−Atmos.* **2002**, *107*, 4214.
(208) Rahn, T.; Wahlen, M. *Global Biogeochem. Cycles* **2000**, *14*, 537.
(209) Zellner, R.; Hartmann, D.; Rosner, I. *Ber. Bunsen-Ges. Phys. Chem.* **1992**, *96*, 385.
(210) McElroy, M. B.; Jones, D. B. A. *Global Biogeochem. Cycles* **1996**, *10*, 651.
(211) Zipf, E. C.; Prasad, S. S. *Geophys. Res. Lett.* **1998**, *25*, 4333.
(212) Prasad, S. S.; Zipf, E. C. *Chemosphere: Global Change Sci.* **2000**, *2*, 235.
(213) Estupiñán, E. G.; Stickel, R. E.; Nicovich, J. M.; Wine, P. H. *J. Phys. Chem. A* **2002**, *106*, 5880.
(214) Estupiñán, E. G.; Stickel, R. E.; Wine, P. H. *Chemosphere: Global Change Sci.* **2000**, *2*, 247.
(215) Wingen, L. M.; Finlayson-Pitts, B. J. *Geophys. Res. Lett.* **1998**, *25*, 517.
(216) Dentener, F.; Crutzen, P. J. *J. Atmos. Chem.* **1994**, 331.
(217) Lindholm, N.; Hershberger, J. F. *J. Phys. Chem. A* **1997**, *101*, 4991.
(218) Park, J.; Lin, M. C. *J. Phys. Chem. A* **1997**, *101*, 2643.
(219) Park, J.; Lin, M. C. *J. Phys. Chem. A* **1996**, *100*, 3317.
(220) Park, J.; Lin, M. C. *Int. J. Chem. Kinet.* **1996**, *28*, 879.
(221) Michalski, G.; Savarino, J.; Böhlke, J. K.; Thiemens, M. *Anal. Chem.* **2002**, *74*, 4989.
(222) Casciotti, K. L.; Sigman, D. M.; Hastings, M. G.; Böhlke, J. K.; Hilkert, A. *Anal. Chem.* **2002**, *74*, 4905.
(223) Glickman, M. H.; Cliff, S.; Thiemens, M.; Klinman, J. P. *J. Am. Chem. Soc.* **1997**, *119*, 11357.
(224) Kim, K.-R.; Joos, F.; Keller, M.; Matson, P.; Craig, H. *Non-CO_2 Greenhouse Gases: Scientific Understanding, Control and Implementation*; Noordwijkerhout: The Netherlands, 2000; p 179.
(225) Röckmann, T.; Kaiser, J.; Brenninkmeijer, C. A. M. *Atmos. Chem. Phys.* **2003**, *3*, 315 [online].
(226) Sowers, T.; Rodebaugh, A.; Yoshida, N.; Toyoda, S. *Global Biogeochem. Cycles* **2002**, *16*, 1129.
(227) Pérez, T.; Trumbore, S. E.; Tyler, S. C.; Matson, P. A.; Ortiz-Monasterio, I.; Rahn, T.; Griffith, D. W. T. *J. Geophys. Res.−Atmos.* **2001**, *106*, 9869.
(228) Weston, R. E. *Abstr. Pap. Am. Chem. Soc.* **2000**, *219*, U313.
(229) Hodder, P. S.; Brenninkmeijer, C. A. M.; Thiemens, M. H. *ICOG proceedings*; U.S. Geological Circulair 1107; U.S. Geological Survey: Washington, DC, 1994.
(230) Huff, A. K.; Thiemens, M. H. *Geophys. Res. Lett.* **1998**, *25*, 3509.
(231) Röckmann, T.; Jöckel, P.; Gros, V.; Bräunlich, M.; Possnert, G.; Brenninkmeijer, C. A. M. *Atmos. Chem. Phys.* **2002**, *2*, 147 [online].
(232) Brenninkmeijer, C. A. M.; Röckmann, T.; Bräunlich, M.; Jöckel, P.; Bergamaschi, P. *Chemosphere: Global Change Sci.* **1999**, *1*, 33.
(233) Mak, J. E.; Yang, W. B. *Anal. Chem.* **1998**, *70*, 5159.
(234) Tsunogai, U.; Nakagawa, F.; Komatsu, D. D.; Gamo, T. *Anal. Chem.* **2002**, *74*, 5695.
(235) Stevens, C. M.; Kaplan, L.; Gorse, R.; Durkee, S.; Compton, M.; Cohen, S.; Bielling, K. *Int. J. Chem. Kinet.* **1980**, *12*, 935.
(236) Röckmann, T. Ph.D. thesis, Ruprecht-Karls-Universität Heidelberg, 1998.
(237) Röckmann, T.; Brenninkmeijer, C. A. M.; Neeb, P.; Crutzen, P. J. *J. Geophys. Res.−Atmos.* **1998**, *103*, 1463.
(238) Röckmann, T.; Brenninkmeijer, C. A. M.; Saueressig, G.; Bergamaschi, P.; Crowley, J. N.; Fischer, H.; Crutzen, P. J. *Science* **1998**, *281*, 544.
(239) Manning, M. R.; Brenninkmeijer, C. A. M.; Allan, W. *J. Geophys. Res.−Atmos.* **1997**, *102*, 10673.
(240) Bergamaschi, P.; Hein, R.; Brenninkmeijer, C. A. M.; Crutzen, P. J. *J. Geophys. Res.−Atmos.* **2000**, *105*, 1929.
(241) Tromp, T. K.; Shia, R.; Allen, M.; Eiler, J. M.; Yung, Y. L. *Science* **2003**, *300*, 1740.
(242) Ehhalt, D. H.; Davidson, J. A.; Cantrell, C. A.; Friedman, I.; Tyler, S. *J. Geophys. Res.−Atmos.* **1989**, *94*, 9831.
(243) Rahn, T.; Kitchen, N.; Eiler, J. *Geochim. Cosmochim. Acta* **2002**, *66*, 2475.
(244) Gerst, S.; Quay, P. *J. Geophys. Res.−Atmos.* **2000**, *105*, 26433.
(245) Gerst, S.; Quay, P. *J. Geophys. Res.−Atmos.* **2001**, *106*, 5021.
(246) Rahn, T.; Eiler, J. M.; Kitchen, N.; Fessenden, J. E.; Randerson, J. T. *Geophys. Res. Lett.* **2002**, *29*, art. no. 1888.
(247) Talukdar, R. K.; Gierczak, T.; Goldfarb, L.; Rudich, Y.; Rao, B. S. M.; Ravishankara, A. R. *J. Phys. Chem.* **1996**, *100*, 3037.
(248) Talukdar, R. K.; Ravidhankara, A. R. *Chem. Phys. Lett.* **1996**, *253*, 177.
(249) Taatjes, C. A. *Chem. Phys. Lett.* **1999**, *306*, 33.
(250) Friedman, I.; Scholz, T. G. *Geochim. Cosmochim. Acta* **1974**, *79*, 785.
(251) Novelli, P. C.; Lang, P. M.; Masarie, K. A.; Hurst, D. F.; Myers, R.; Elkins, J. W. *J. Geophys. Res.−Atmos.* **1999**, *104*, 30427.
(252) Rahn, T.; Eiler, J.; McCarthy, M.; Boering, K.; Wennberg, P.; Atlas, E.; Schauffler, S. *Geochim. Cosmochim. Acta* **2002**, *66*, A622.
(253) Röckmann, T.; Rhee, T. S.; Engel, A. *Atmos. Chem. Phys. Discuss.* **2003**, *3*, 3745 [online].
(254) Keith, D. W. *J. Geophys. Res.−Atmos.* **2000**, *105*, 15167.
(255) Moyer, E. J.; Irion, F. W.; Yung, Y. L.; Gunson, M. R. *Geophys. Res. Lett.* **1996**, *23*, 2385.
(256) Irion, F. W. *Geophys. Res. Lett.* **1996**, *23*, 2381.
(257) Ridal, M.; Jonsson, A.; Werner, M.; Murtagh, D. P. *J. Geophys. Res.−Atmos.* **2001**, *106*, 32283.
(258) Bechtel, C.; Zahn, A. *Atmos. Chem. Phys. Discuss.* **2003**, *3*, 3991 [online].
(259) Savarino, J.; Thiemens, M. H. *Atmos. Environ.* **1999**, *33*, 3683.
(260) Savarino, J.; Thiemens, M. H. *J. Phys. Chem. A* **1999**, *103*, 9221.
(261) Johnson, B. J.; Dawson, G. A. *Environ. Sci. Technol.* **1990**, *24*, 898.
(262) Tanner, R. L.; Zielinska, B.; Uberna, E.; Harshfield, G.; McNichol, A. P. *J. Geophys. Res.−Atmos.* **1996**, *101*, 28961.
(263) Rudolph, J.; Czuba, E.; Norman, A. L.; Huang, L.; Ernst, D. *Atmos. Environ.* **2002**, *36*, 1173.
(264) Tsunogai, U.; Yoshida, N.; Gamo, T. *J. Geophys. Res.−Atmos.* **1999**, *104*, 16033.
(265) Rudolph, J.; Czuba, E.; Huang, L. *J. Geophys. Res.−Atmos.* **2000**, *105*, 29329.
(266) Stone, T.; Johnson, B. J.; Dawson, G. A.; Long, A. *EOS* **1989**, *70*, 1017.
(267) Beukes, J. A.; D'Anna, B.; Bakken, V.; Nielsen, C. J. *Phys. Chem. Chem. Phys.* **2000**, *2*, 4049.
(268) D'Anna, B.; Bakken, V.; Beukes, J. A.; Nielsen, C. J.; Brudnik, K.; Jodkowski, J. T. *Phys. Chem. Chem. Phys.* **2002**, *5*, 1790.

(269) Goldman, A.; Coffey, M. T.; Stephen, T. M.; Rinsland, C. P.; Mankin, W. G.; Hannigan, J. W. *J. Quant. Spectrosc. Radiat. Transfer* **2000**, *67*, 447.
(270) Castleman, J. A. W.; Munkelwitz, H. R.; Manowitz, B. *Tellus* **1974**, *26*, 222.
(271) Thiemens, M. H.; Savarino, J.; Farquhar, J.; Bao, H. M. *Acc. Chem. Res.* **2001**, *34*, 645.
(272) Lee, C. C.-W.; Savarino, J.; Thiemens, M. H. *Geophys. Res. Lett.* **2001**, *28*, 1783.
(273) Savarino, J.; Alexander, B.; Darmohusodo, V.; Thiemens, M. H. *Anal. Chem.* **2001**, *73*, 4457.
(274) Savarino, J.; Lee, C. C. W.; Thiemens, M. H. *J. Geophys. Res.−Atmos.* **2000**, *105*, 29079.
(275) Lee, C. C.-W.; Thiemens, M. H. *J. Geophys. Res.−Atmos.* **2001**, *106*, 17359.
(276) Lee, C. C.-W.; Savarino, J.; Cachier, H.; Thiemens, M. H. *Tellus* **2002**, *54B*, 193.
(277) Farquhar, J.; Savarino, J.; Airieau, S.; Thiemens, M. H. *J. Geophys. Res.−Planets* **2001**, *106*, 32829.
(278) Bao, H.; Reheis, M. C. *J. Geophys. Res.−Atmos.* **2003**, *108*, 4430 (doi: 10.1029/2002JD003022).
(279) Bao, H.; Michalski, G. M.; Thiemens, M. H. *Geochim. Cosmochim. Acta* **2001**, *65*, 2029.
(280) Michalski, G.; Hernandez, L.; Meixner, T.; Fenn, M.; Thiemens, M. H. *EOS Trans. Suppl.* **2001**, *82*, Abstract H11D.
(281) Hernandez, L.; Michalski, G.; Meixner, T.; Fenn, M.; Thiemens, M. H. *EOS Trans. Suppl.* **2002**, *83*, Abstract B71A.
(282) Michalski, G.; Scott, Z.; Kabiling, M.; Thiemens, M. *Geophys. Res. Lett.* **2003**, *30*, doi 10.1029/2003GL017015.
(283) Hastings, M. G.; Sigman, D. M.; Lipschultz, F. *J. Geophys. Res.−Atmos.* **2003**, in press.
(284) Saueressig, G.; Crowley, J. N.; Bergamaschi, P.; Brühl, C.; Brenninkmeijer, C. A. M.; Fischer, H. *J. Geophys. Res.−Atmos.* **2001**, *106*, 23127.
(285) Cantrell, C. A.; Shetter, R. E.; McDaniel, A. H.; Calvert, J. G.; Davidson, J. A.; Lowe, D. C.; Tyler, S. C.; Cicerone, R. J.; Greenberg, J. P. *J. Geophys. Res.−Atmos.* **1990**, *95*, 22455.
(286) Gierczak, T.; Talukdar, R. K.; Herndon, G. L.; Vaghjiani, G. L.; Ravishankara, A. R. *J. Phys. Chem. A* **1997**, *101*, 3125.
(287) Tyler, S. C.; Ajie, H. O.; Rice, A. J.; Cicerone, R. J. *Geophys. Res. Lett.* **2000**, *27*, 1715.
(288) Boone, G. D.; Agyin, D. J.; Robichaud, F. M.; Tao, F. M.; Hewitt, S. A. *J. Phys. Chem. A* **2001**, *105*, 1456.
(289) Crowley, J. N.; Saueressig, G.; Bergamaschi, P.; Fischer, H.; Harris, G. W. *Chem. Phys. Lett.* **1999**, *303*, 268.
(290) Saueressig, G.; Bergamaschi, P.; Crowley, J. N.; Fischer, H.; Harris, G. W. *Geophys. Res. Lett.* **1995**, *22*, 1225.
(291) Saueressig, G.; Bergamaschi, P.; Crowley, J. N.; Fischer, H.; Harris, G. W. *Geophys. Res. Lett.* **1996**, *23*, 3619.
(292) Davidson, J. A.; Cantrell, S. C.; Tyler, S. C.; Shetter, R. J.; Cicerone, R. J.; Calvert, J. G. *J. Geophys. Res.−Atmos.* **1987**, *92*, 2195.
(293) Alexander, B.; Vollmer, M. K.; Jackson, T.; Weiss, R. F.; Thiemens, M. H. *Geophys. Res. Lett.* **2001**, *28*, 4103.
(294) Yoshino, K.; Freeman, D. E.; Parkinson, W. H. *Planet. Space Sci.* **1984**, *32*, 1219.
(295) Selwyn, G.; Podolske, J.; Johnston, H. S. *Geophys. Res. Lett.* **1977**, *4*, 427.
(296) Mérienne, M. F.; Coquart, B.; Jenouvrier, A. *Planet. Space Sci.* **1990**, *38*, 617.
(297) Leung, F.-Y. T.; Colussi, A. J.; Hoffmann, M. R.; Toon, G. C. *Geophys. Res. Lett.* **2002**, *29*, 112.
(298) Perri, M. J.; Van Wyngarden, A. L.; Boering, K. A.; Lin, J. J.; Lee, Y. T. *J. Chem. Phys.* **2003**, *119*, 8213.

CR020644K